THE INSTITUTE OF PAPER CHEMISTRY, APPLETON, WISCONSIN

SLIDE MATERIAL

for the

Engineering Project Advisory Committee

October 23-24, 1985
The Institute of Paper Chemistry
Continuing Education Center
Appleton, Wisconsin

2

TABLE OF CONTENTS

Project 3556

FUNDAMENTALS OF KRAFT LIQUOR CORROSIVITY

David Crowe

PROJECT 3556

FUNDAMENTALS OF KRAFT LIQUOR CORROSIVITY

David C. Crowe

FUNDAMENTALS OF KRAFT LIQUOR CORROSIVITY

OBJECTIVE

REDUCE COSTS OF CORROSION OF CARBON STEEL BY KRAFT LIQUORS

APPROACH

- MONITOR CORROSIVITY
- DETECT HIGH CORROSIVITY
- TRACE ORIGINS OF HIGH CORROSION RATE
- CORRECT

PROGRESS

- CONTINUED MONITORING OF CORROSIVITY IN THE FIELD
  - LPR
  - ER
  - WEIGHT LOSS
  - LIQUOR SAMPLING
  - VELOCITY EFFECT
- CONSTRUCTION AND PROGRAMMING OF MICROPROCESSOR FOR REMOTE DATA ACQUISITION

PROGRESS (Contd.)

- COMPLETION OF STUDY OF THIOSULFATE ADDITIONS ON CORROSION RATE
- COMMENCEMENT OF STUDY OF SULFITE ADDITIONS ON CORROSION RATE
- CONSTRUCTION OF APPARATUS TO STUDY VELOCITY EFFECTS BY MEANS OF ROTATING CYLINDER ELECTRODE

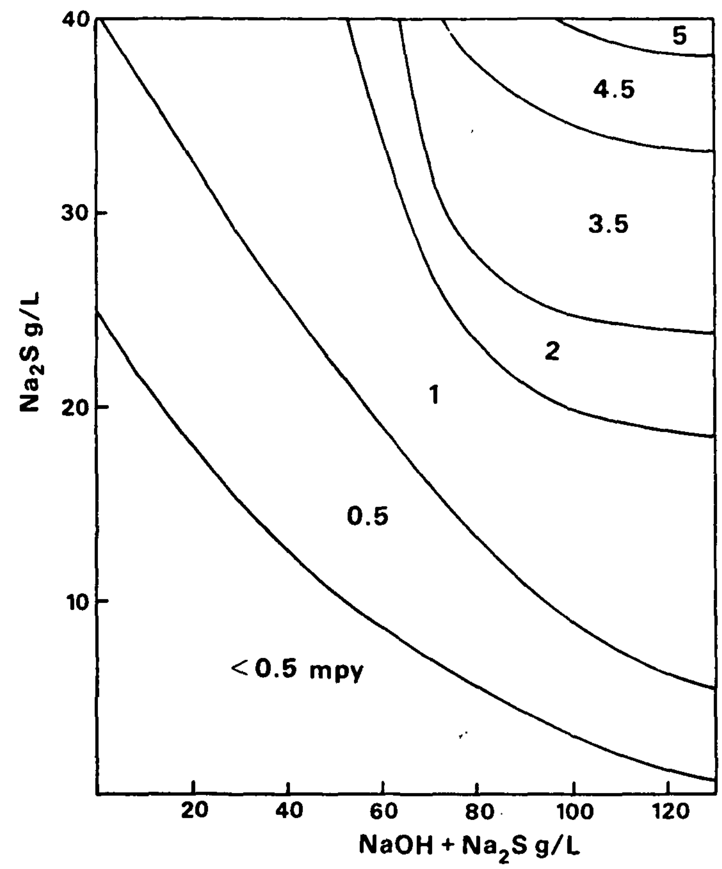

Iso-corrosion plot for NaOH + Na_2S solutions.

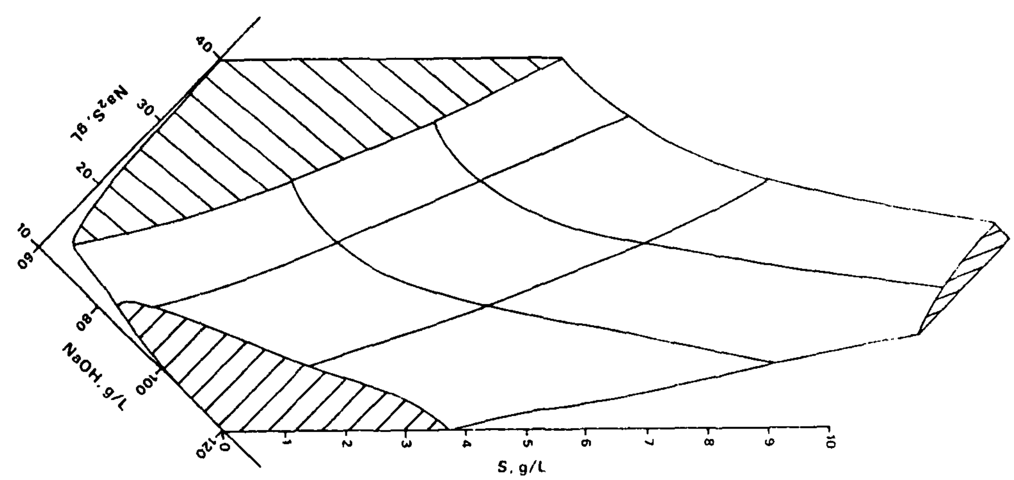

Isocorrosion surface 5 mpy in NaOH + Na_2S + S solution after 2 weeks exposure.

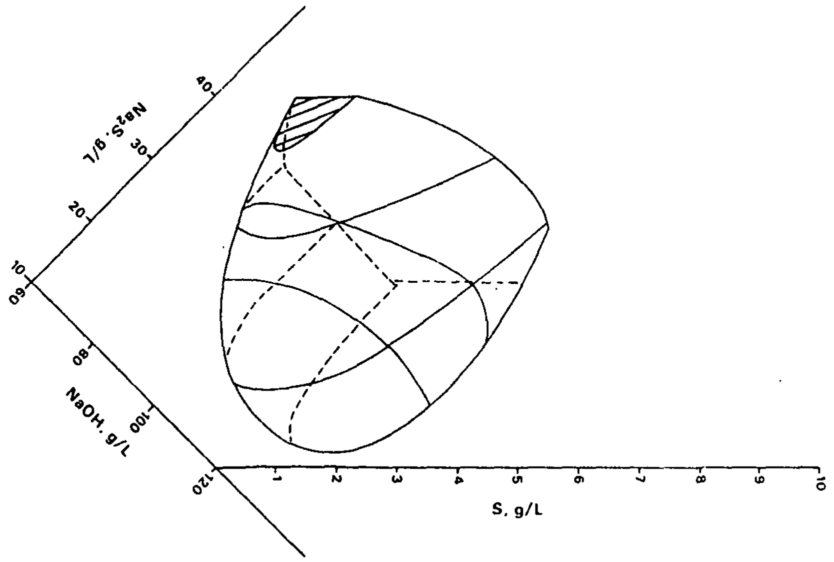

Isocorrosion surface 5 mpy in NaOH + Na_2S + S solution after 8 weeks exposure.

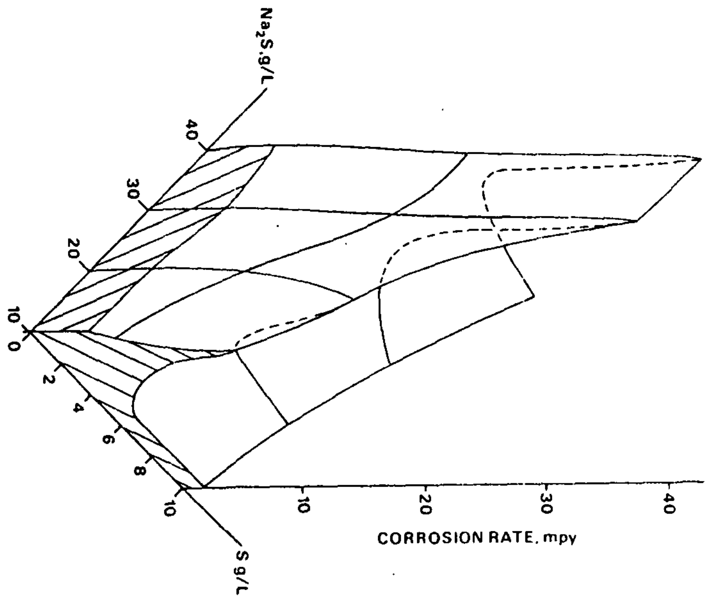

Corrosion rates in Na_2S + S + 120 g/L NaOH solution after 2 week exposure.

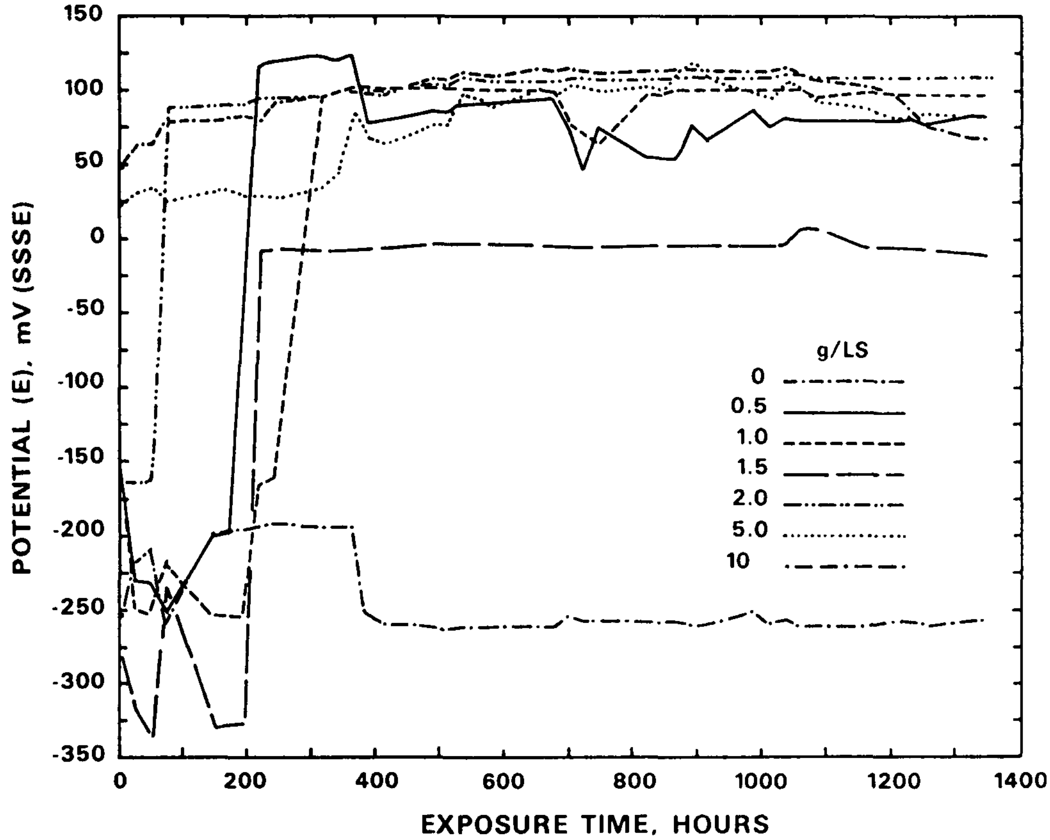

Corrosion potential as a function of exposure time in 100 g/L NaOH + 30 g/L Na_2S + 0–10 g/L S.

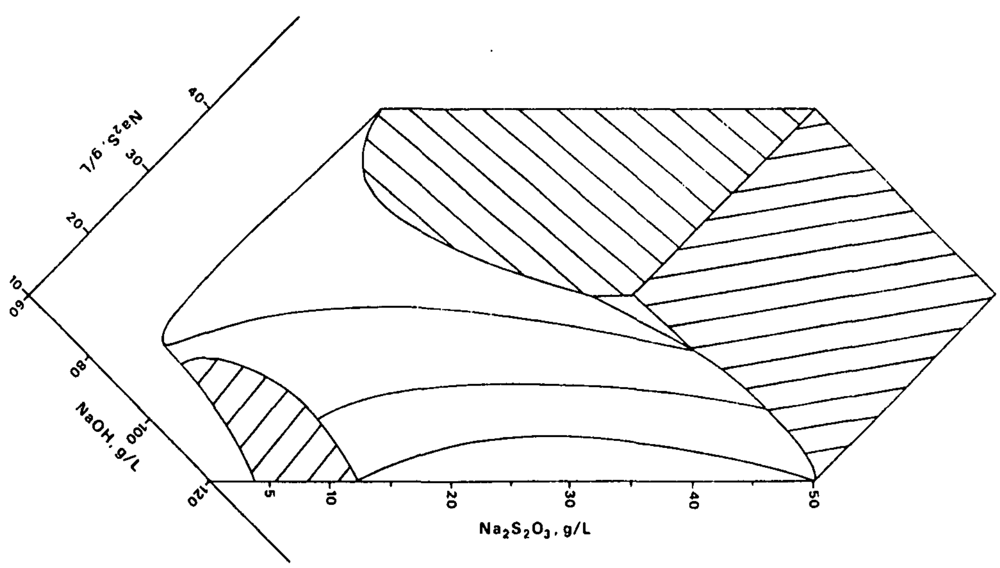

Isocorrosion plot of 15 mpy surface in NaOH + Na_2S + $Na_2S_2O_3$ solutions after 2 weeks exposure.

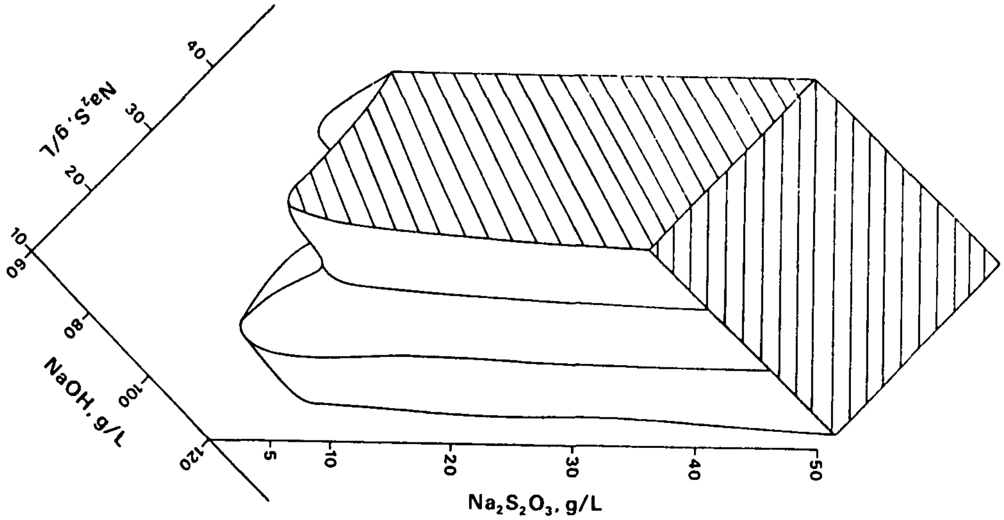

Isocorrosion plot of 15 mpy surface in NaOH + Na_2S + $Na_2S_2O_3$ solutions after 8 weeks exposure.

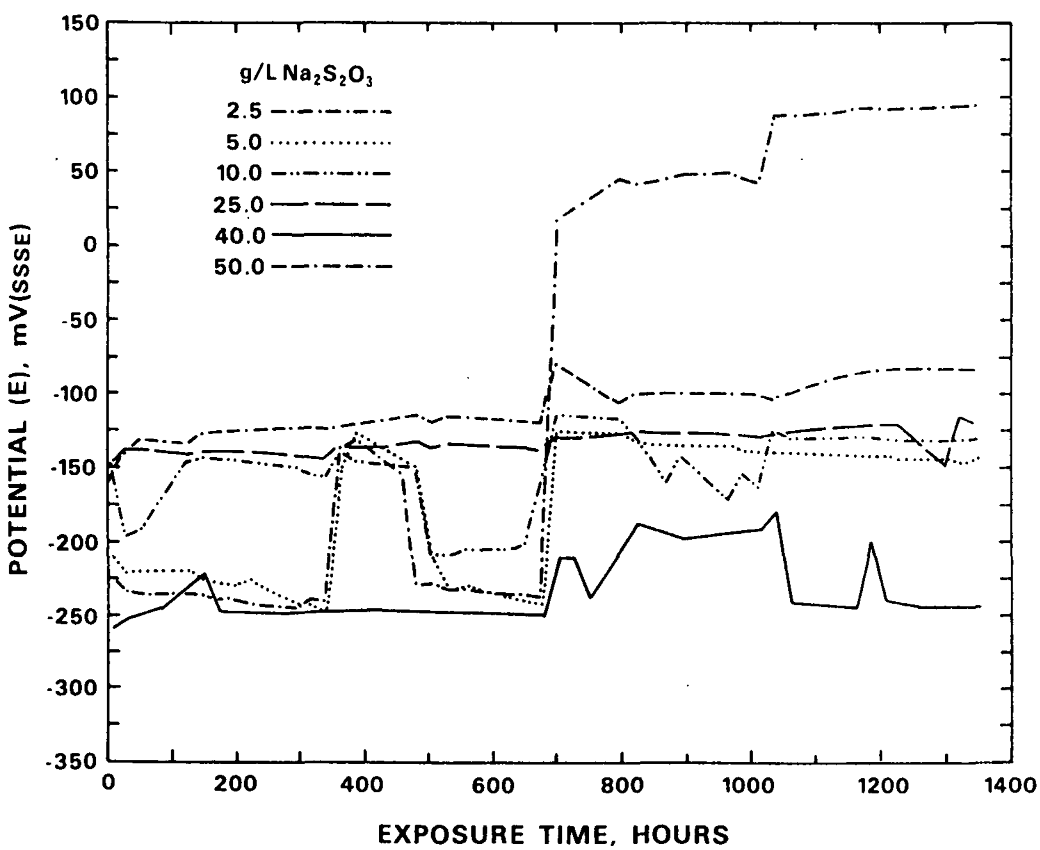

Corrosion potential during exposure in 80 g/L NaOH + 40 g/L Na_2S + 0-50 g/L $Na_2S_2O_3$.

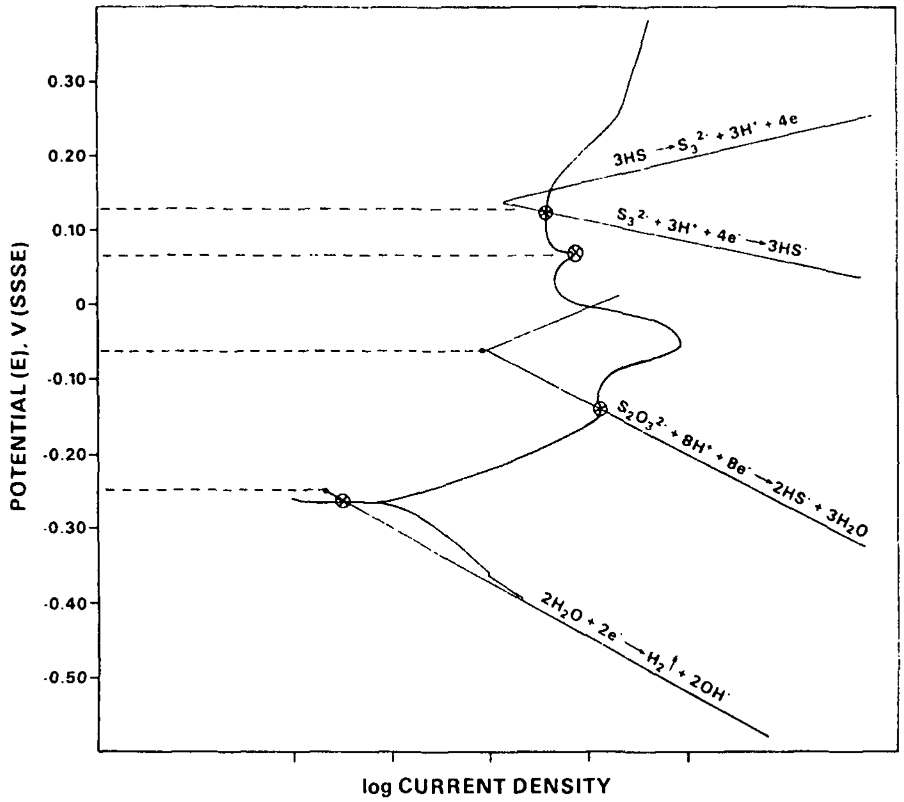

Schematic diagram illustrating the reactions which may control the corrosion potential.

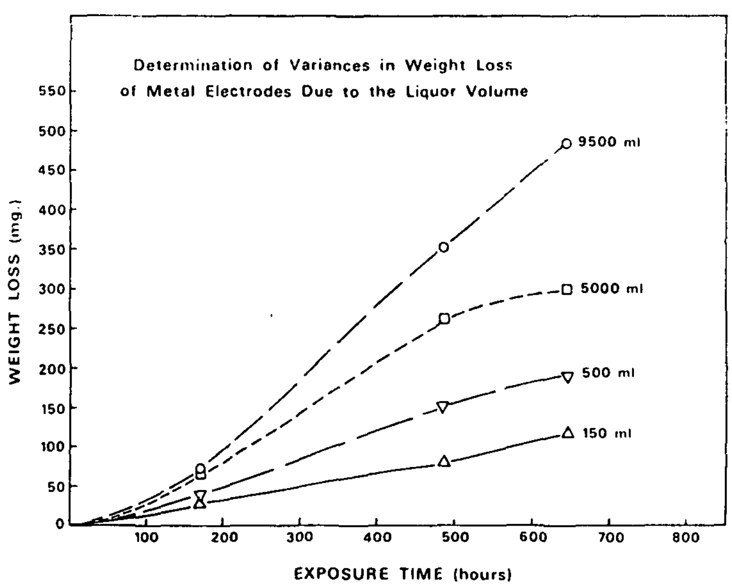

Determination of variances in weight loss of metal electrodes due to the liquor volume.

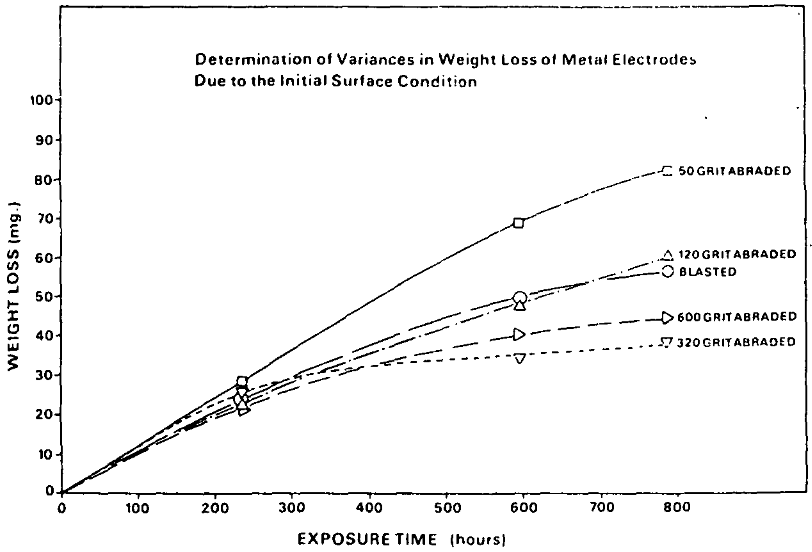

Determination of variances in weight loss of metal electrodes due to the initial surface condition.

IN-MILL LPR RESULTS

- MEASURED VALUES AGREED VERY WELL WITH WEIGHT LOSS, WHEN APPROPRIATE CORRECTIONS ARE APPLIED, CONSISTENT WITH TAFEL SLOPES MEASURED FROM IN SITU POLARIZATION CURVES.
- GIVES AN INSTANTANEOUS MEASUREMENT OF CORROSION RATE.

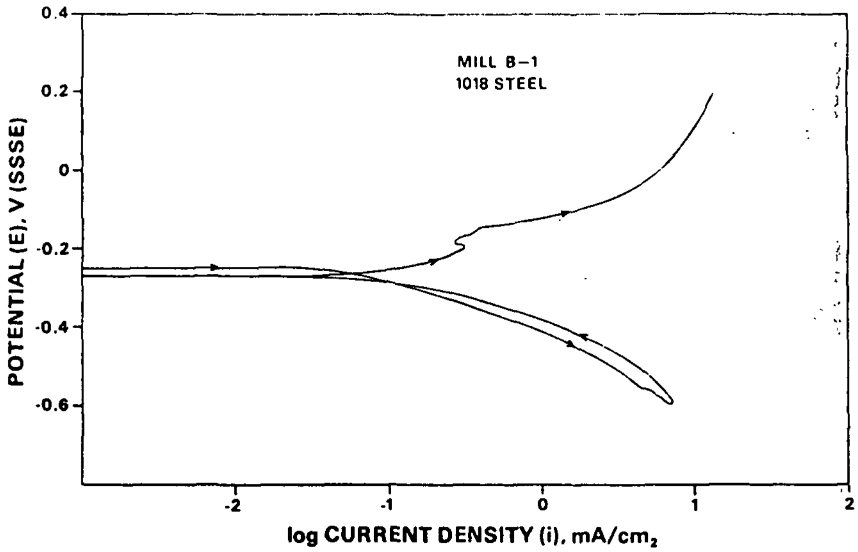

Representative polarization curve
for 1018 steel in mill white liquor

ELECTRICAL RESISTANCE RESULTS

- EXCELLENT AGREEMENT WITH WEIGHT LOSS TESTS.
- A PERIOD OF EXPOSURE OF AS MUCH AS ONE MONTH IS NECESSARY TO OBTAIN AN ACCURATE MEASUREMENT.
- NEEDS NO CORRECTION OR INTERPRETATION.

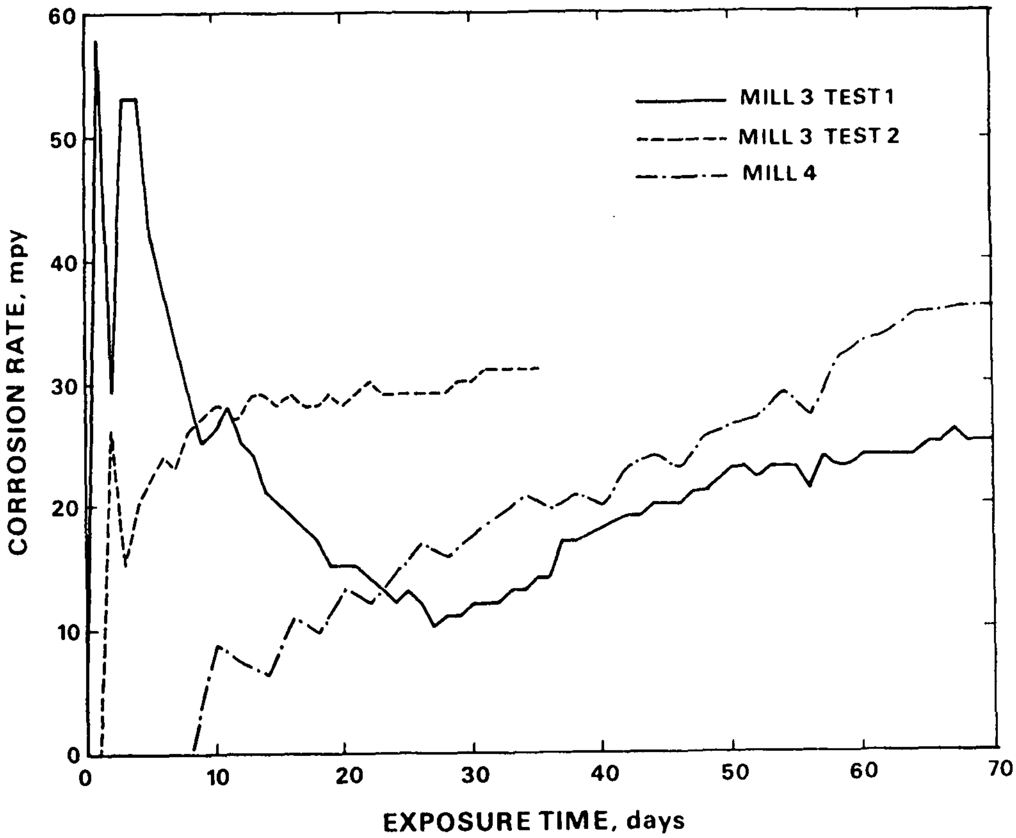

Corrosion rate measured by electrical
resistance technique in mill white liquor

MATERIALS

- MATERIALS, IN ORDER OF DECREASING CORROSION RESISTANCE:

  A285 SPECIAL
  A283
  A285C
  1018

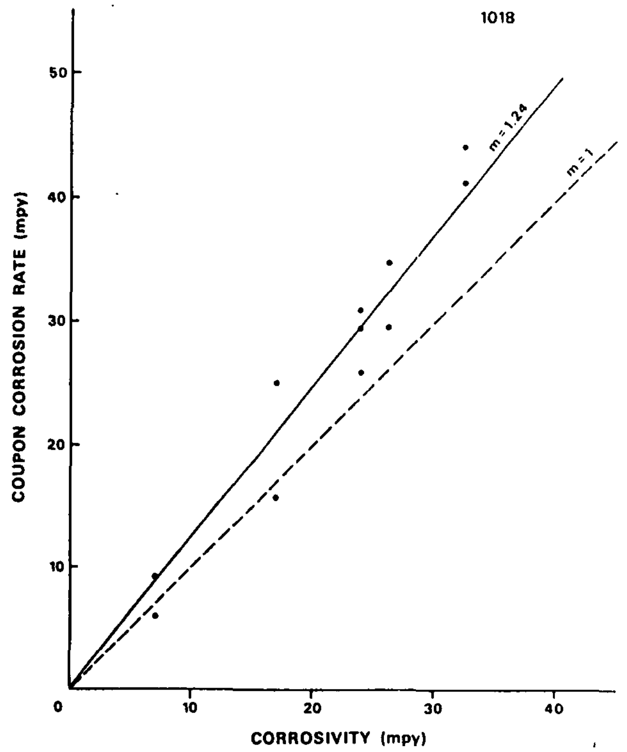

Corrosion rate of 1018 steel in mill
white liquors of various corrosivity

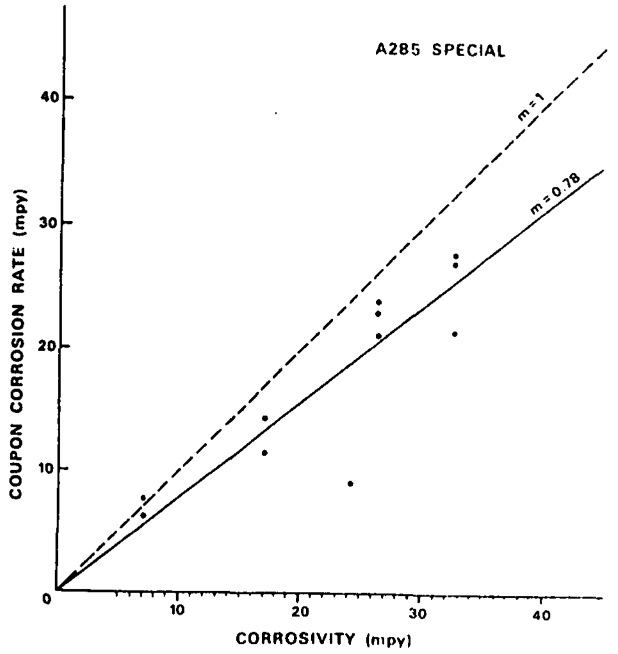

Corrosion rate of A285 - special steel
in mill white liquors of various corrosivity

LIQUOR CORROSIVITY

- THE MOST SIGNIFICANT FACTOR
- THIOSULFATE, SULFIDE, HYDROXIDE } AFFECTED CORROSION RATES IN-MILL

PLANS FOR NEXT PERIOD

- FIELD TEST THE MICROPROCESSOR-BASED DATA ACQUISITION SYSTEM
- COLLECT MORE MILL DATA
- MEASURE EFFECTS OF SULFITE ON CORROSION RATES
- TESTING OF VELOCITY EFFECTS WITH A ROTATING CYLINDER ELECTRODE
- COMPLETE MODIFICATIONS TO FLOW LOOP AND RESUME TESTING
- TESTING OF A NEW DESIGN OF Ag/Ag_2S REFERENCE ELECTRODE

SIGNIFICANCE TO THE INDUSTRY

- CORROSION MONITORING METHODS MAY BE APPLIED RELIABLY IN WHITE LIQUOR SYSTEMS
- CORROSION RATE IS INFLUENCED MORE STRONGLY BY LIQUOR CORROSIVITY THAN BY STEEL COMPOSITION
- CORROSION IS STIMULATED BY THIOSULFATE AND POLYSULFIDE RESULTING FROM LIQUOR OXIDATION

Project 3309

FUNDAMENTALS OF CORROSION CONTROL IN PAPER MILLS

Ronald Yeske

FUNDAMENTALS OF CORROSION CONTROL IN PAPER MILLS

Project 3309

OBJECTIVE

- IMPROVE LIFETIME OF SUCTION ROLLS

SHORT TERM OBJECTIVES

- IDENTIFY A PREDICTIVE LABORATORY TEST
- NORMALIZE DIFFERENT FATIGUE METHODS

A PREDICTIVE LABORATORY TEST

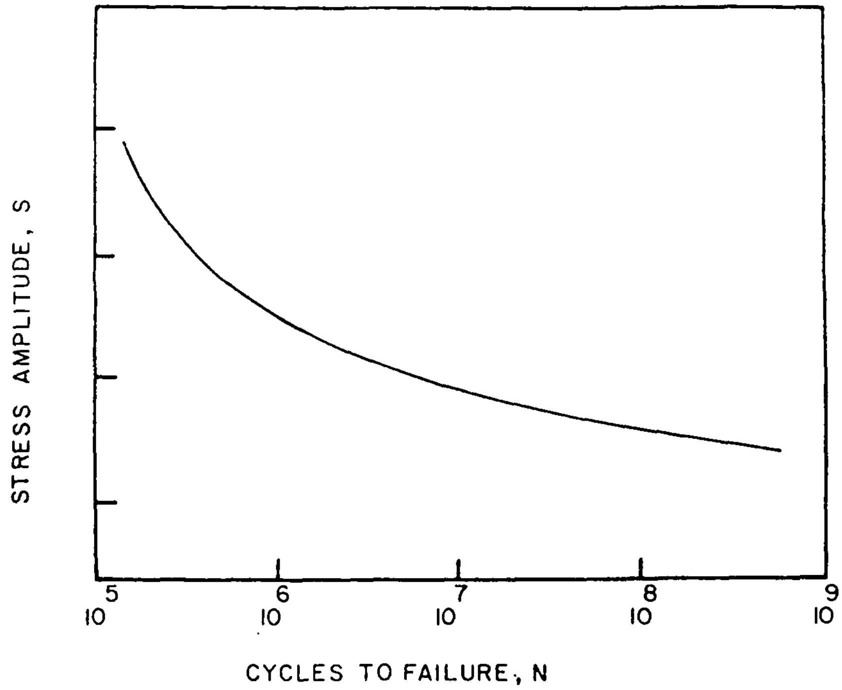

Schematic S-N curve depicting resistance to fatigue crack initiation.

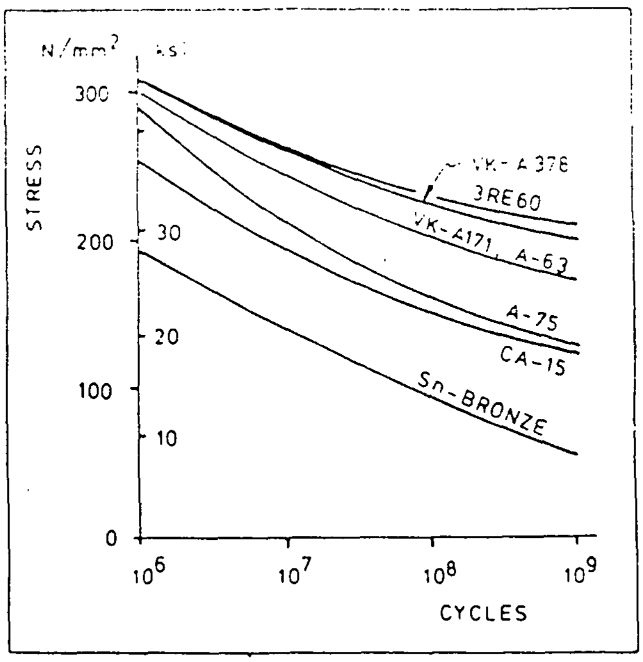

S-N curves for seven suction roll alloys in white water (pH 3.5, chloride 20-400 ppm, sulfate 250-1000 ppm) from rotating beam tests at 1500-1750 rpm

Although Alloy 75 is superior to Alloy 63 in service, the results of this S-N curve generated in the laboratory would indicate otherwise.

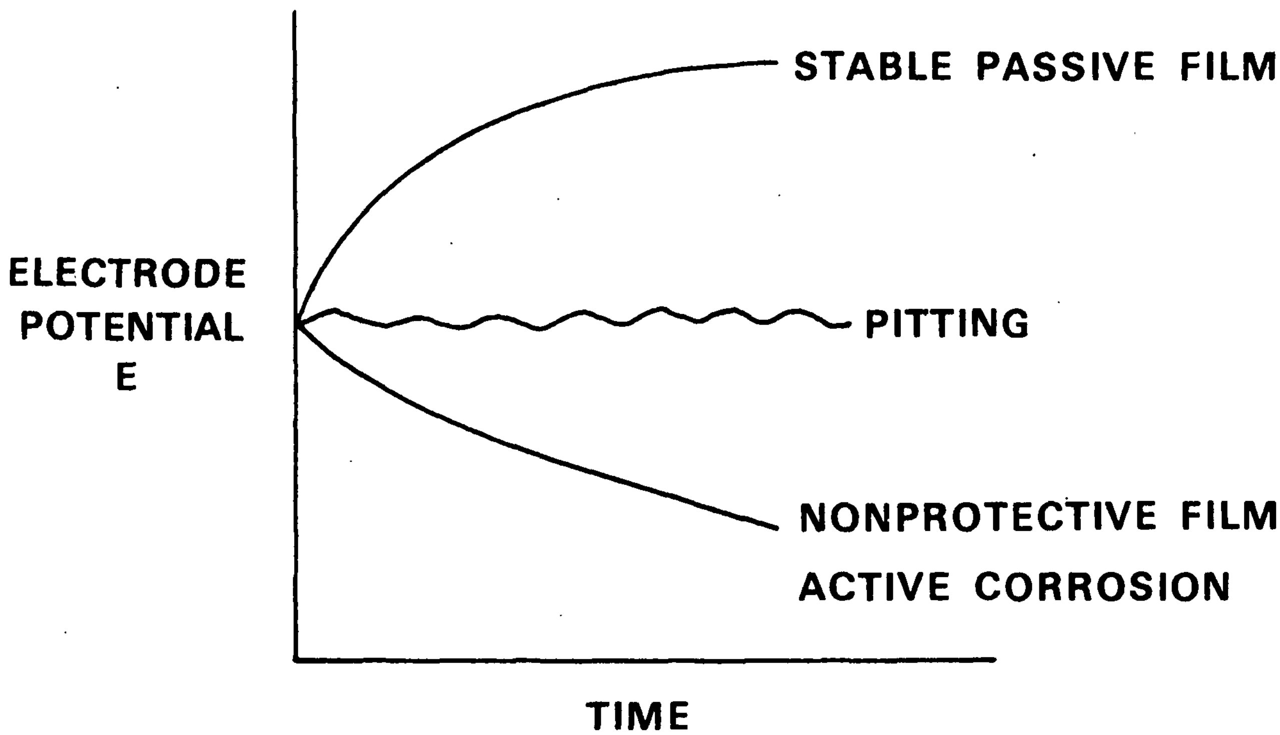

Variation in electrochemical potentials developed at the wetted surfaces of suction roll specimens exposed to a simulated white water.

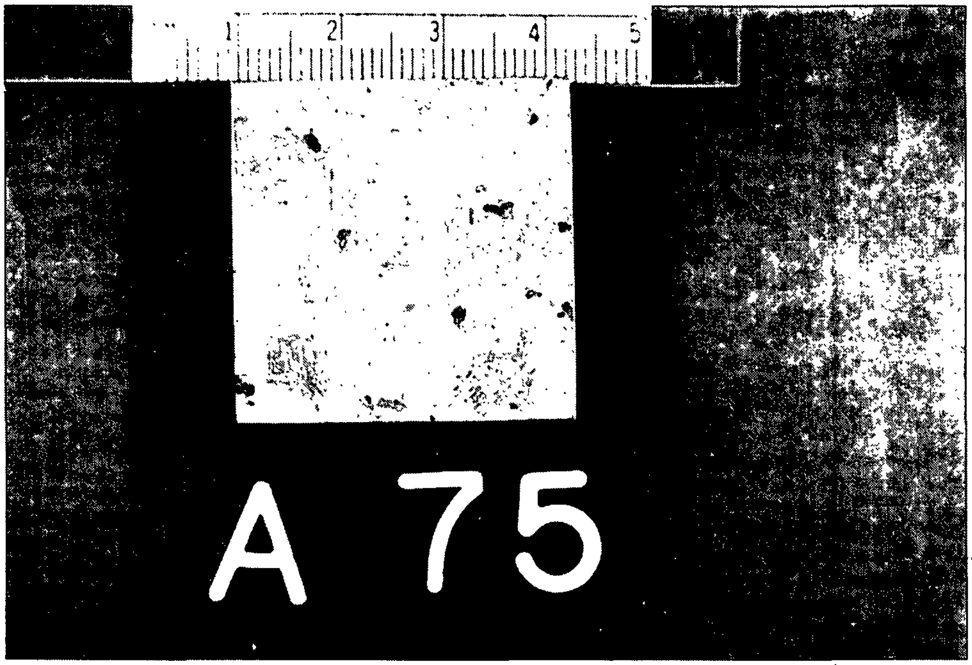

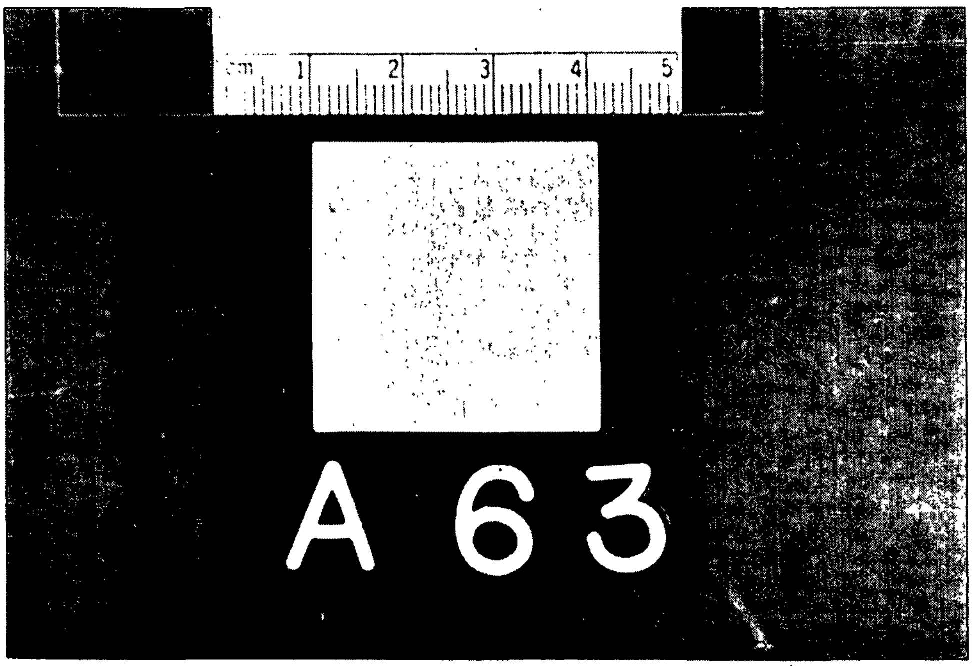

Examples of pitting corrosion resistance of Alloys 75 and 63 in simulated paper machine white waters. Alloy 75 has a superior service record.

NORMALIZE FATIGUE METHODS

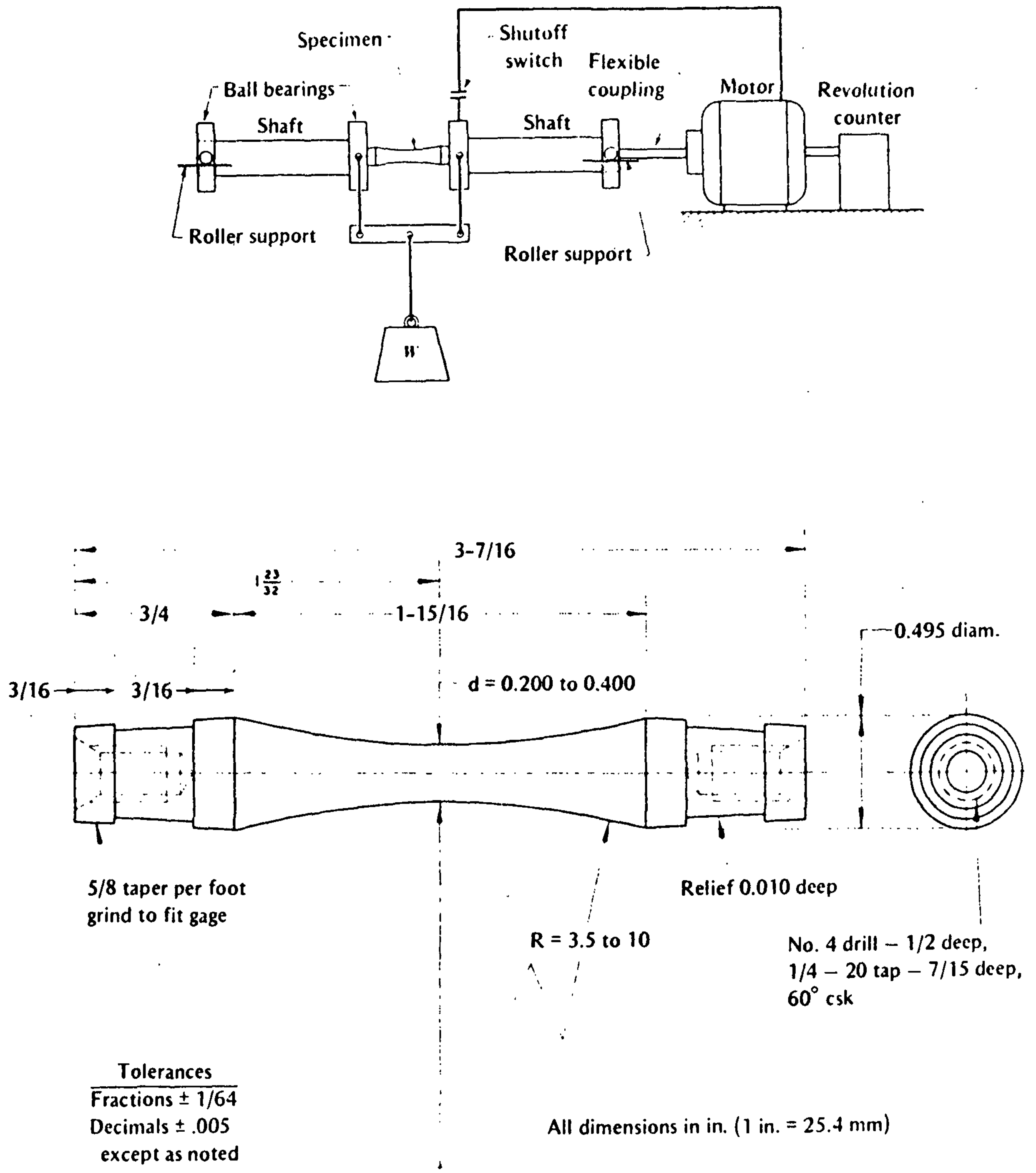

Schematic illustration of rotating beam testing machine (upper) and geometry/dimensions of the specimen (R. R. Moore type).

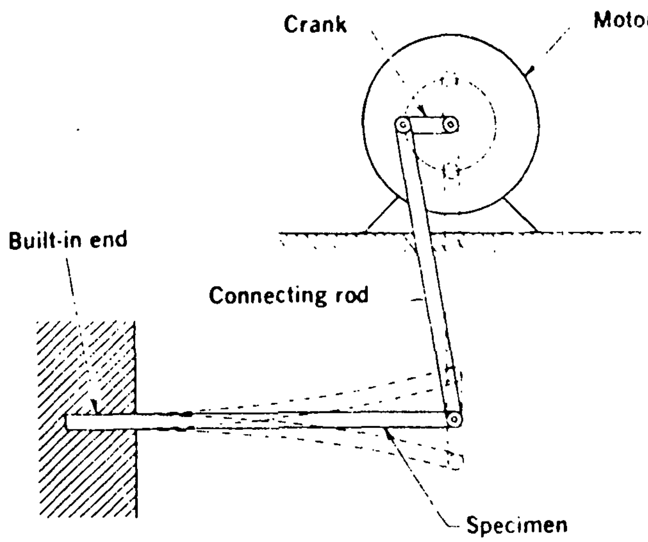

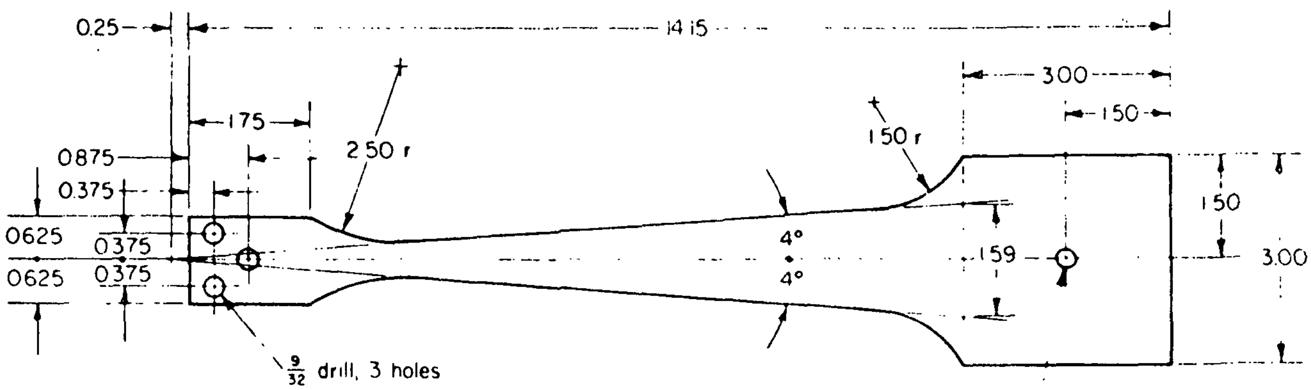

Notes 1. Specimen to be symmetrical about ℄.
2. Specimen thickness shall be 0.400 ± .001 in.
3. All dimensions in inches.

Schematic illustration of reversed plate bending test machine (upper) and specimen geometry/dimensions, below.

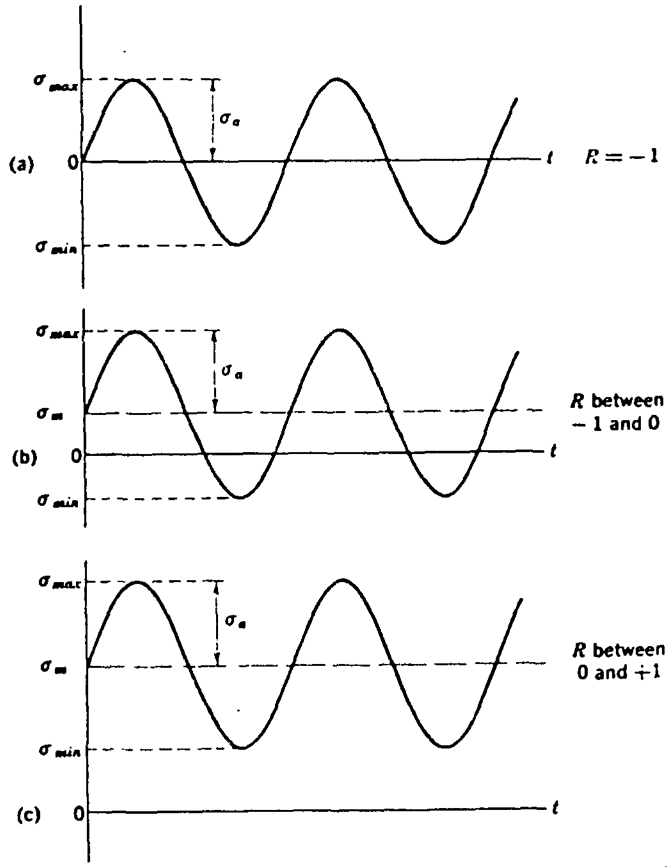

Schematic illustration of three alternating load forms as a function of time (t) in fatigue

IMPORTANT VARIABLES

- STRESS AMPLITUDE
- MEAN STRESS
- SPECIMEN GEOMETRY
- FREQUENCY
- NOTCH/SMOOTH
- SURFACE FINISH
- TEMPERATURE
- Cl^-, $S_2O_3^=$ CONCENTRATION
- pH

CORROSION TESTING PROGRAM

COMPARISON OF WEIGHT LOSSES
DUE TO PITTING OF SUCTION ROLL ALLOYS

ALLOY	CORROSION RATE, mpy	ALLOY	CORROSION RATE, mpy
A75	3.4	CF3M	1.0
CA15	12.1	1811	0.1
KA171	0.04	1804	0.5
2505	0.7	304L	3.0
KA171	0.08	VKA 378	0.06
A63	0.0	1300	14.3

NORMALIZATION OF FATIGUE METHODS

- ACQUISITION OF ALTERNATING BENDING APPARATUS
- ACQUISITION OF THREE ROTATING BENDING MACHINES
- TEST CHAMBER DESIGN, SHAKEDOWN

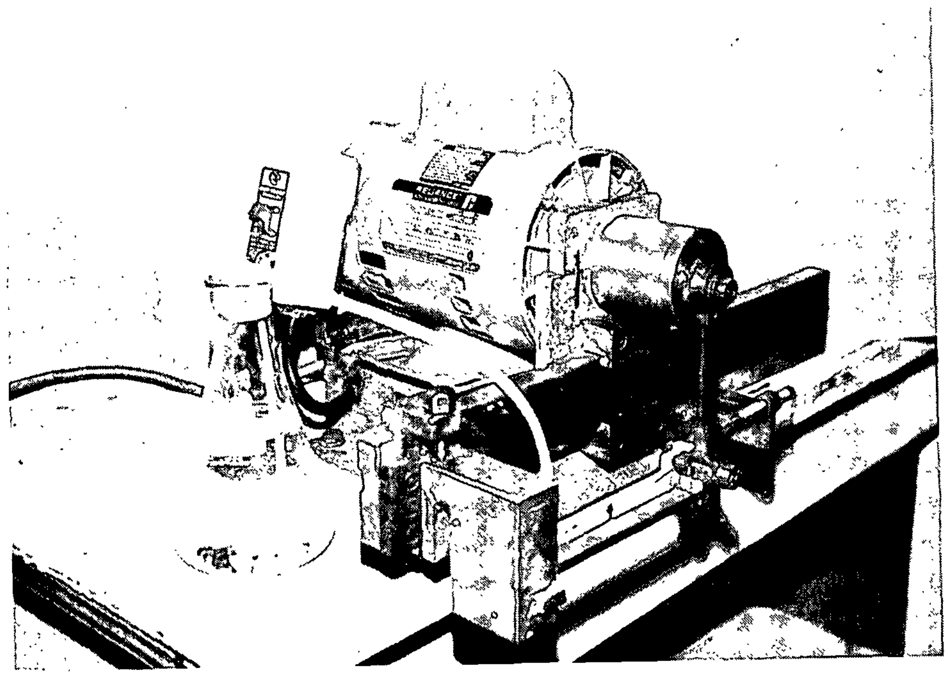

Tatnall Krause alternating bending fatigue machine fitted with a wick arrangement for delivery of corrosive solutions to a stress concentrating hole in the test plate.

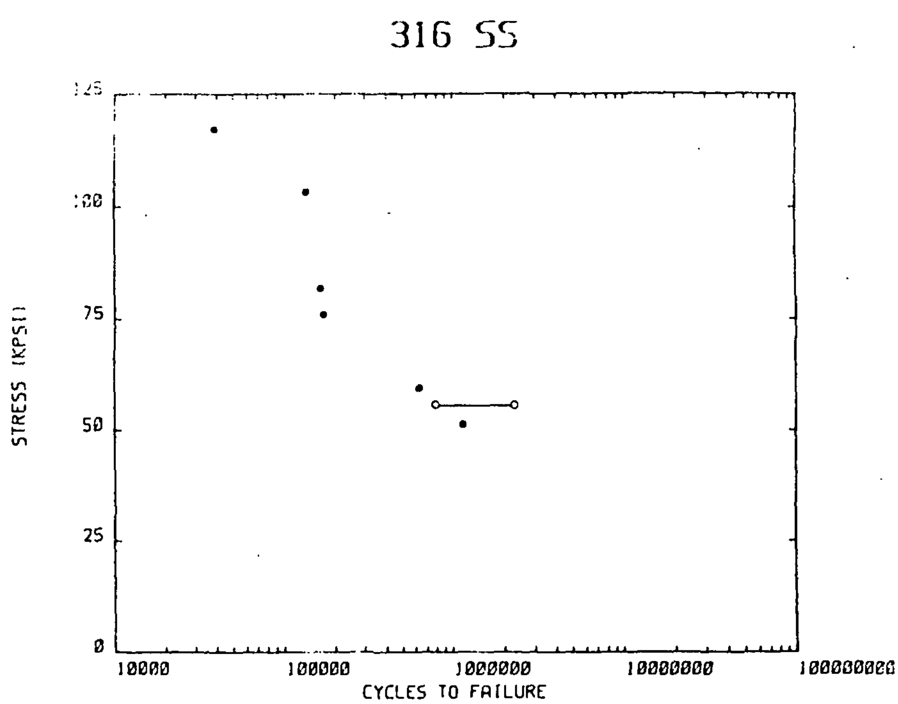

S-N curve for 316L stainless steel exposed to Environment #1 (1000 ppm chloride, pH 4.7), as generated with the Tatnall Krause alternating bending machine.

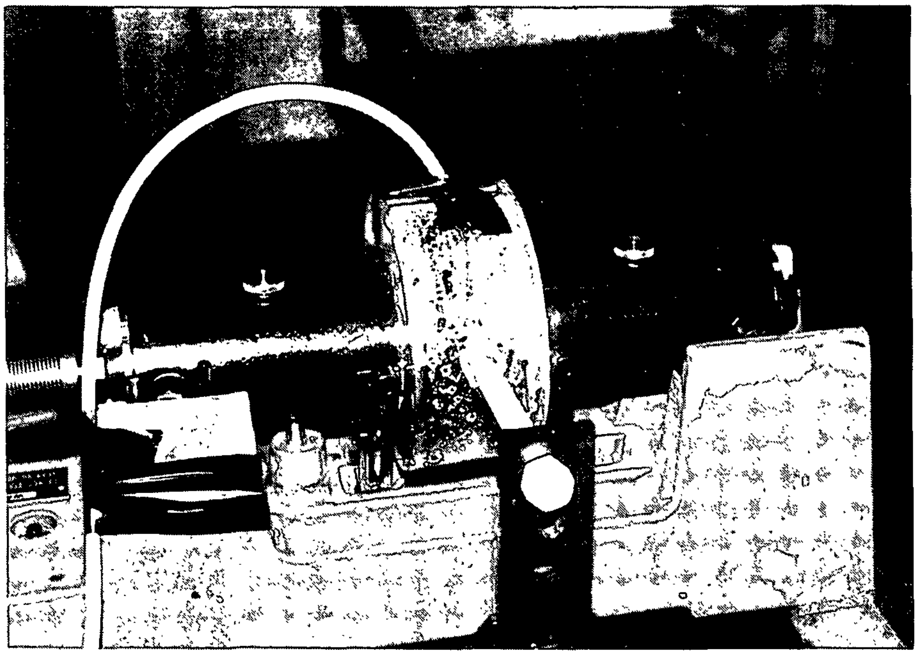

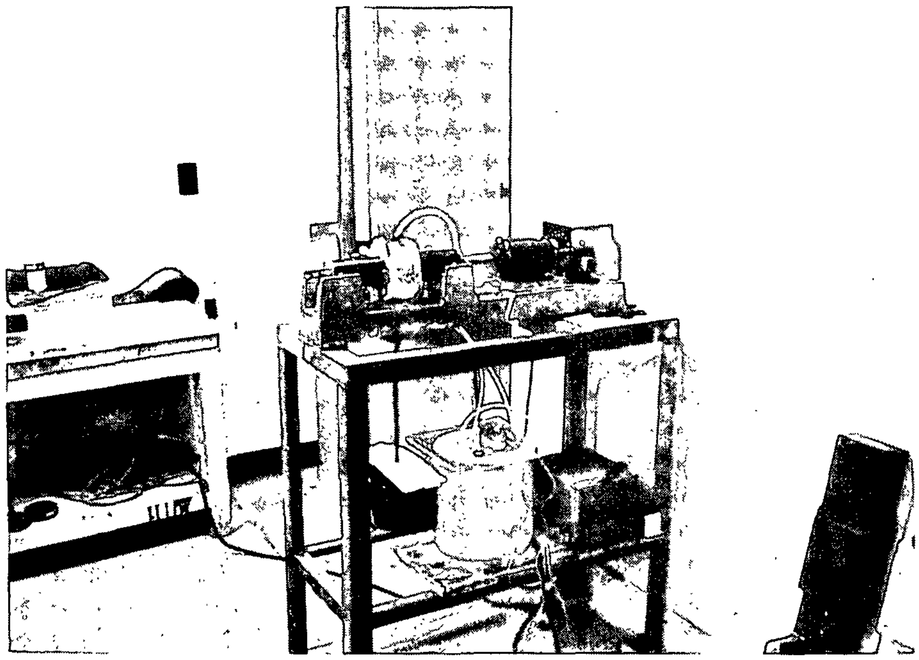

R. R. Moore rotating bending fatigue machine fitted with a recent version of a corrosion test chamber.

PREDICTIVE TEST DEVELOPMENT

INITIATION VS. PROPAGATION

STRESS INTENSITY CONCEPT

$$\text{DRIVING FORCE FOR GROWTH} = \begin{cases} \text{NOMINAL STRESS} \\ \text{CRACK LENGTH} \\ \text{GEOMETRY} \end{cases}$$

$$\Delta K = \text{(STRESS RANGE) (CRACK LENGTH)}^{\frac{1}{2}} \text{ (GEOMETRY)}$$

$$= S_R(a)^{\frac{1}{2}} \text{ fn } (a/w)$$

STRESS INTENSITY NORMALIZES

- LONG CRACK, LOW STRESS
- SHORT CRACK, HIGH STRESS
- LOADING GEOMETRY

MEAN STRESS EFFECTS

"R" RATIO = K_{max}/K_{min}

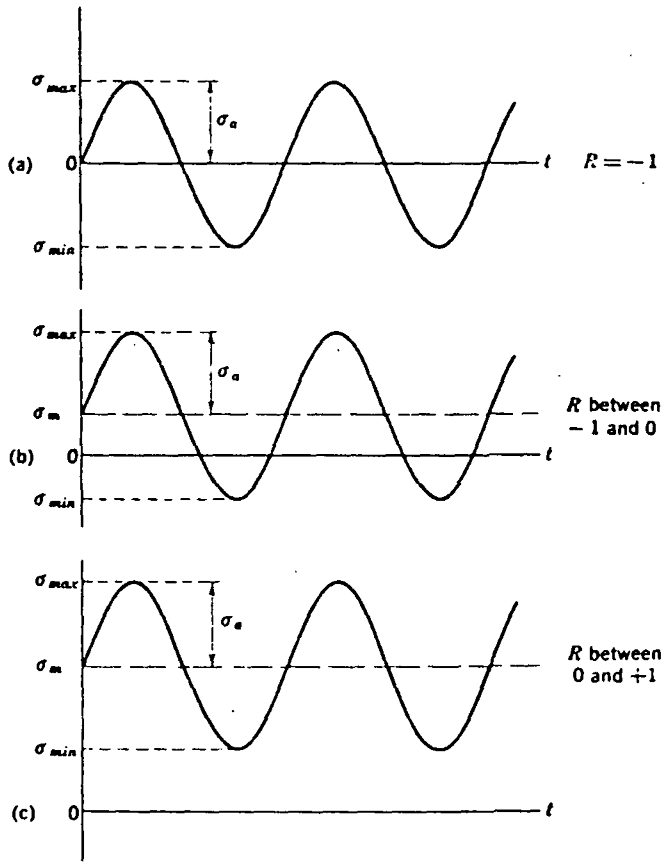

Schematic illustration of three alternating load forms as a function of time (t) in fatigue

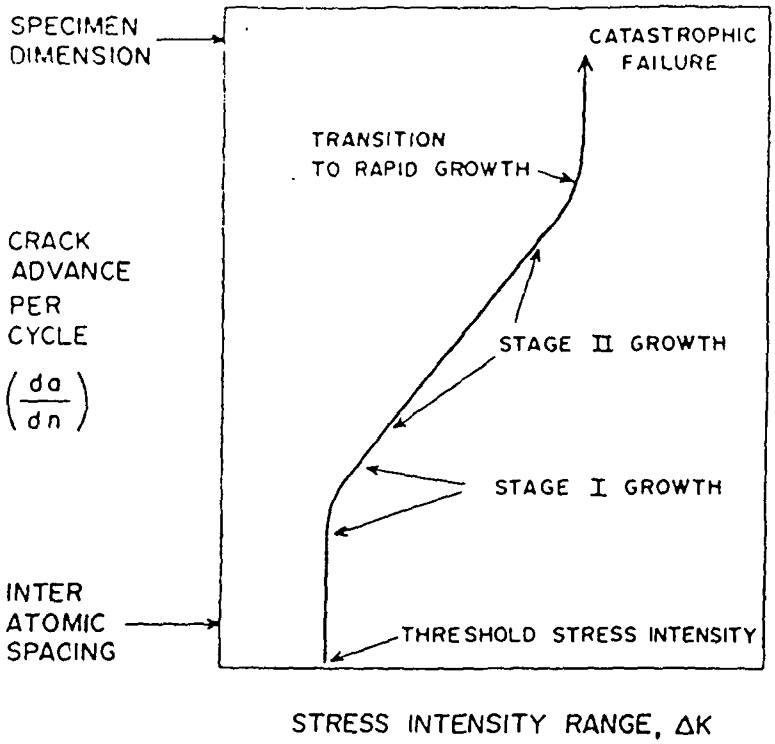

Schematic diagram showing the dependence of crack growth rates on the cyclic stress intensity.

ΔK_{th} DETERMINATION

- CRACK SHARPNESS
- LOAD SHEDDING
- COMPRESSIVE RESIDUAL STRESSES

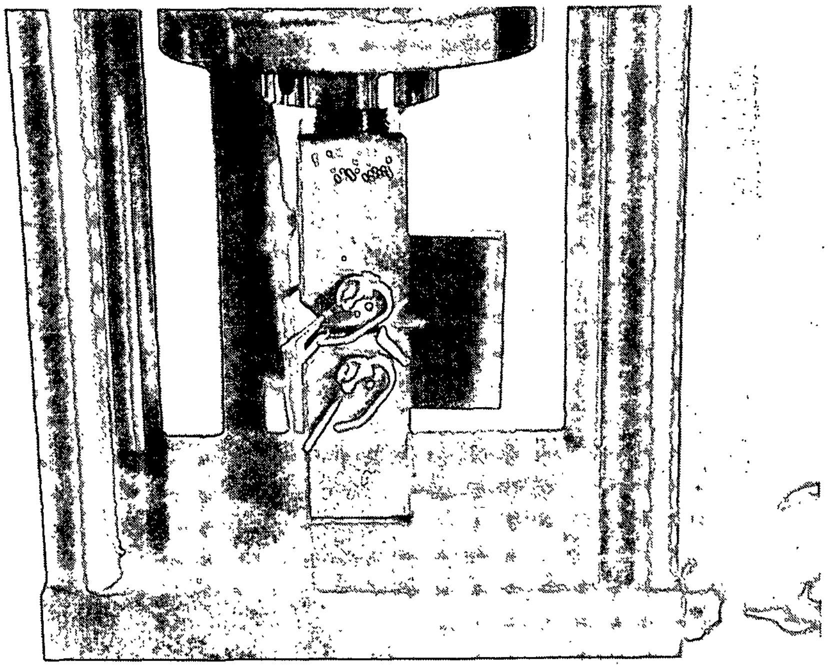

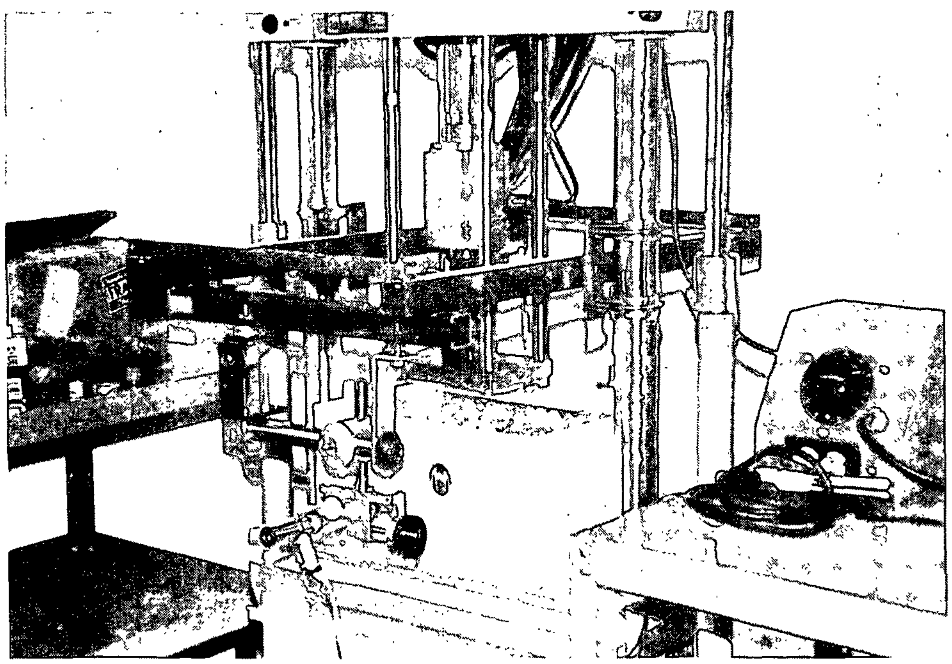

The MTS electrohydraulic testing machine equipped with modified test frame and environmental chamber for fatigue testing in simulated paper machine white waters.

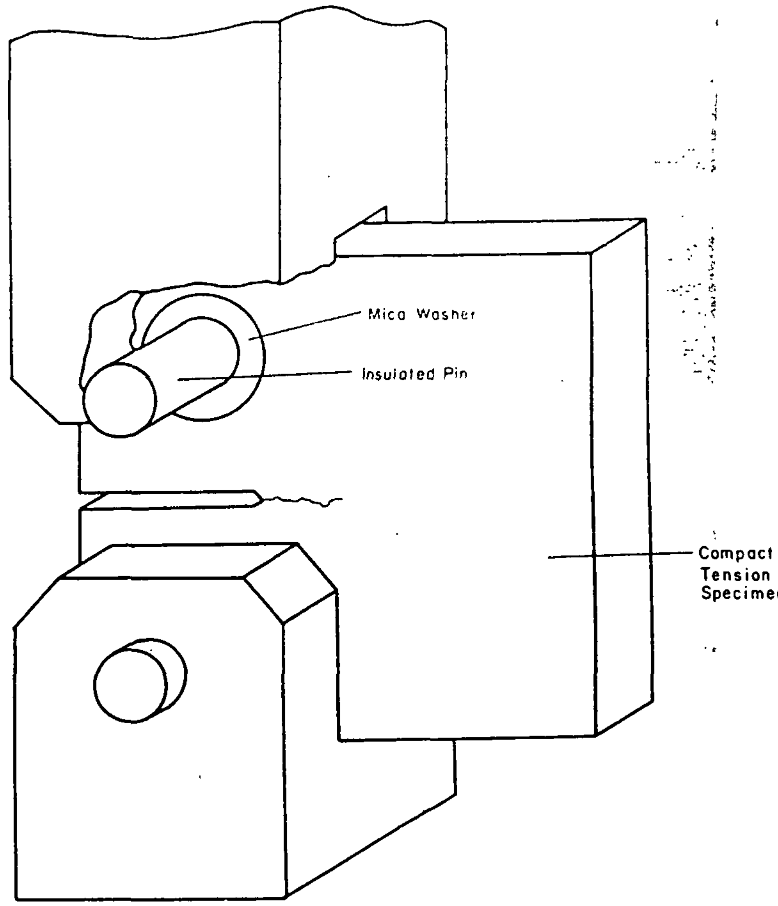

Cut-away view of the gripping arrangements used in near-threshold fatigue testing.

TEST ENVIRONMENTS

ENVIRONMENT	CHLORIDE, ppm	SULFATE, ppm	THIOSULFATE, ppm	pH
A	1000	0	0	4.7
B	100	1000	0	3.6
C	1000	1000	0	3.5
D	200	500	50	4.1

REPRODUCIBILITY

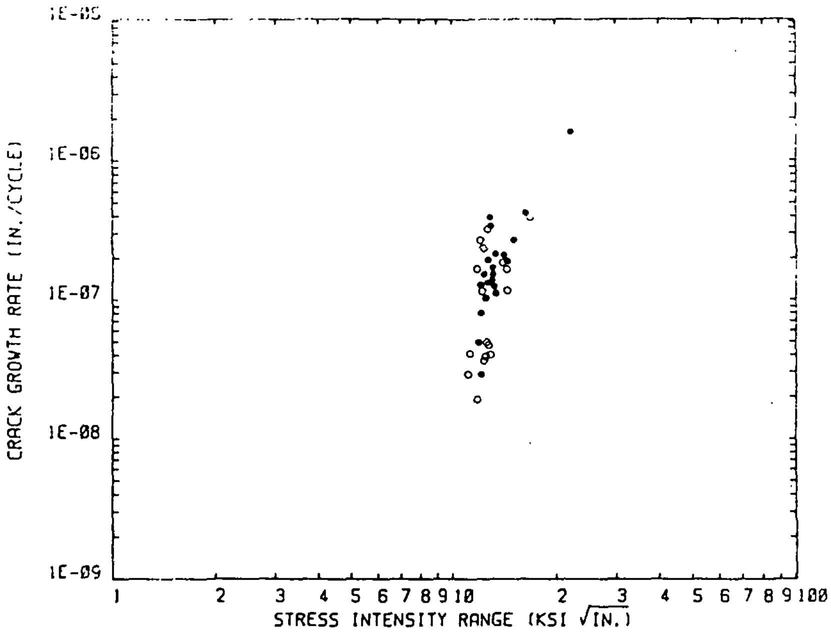

A comparison of fatigue crack growth rates measured in two separate tests on Alloy 63 in Environment A.

ENVIRONMENTAL EFFECT

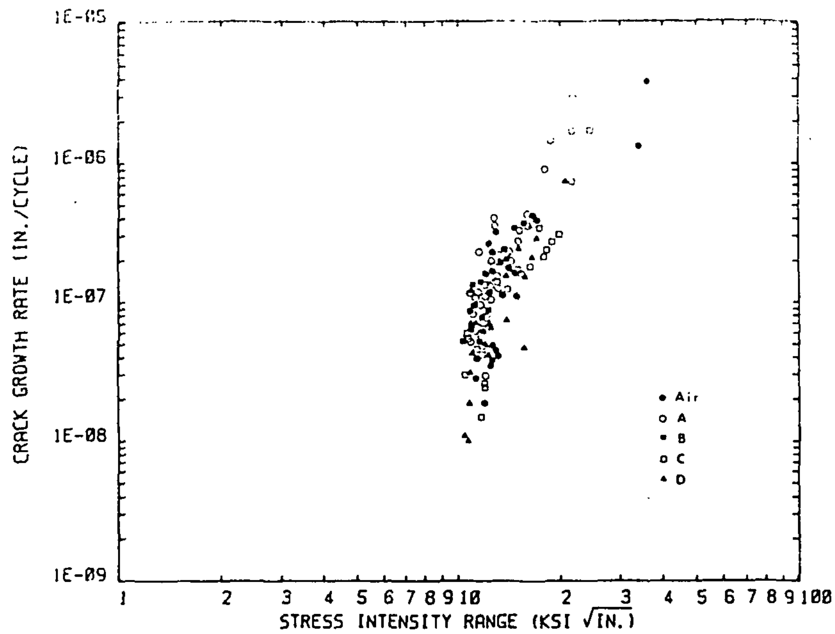

Comparison of the effects of test environment on fatigue crack growth in Alloy 63. R = 0.1, T = 50°C.

ALLOY 63 VS. ALLOY 75

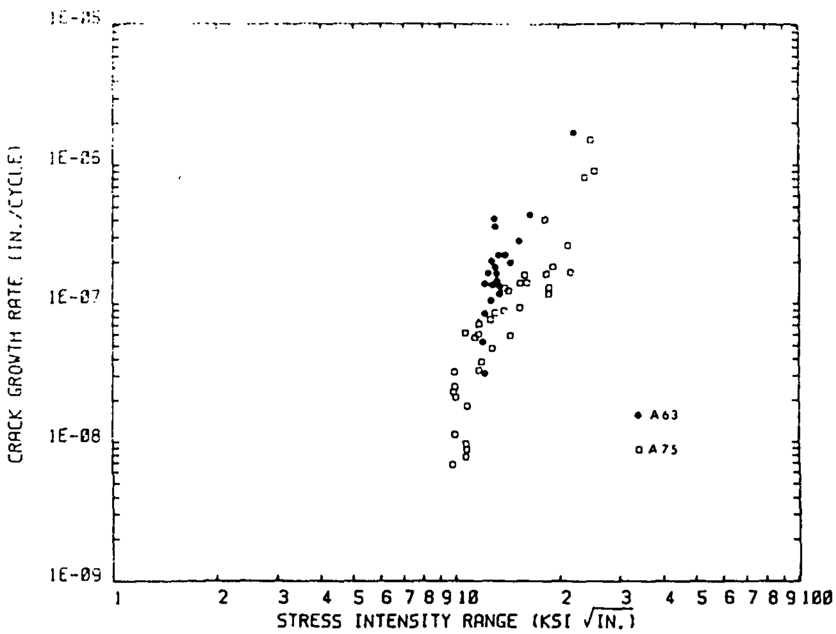

A comparison of the fatigue crack growth characteristics exhibited by Alloys 75 and 63 in a simulated white water containing 1000 ppm chloride.

MEAN STRESS EFFECTS (RESIDUAL STRESS)

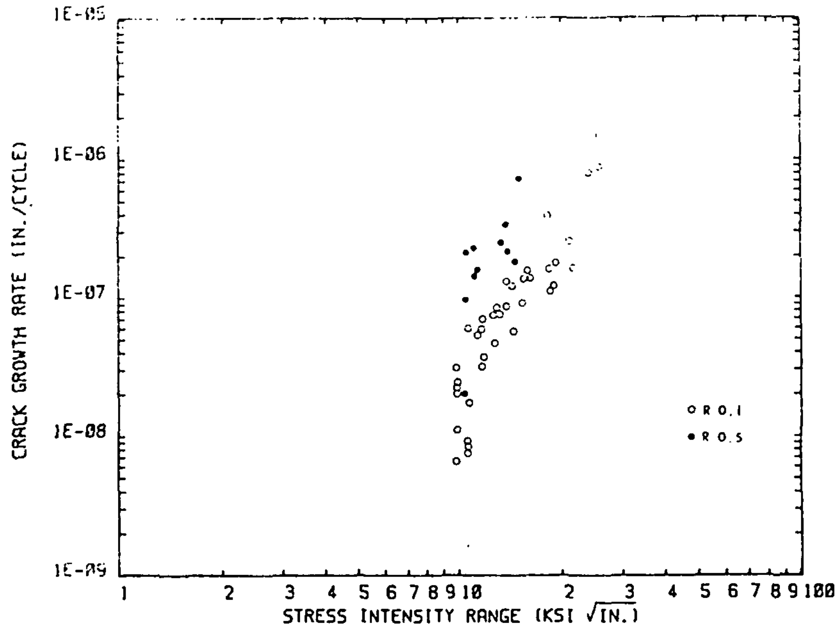

Crack growth rate data for Alloy 75 in a simulated paper machine white water showing the effects of mean stress on growth rate.

FRACTOGRAPHY

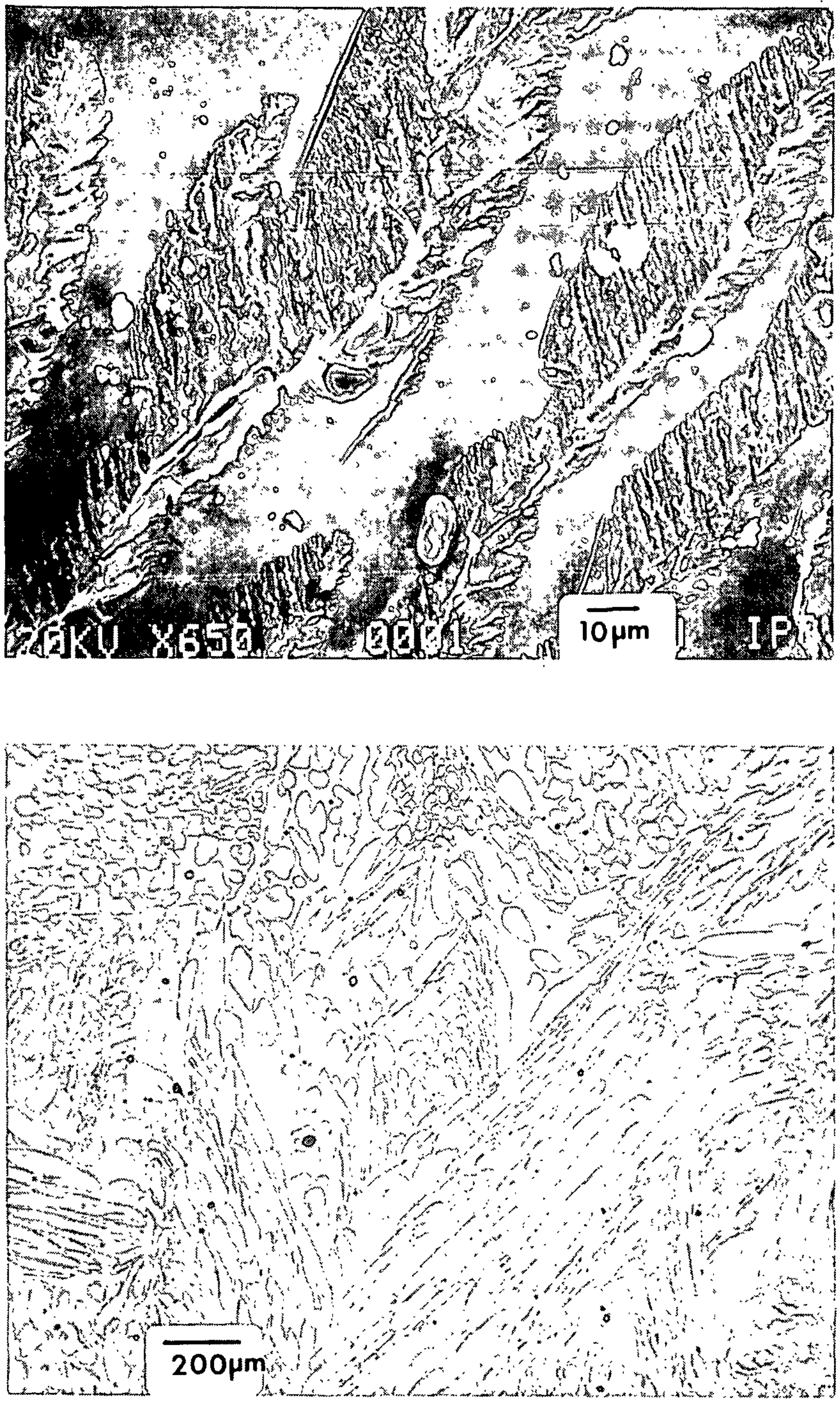

A typical scanning electron fractograph showing features on the fracture surface of an Alloy 63 specimen used in the fatigue crack growth studies.

CONCLUSIONS — NEAR THRESHOLD CRACKING

- MEAN STRESS EFFECT IN STAGE I ONLY
- NO STRONG ENVIRONMENT EFFECT
- NO APPARENT CORRELATION WITH SERVICE

SLOW STRAIN RATE TESTING

MATERIALS ACQUISITION

ALLOY 75

VKA 378

AVESTA 3RE60

VKA 171

ALLOY 63

FUTURE WORK

- NEAR THRESHOLD, STRONGER ENVIRONMENT
- NEAR THRESHOLD, LOWER FREQUENCY
- S-N TESTING
- SLOW STRAIN RATE TESTS
- PITTING, CREVICE CORROSION TESTING
- METALLOGRAPHY

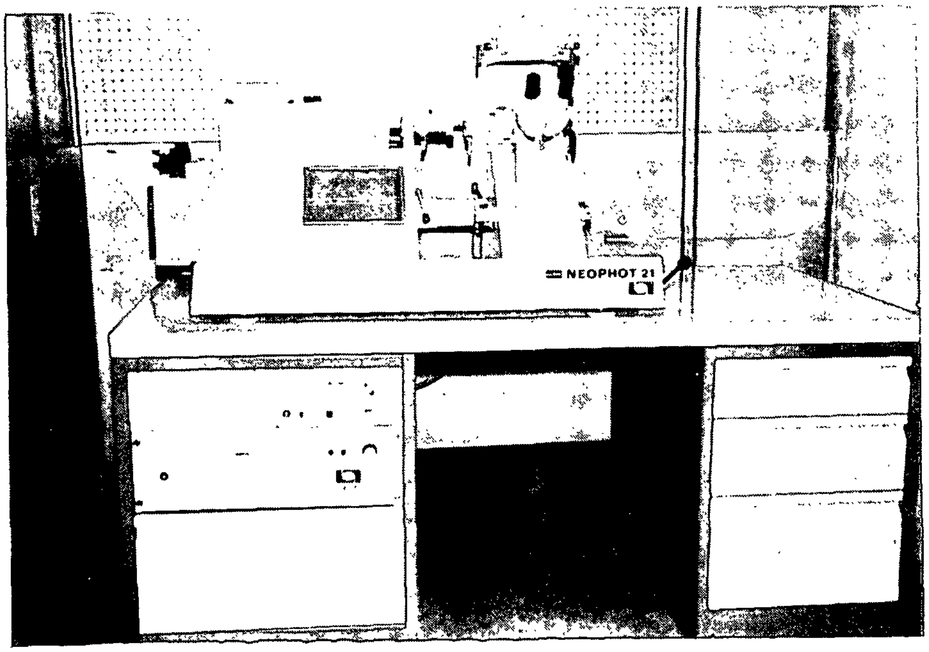

METALURGICAL MICROSCOPE RECENTLY INSTALLED
IN THE CORROSION RESEARCH BUILDING.

SIGNIFICANCE TO THE INDUSTRY

- EMBRYONIC STAGE, BUT...
- BRIGHT PROSPECTS FOR REDUCING SUCTION ROLL COSTS

Project 3384

REFINING OF CHEMICAL PULPS FOR IMPROVED PROPERTIES

Clyde Sprague

PROJECT 3384 - REFINING OF CHEMICAL PULPS
FOR IMPROVED PROPERTIES

OBJECTIVES

- ON-LINE MEASURE OF REFINING INTENSITY
- MODEL BETWEEN INTENSITY AND PROPERTIES
- ON-LINE CONTROL OF PROPERTY DEVELOPMENT

CONTROL OF REFINING SEVERITY

SPECIFIC EDGE LOAD $SEL = \frac{P}{\Omega Z^2 L}$

ACTIVE BAR CROSSING AREA

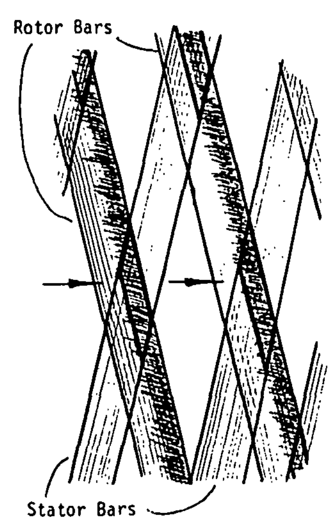

Normal stress $\overline{P}_N = \dfrac{T}{Z^2 L\overline{\ell}} = \dfrac{P}{\pi\mu\Omega Z^2 L\overline{\ell}(D - \frac{1}{2}L\cos\theta)}$

Shear stress $\overline{\tau}_f = \mu_f \overline{P}_N = \dfrac{\mu_f T}{Z^2 L\overline{\ell}} = \dfrac{(\mu_f/\mu)P}{\pi\Omega Z^2 L\overline{\ell}(D - \frac{1}{2}L\cos\theta)}$

Tensile stress $\overline{\sigma}_f = \dfrac{\mu_f \overline{P}_N \ell_f}{t_f} = \dfrac{\mu_f T \ell_f}{Z^2 L\overline{\ell} t_f} = \dfrac{(\mu_f/\mu)P\ell_f}{\pi\Omega Z^2 L\overline{\ell}(D - \frac{1}{2}L\cos\theta)t_f}$

EXPERIMENTAL APPROACHES

- IN-REFINER MEASUREMENT OF P_N
- VERIFICATION OF $\overline{\tau}_f$ AND $\overline{\sigma}_f$ EXPRESSIONS

MODEL EQUATIONS FOR
VALLEY BEATER

$$\overline{P}_N = \frac{\Lambda}{189\mu\overline{\ell}}$$

$$\overline{\tau}_f = \frac{(\mu_f/\mu)\Lambda}{189\overline{\ell}}$$

$$\overline{\sigma}_f = \frac{(\mu_f/\mu)\Lambda\ell_f}{189\overline{\ell}t}$$

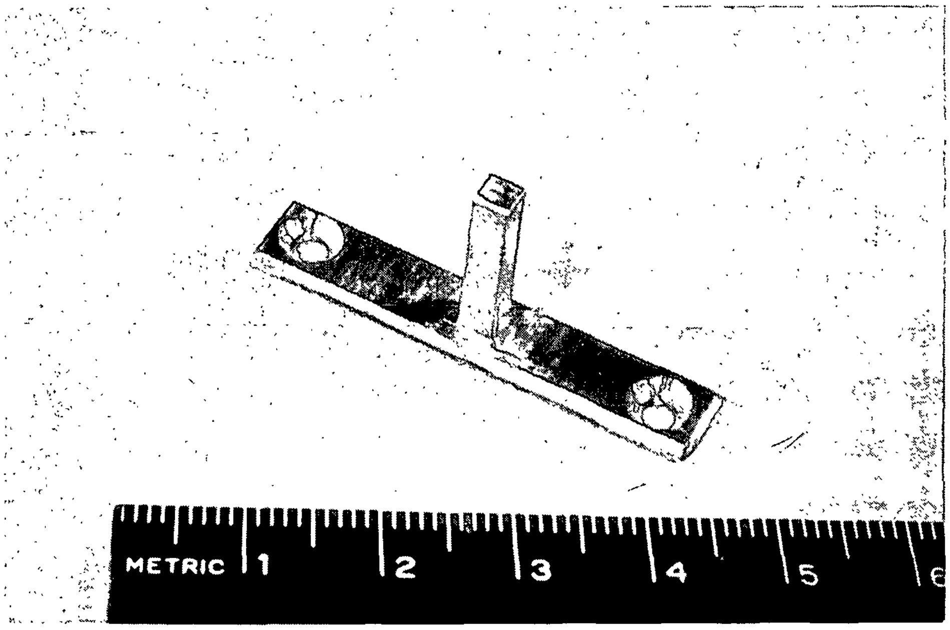

Bar segment and beam prior to strain gage attachment.

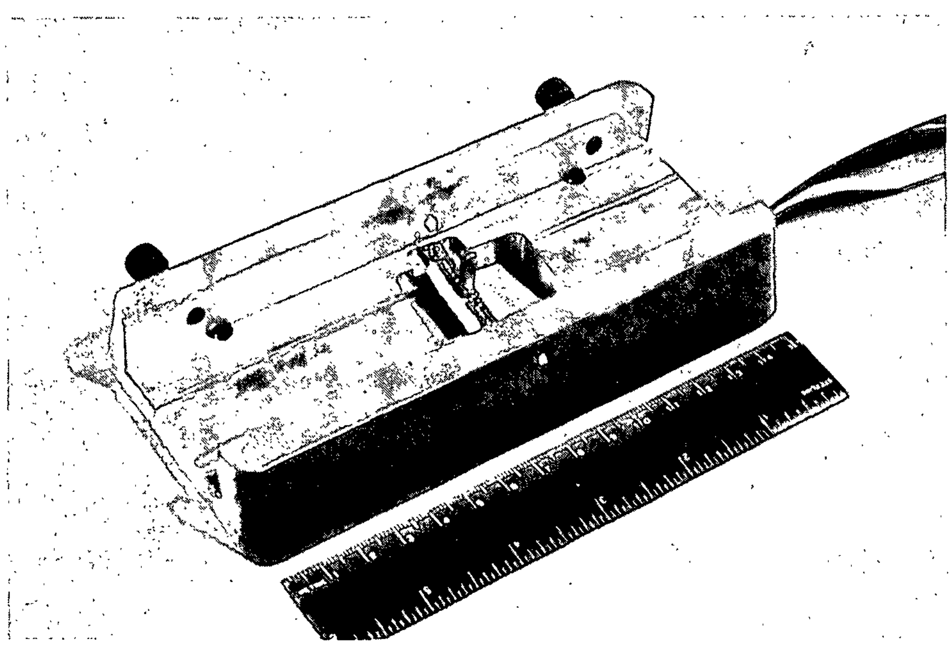

Strain gages attached to beam, bar segment installed in bedplate holder.

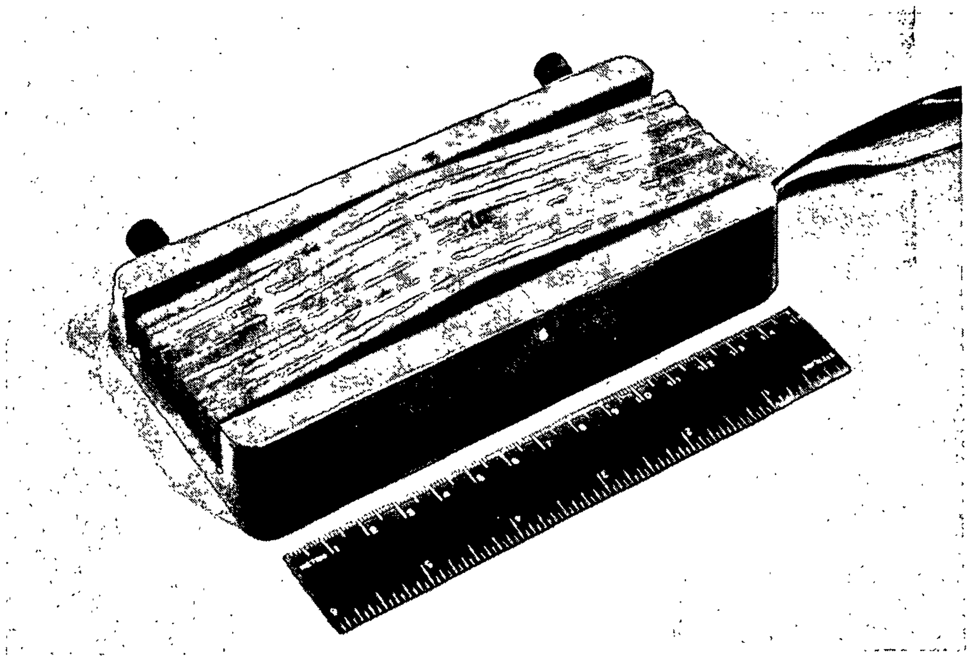

Beater bar assembly in place around instrumented bar segment, prior to potting.

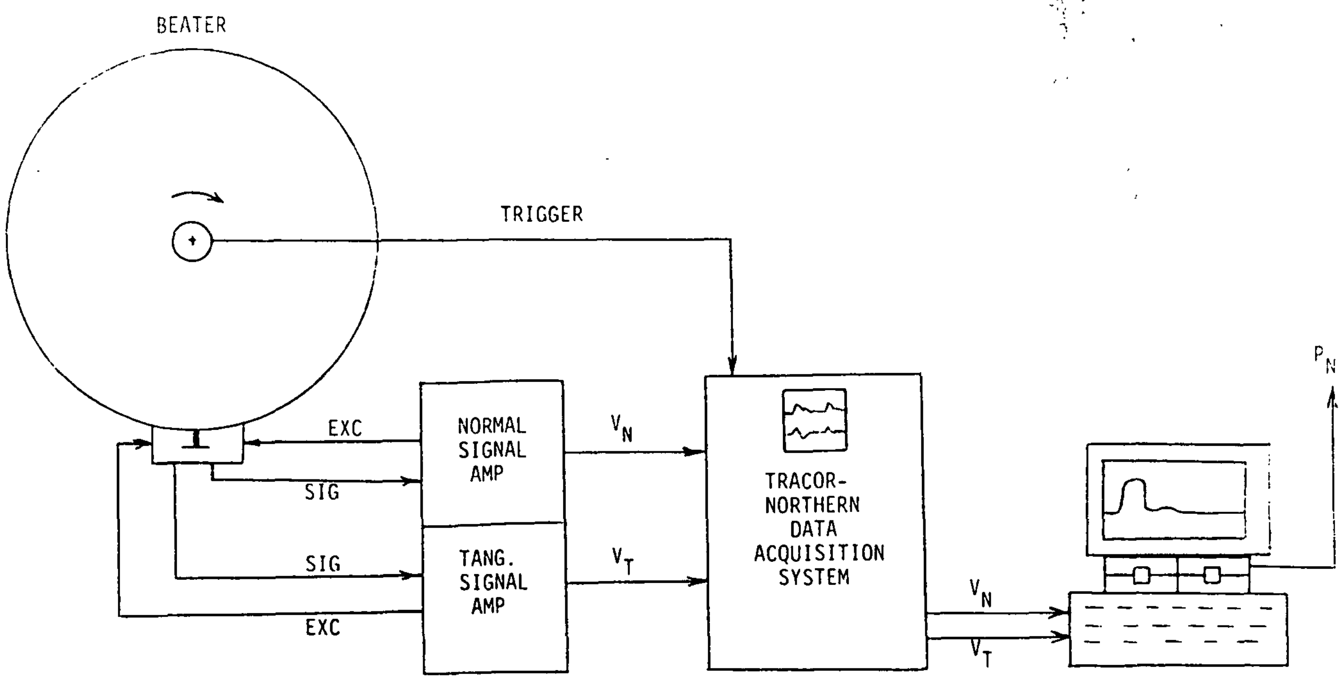

NORMAL PRESSURE MEASURING SYSTEM

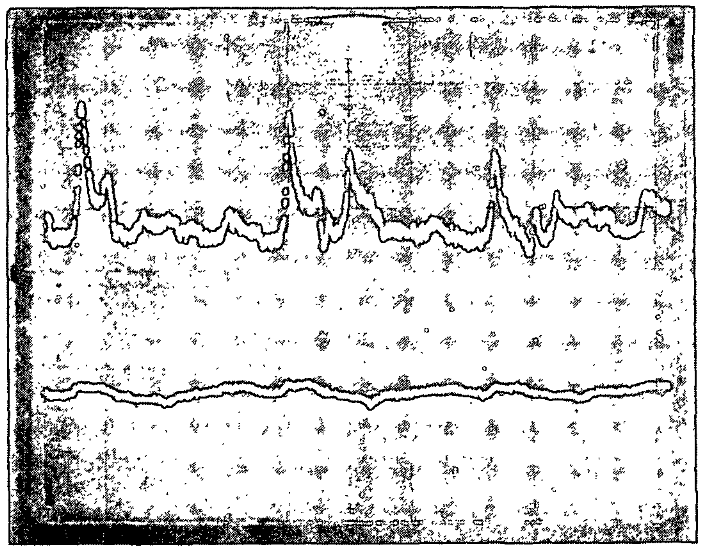

Oscilloscope trace of normal (top) and tangential (bottom) voltage outputs.

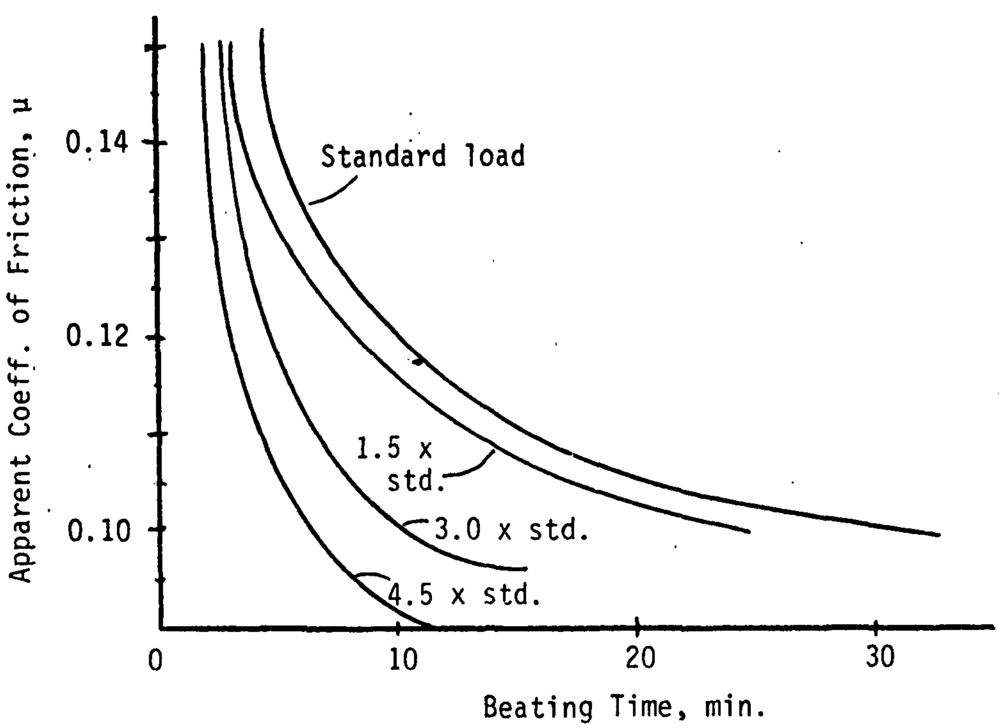

Apparent coefficient of friction as a function of beating time for several load levels.

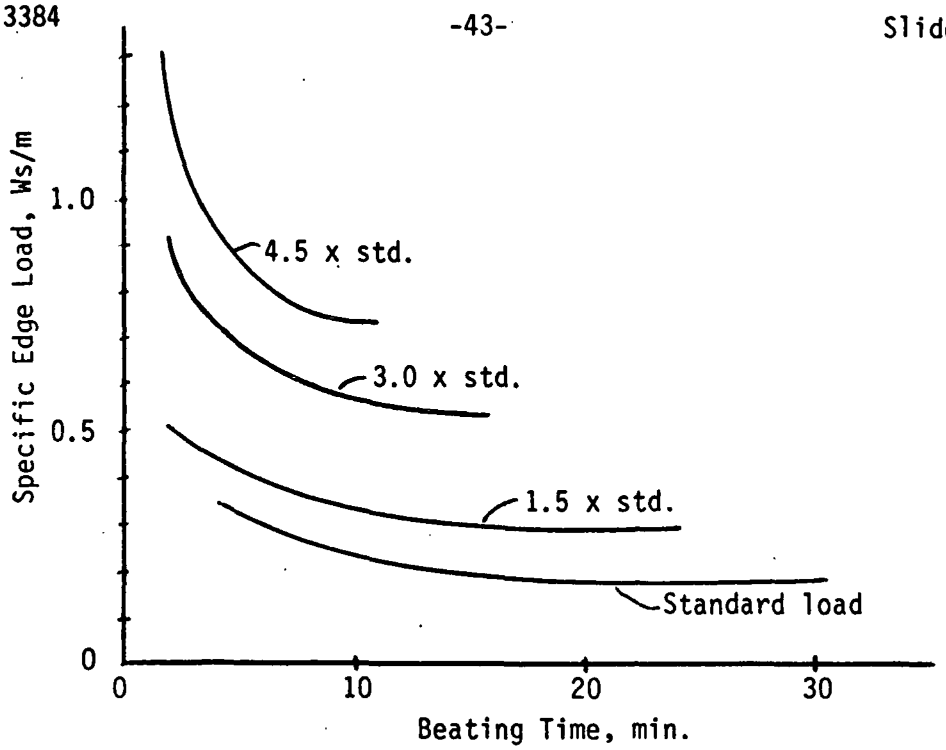

Specific edge load as a function of beating time for several levels of load.

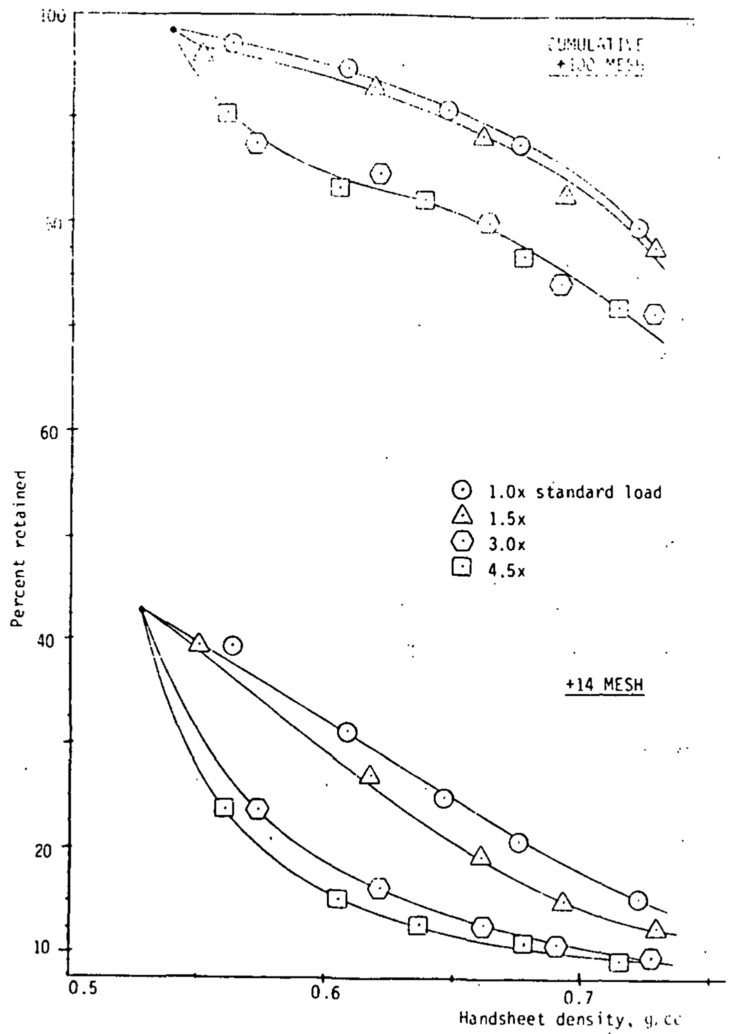

Fiber classification vs. density.

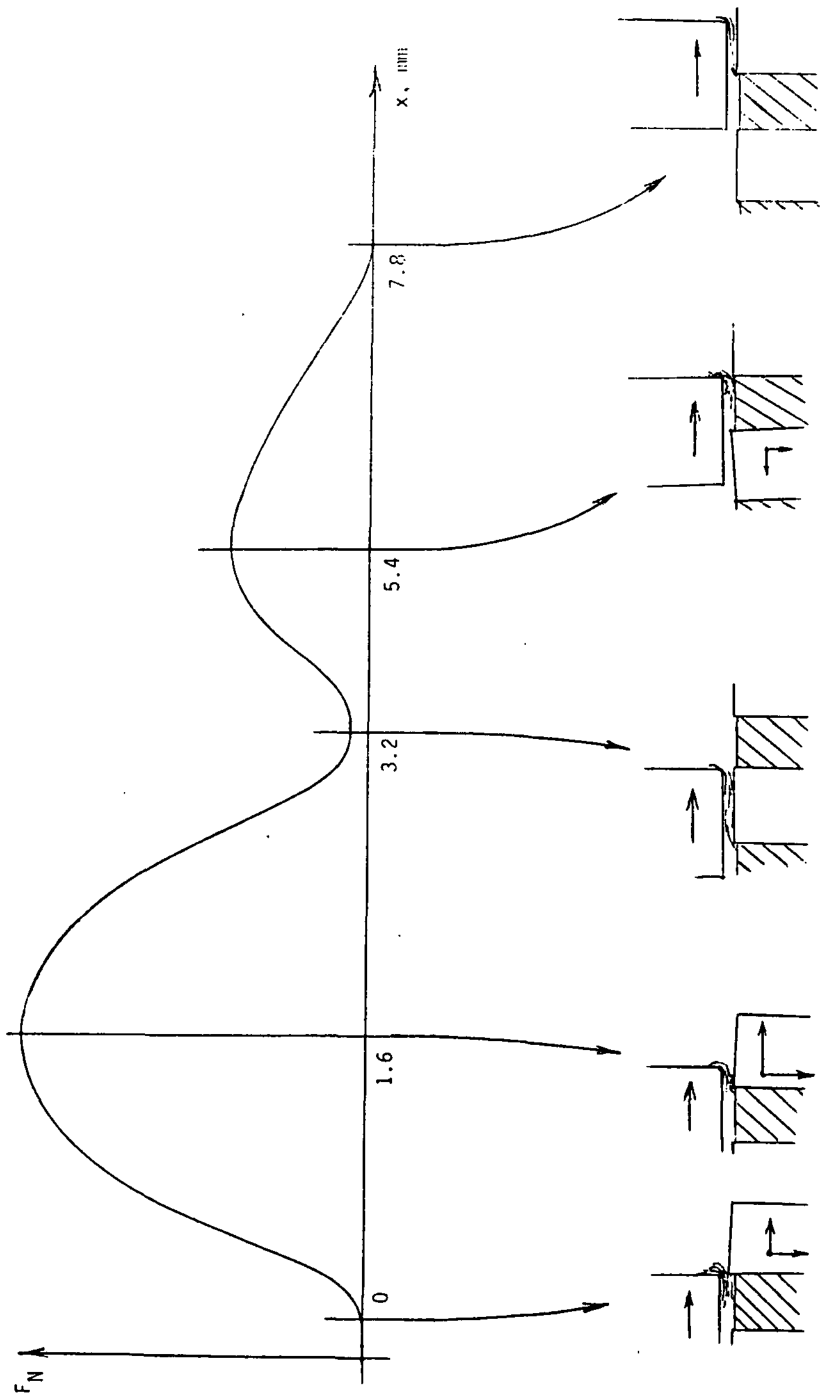

BAR POSITION VS. MEASURED NORMAL FORCE

FREQUENCY HISTOGRAM

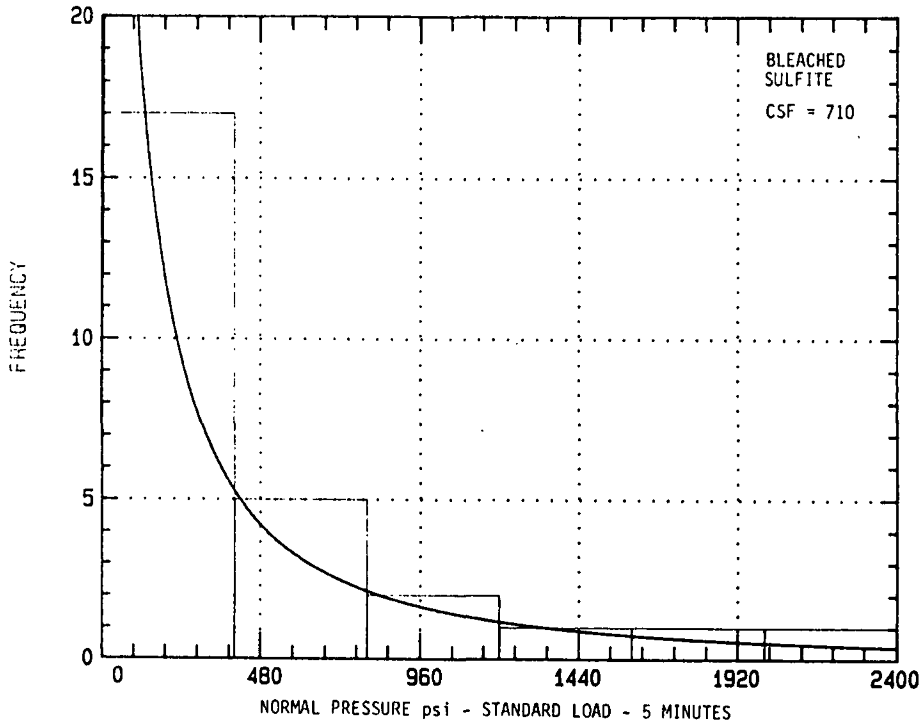

FREQUENCY HISTOGRAM

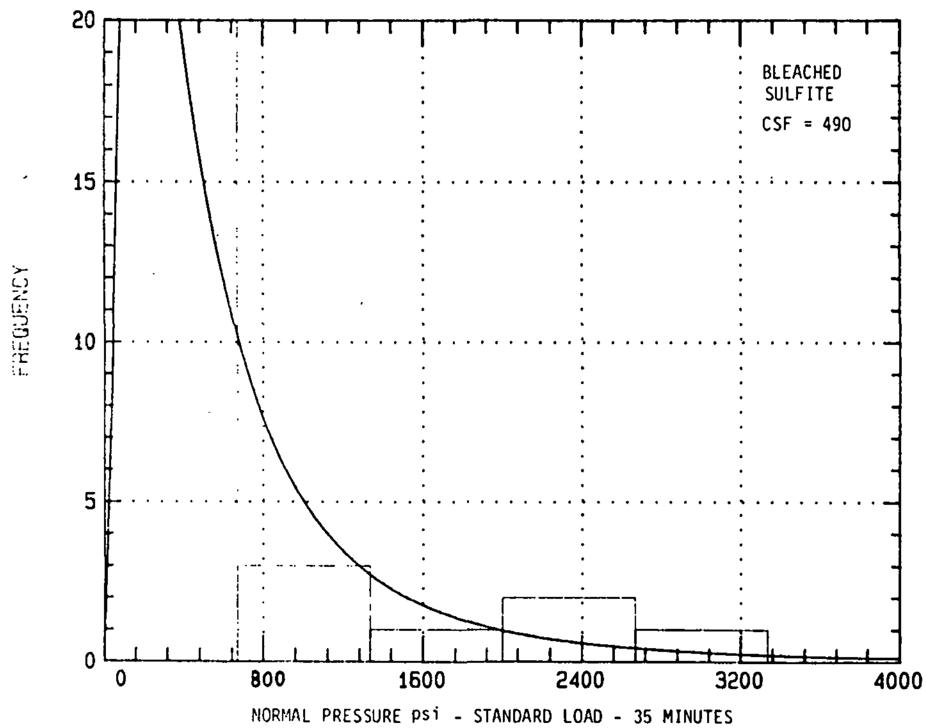

Valley Beater normal pressure histogram and log-normal fitted frequency distribution for a bleached sulfite softwood pulp.

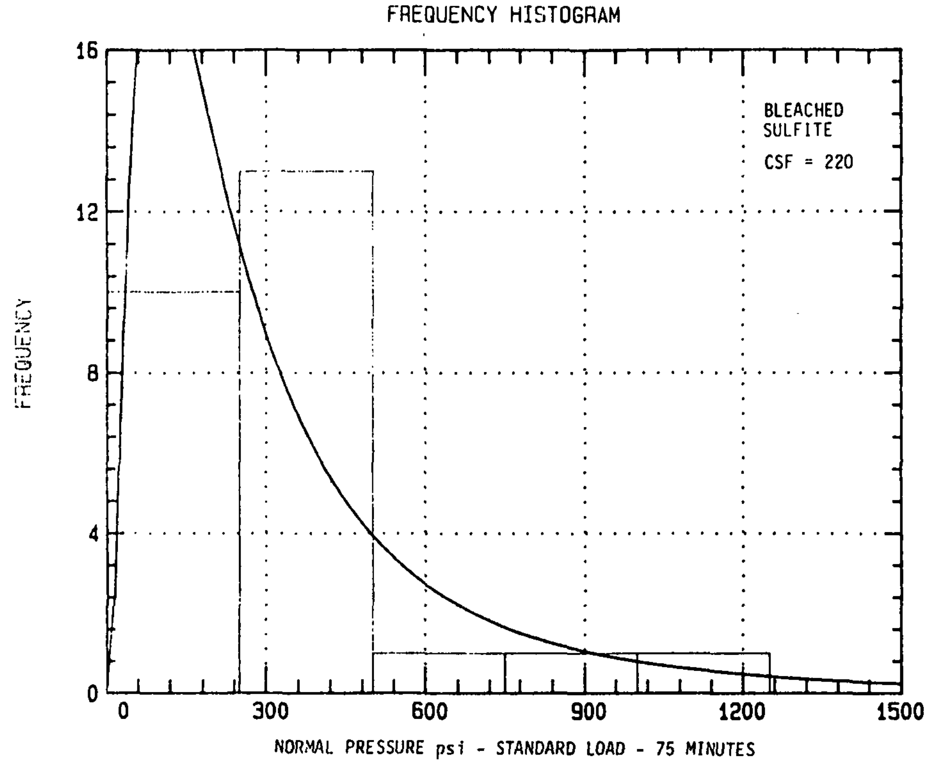

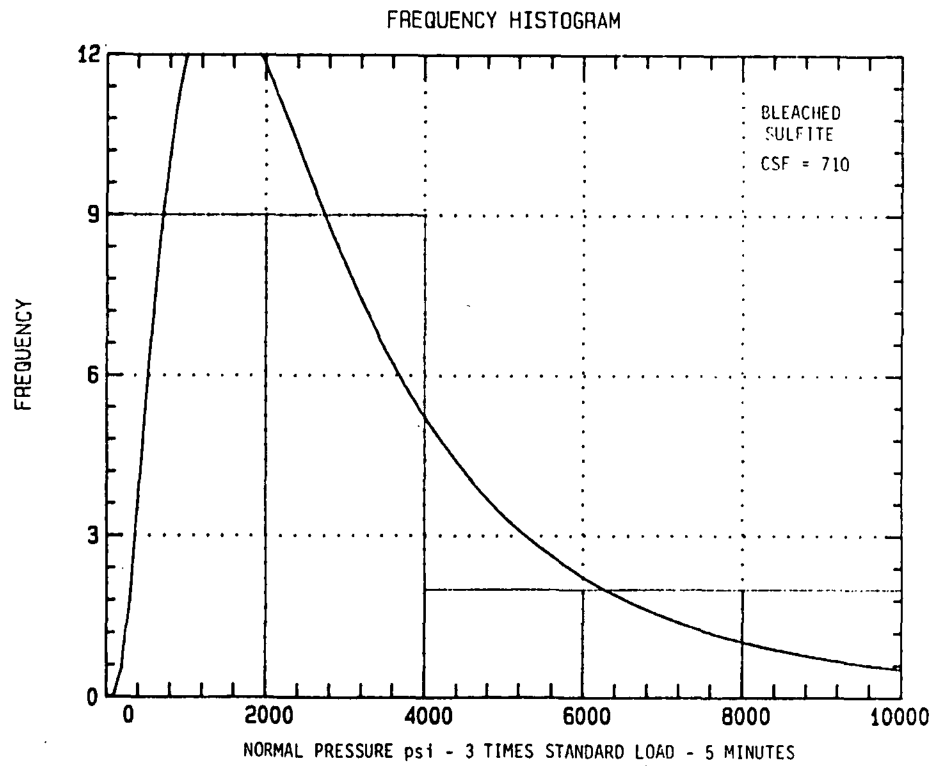

Valley Beater normal pressure histogram and log-normal fitted frequency distribution for a bleached sulfite softwood pulp.

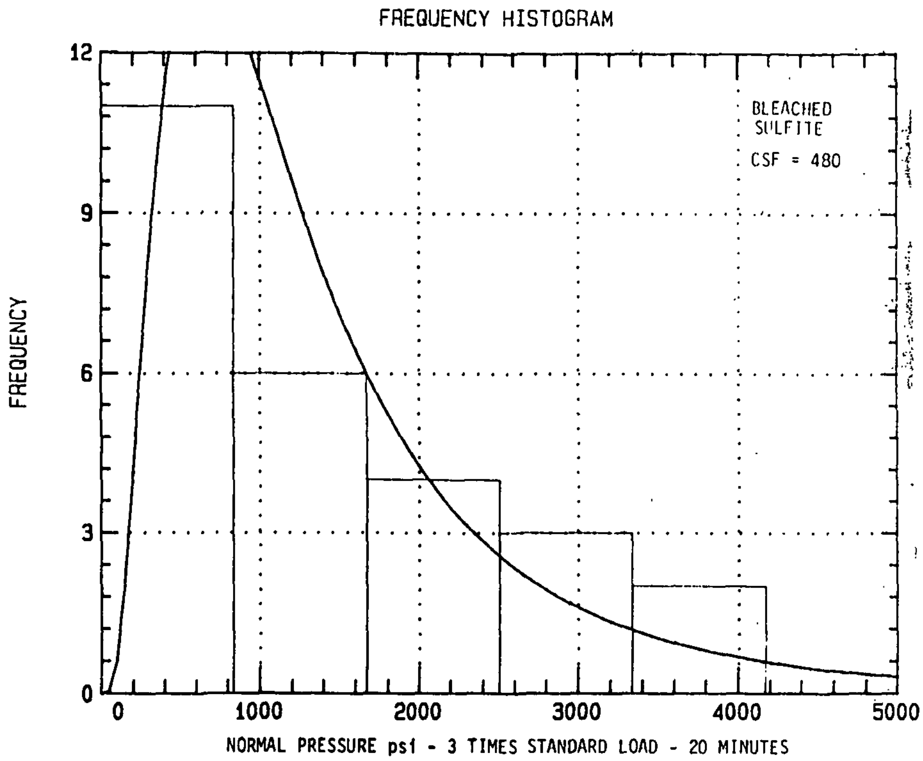

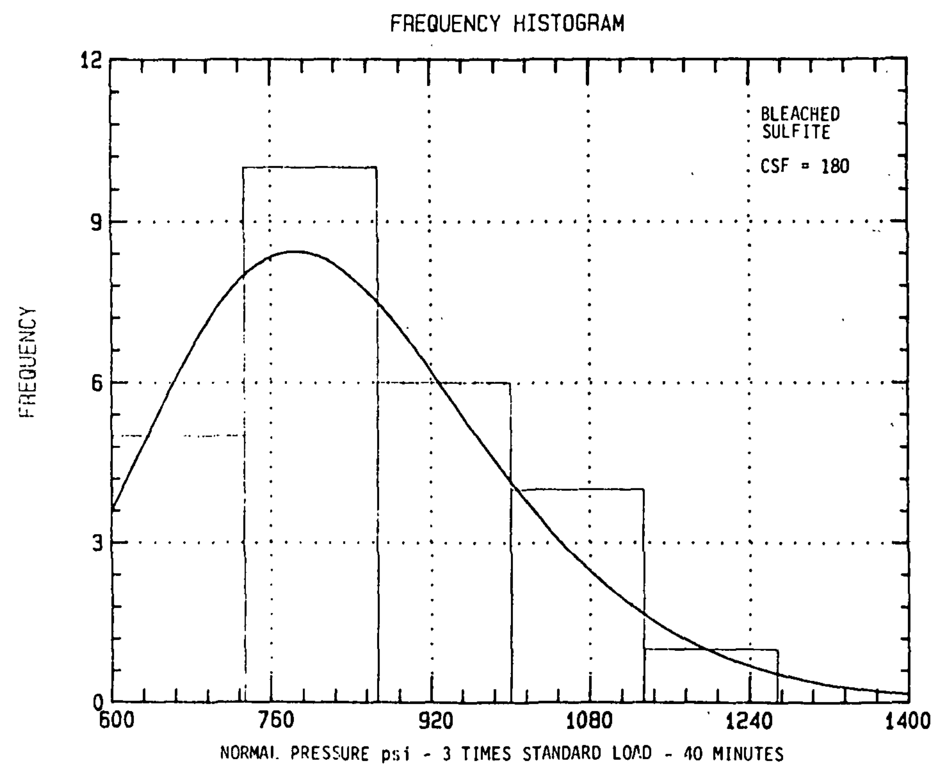

Valley Beater normal pressure histogram and log-normal fitted frequency distribution for a bleached sulfite softwood pulp.

VALLEY BEATER DATA - BLEACHED SULFITE PULP

LOAD	BEATING TIME	CSF	AVE. FIBER LENGTH	SEL WS/M
1X	5	710	2.19	0.263
	20	595	2.04	0.229
	40	450	1.90	0.229
3X	5	710	2.16	0.604
	10	630	1.82	0.553
	20	480	1.68	0.536

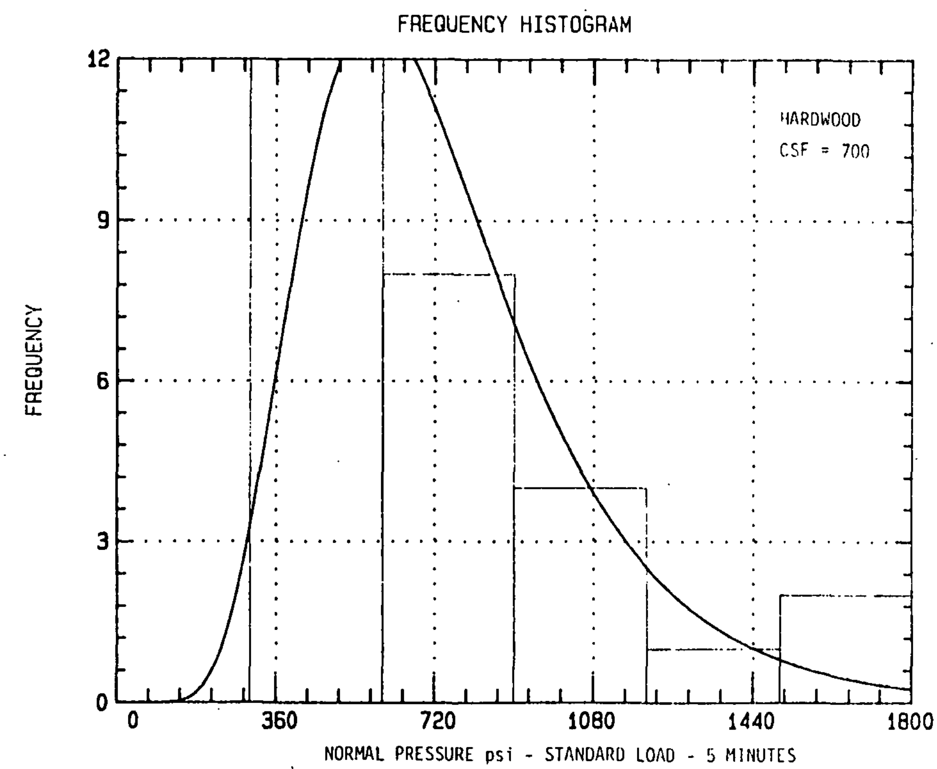

Valley Beater normal pressure histogram and log-normal fitted frequency distribution for hardwood pulp.

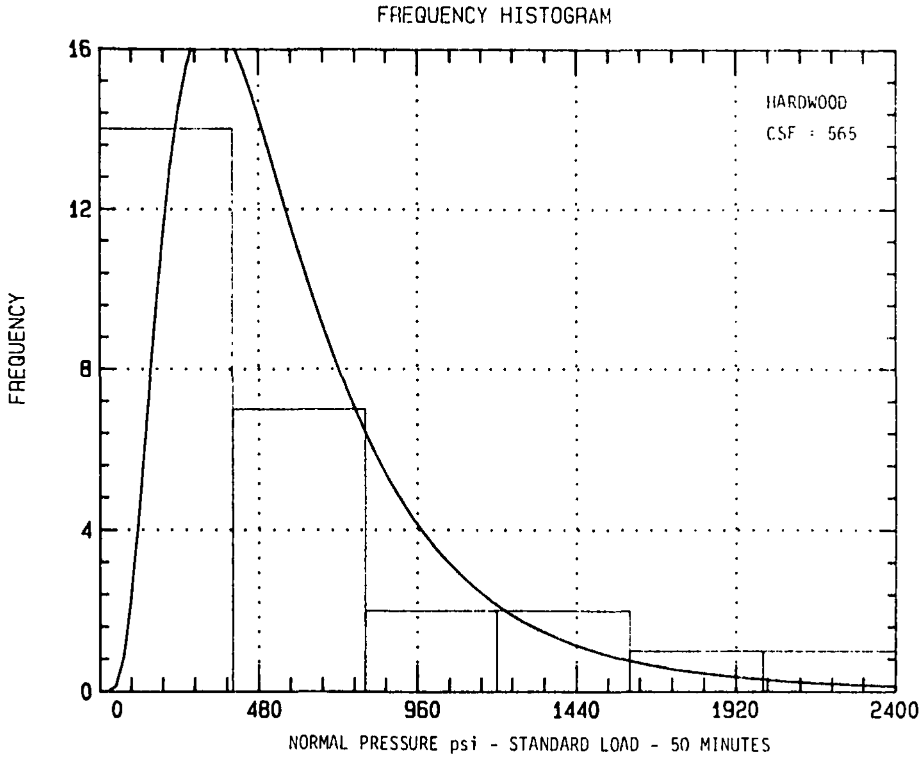

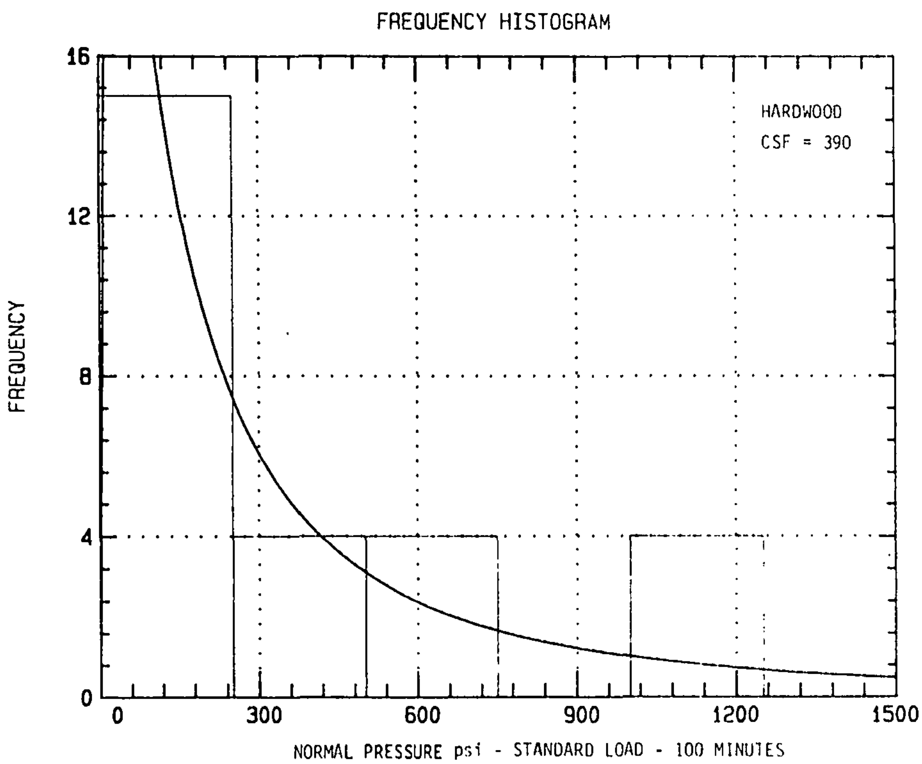

Valley Beater normal pressure histogram and log-normal fitted frequency distribution for hardwood pulp.

Project 3480/3584

PROCESS FUNDAMENTALS OF WET PRESSING

Clyde Sprague

PROJECT 3480/3584

WET PRESSING FUNDAMENTALS

OBJECTIVES: DETERMINE FEASIBILITY AND PERFORMANCE OF DISPLACEMENT PRESSING

DEVELOP A PREDICTIVE MODEL FOR WET PRESSING

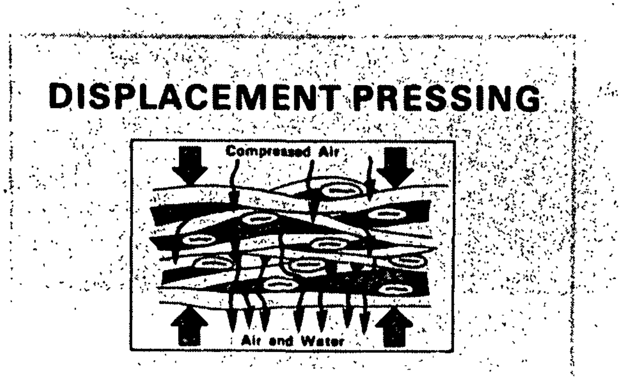

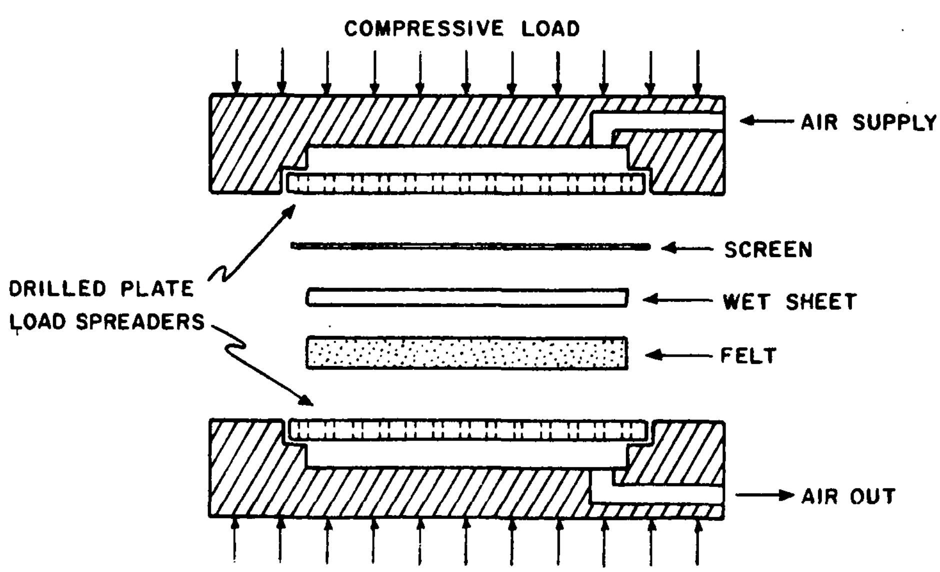

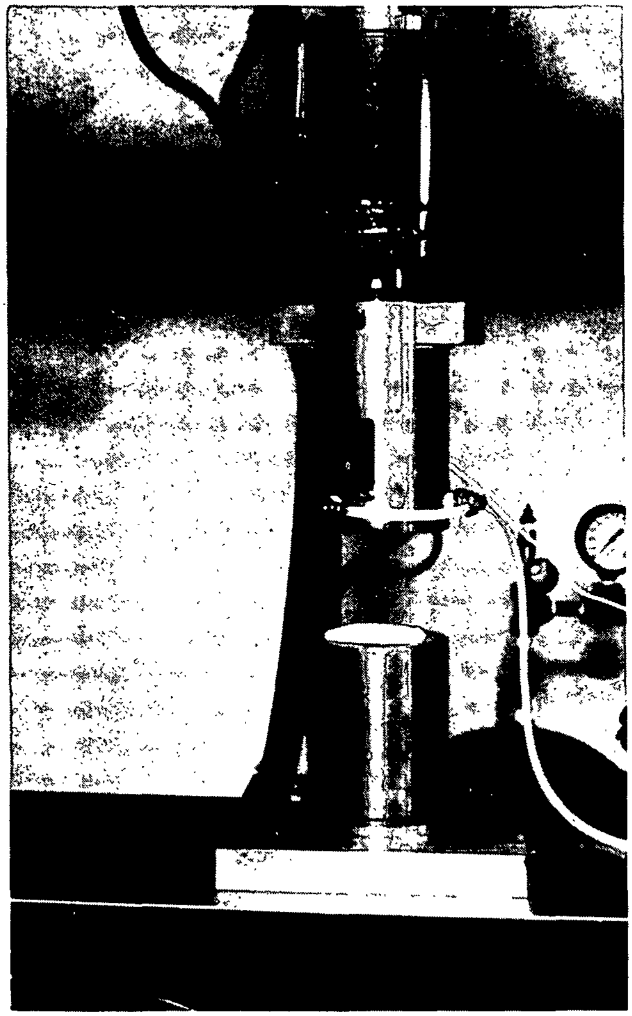

Electrohydraulic displacement pressing system.

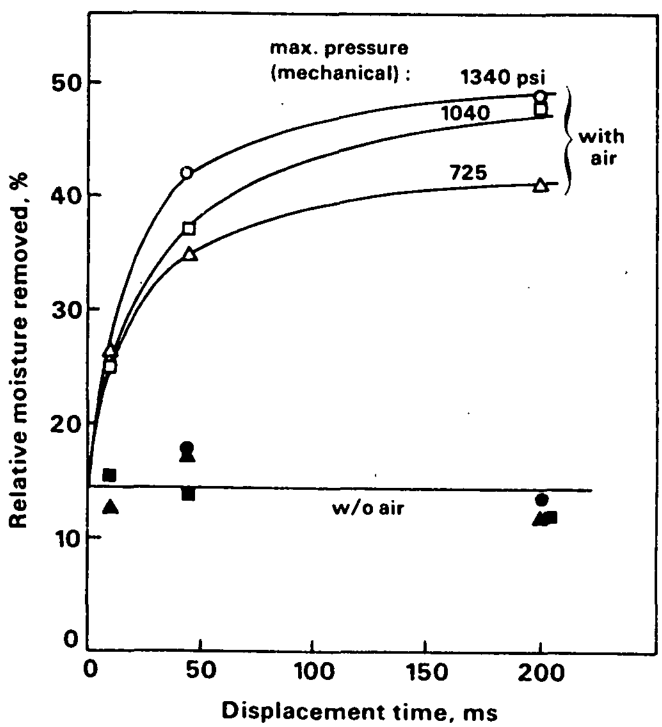

Results of displacement pressing of 63 g/m^2 handsheets

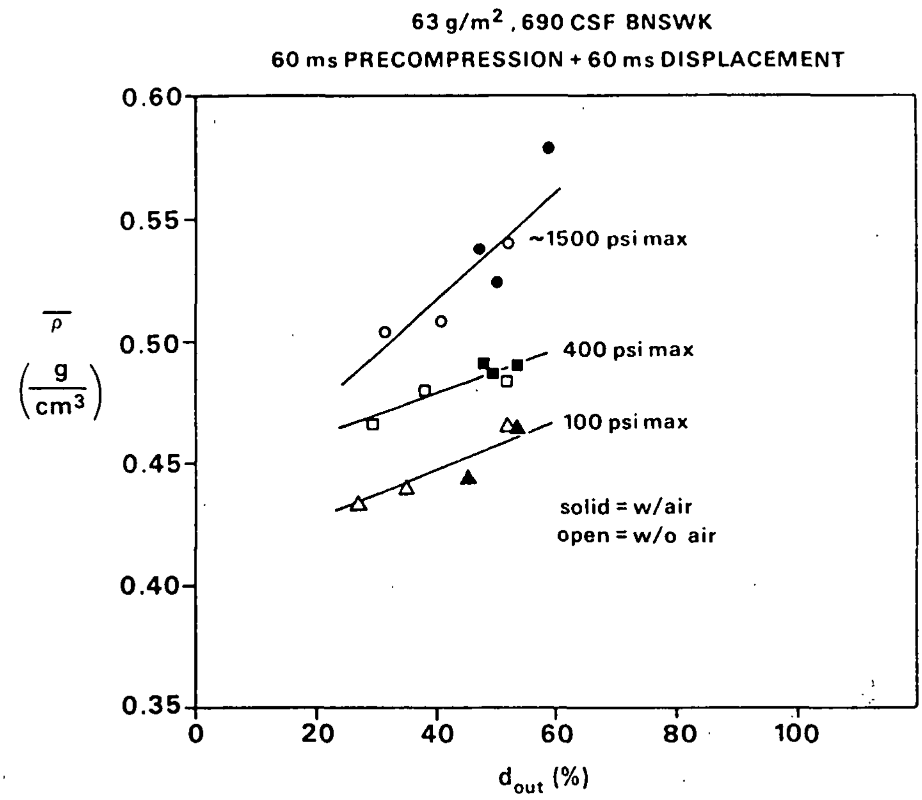

Density - dryness relationships
for various pressing conditions.

THIRD GENERATION EQUIPMENT REQUIREMENTS

- FASTER RISE ON AIR PRESSURE
- EFFECTIVE PRESS CHAMBER SEALING
- INTERCHANGEABLE LOAD SPREADERS
- AIR FLOW MEASUREMENTS
- SYNCHRONIZED AIR DELIVERY

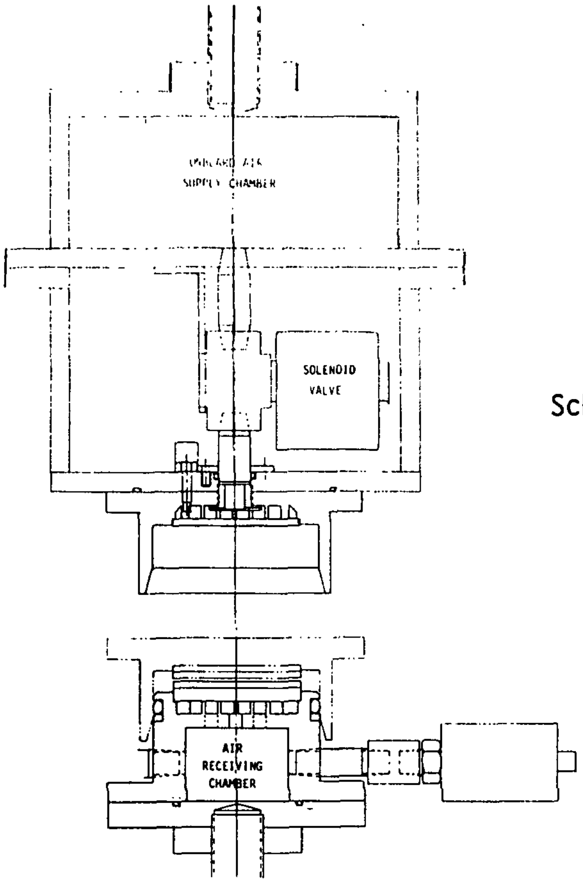

Schematic of displacement pressing head.

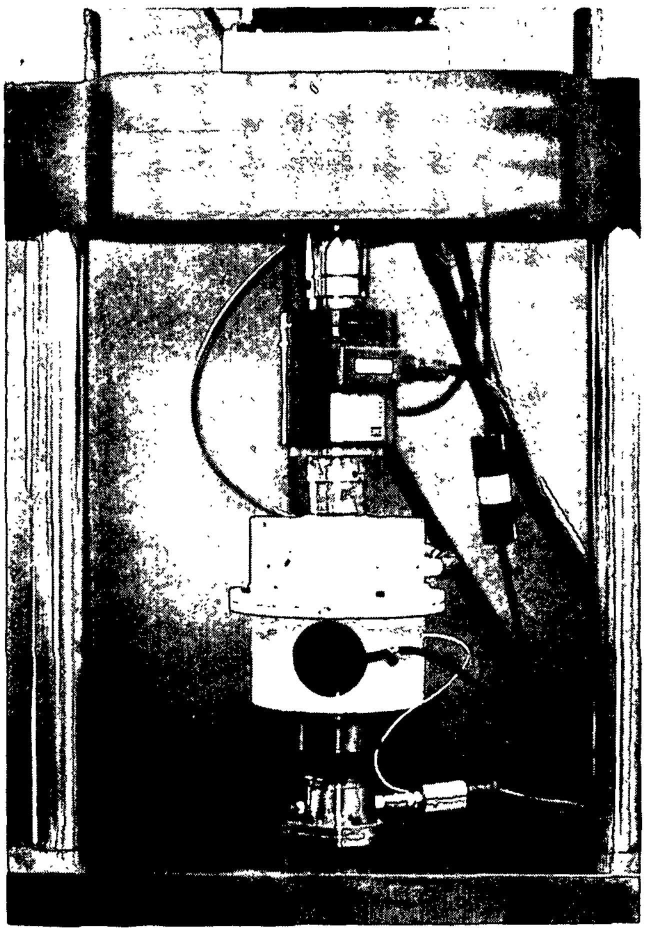

DP head installed in electrohydraulic

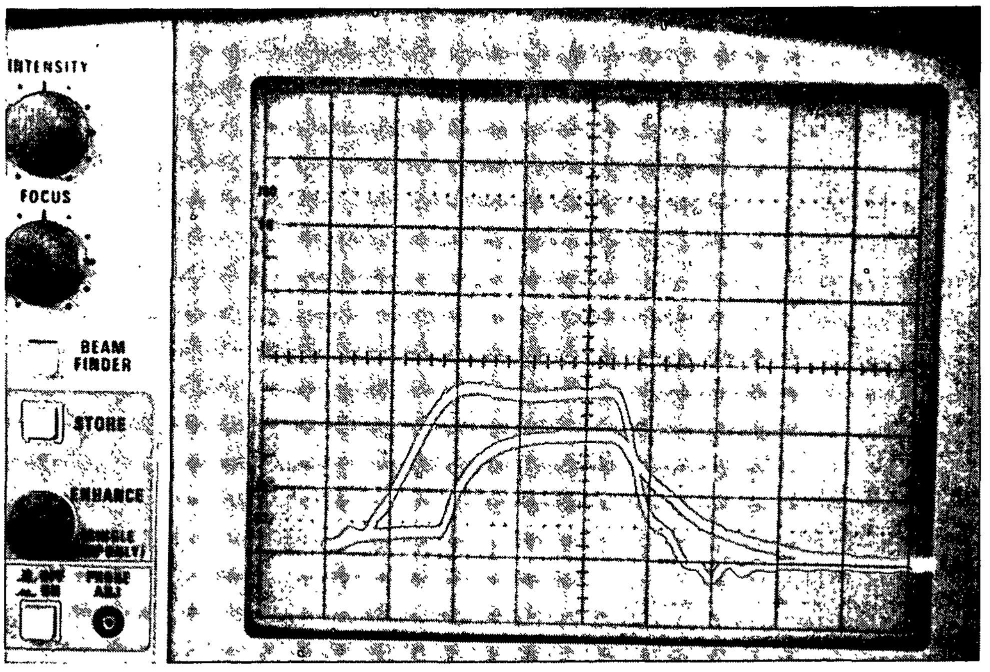

Load and air pressure traces.

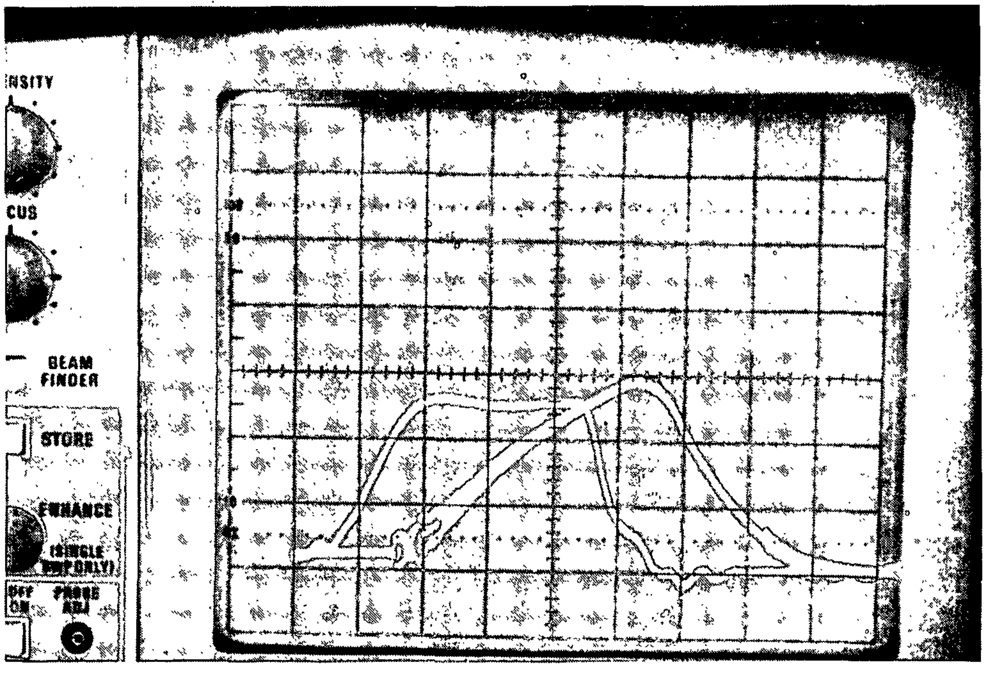

Load and receiving chamber pressure pulses.

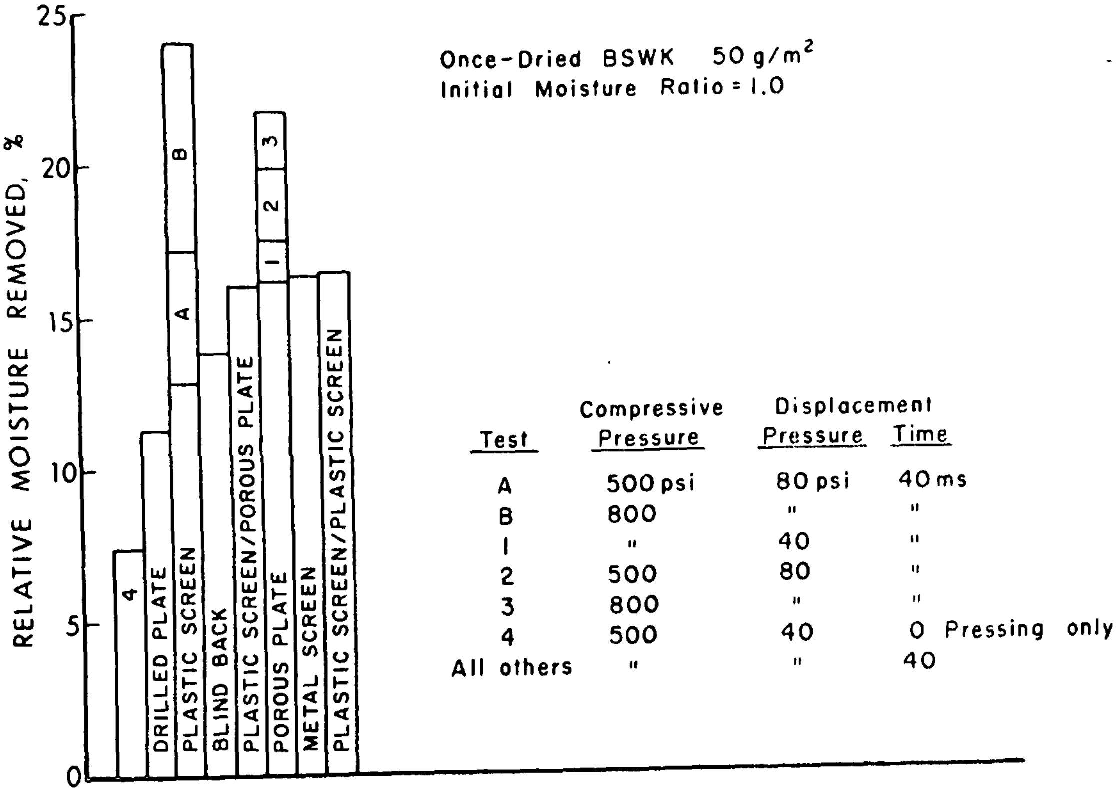

Relative moisture removal values for
various displacement pressing conditions.

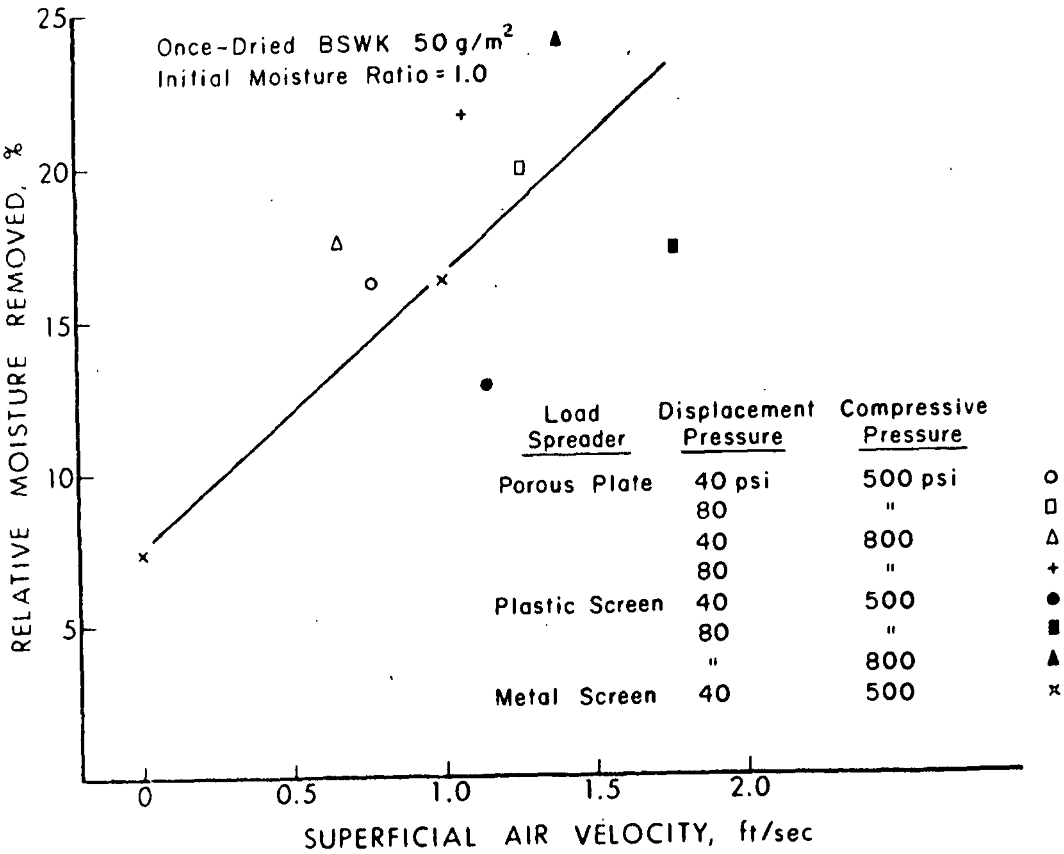

The effect of superficial air velocity on water removal

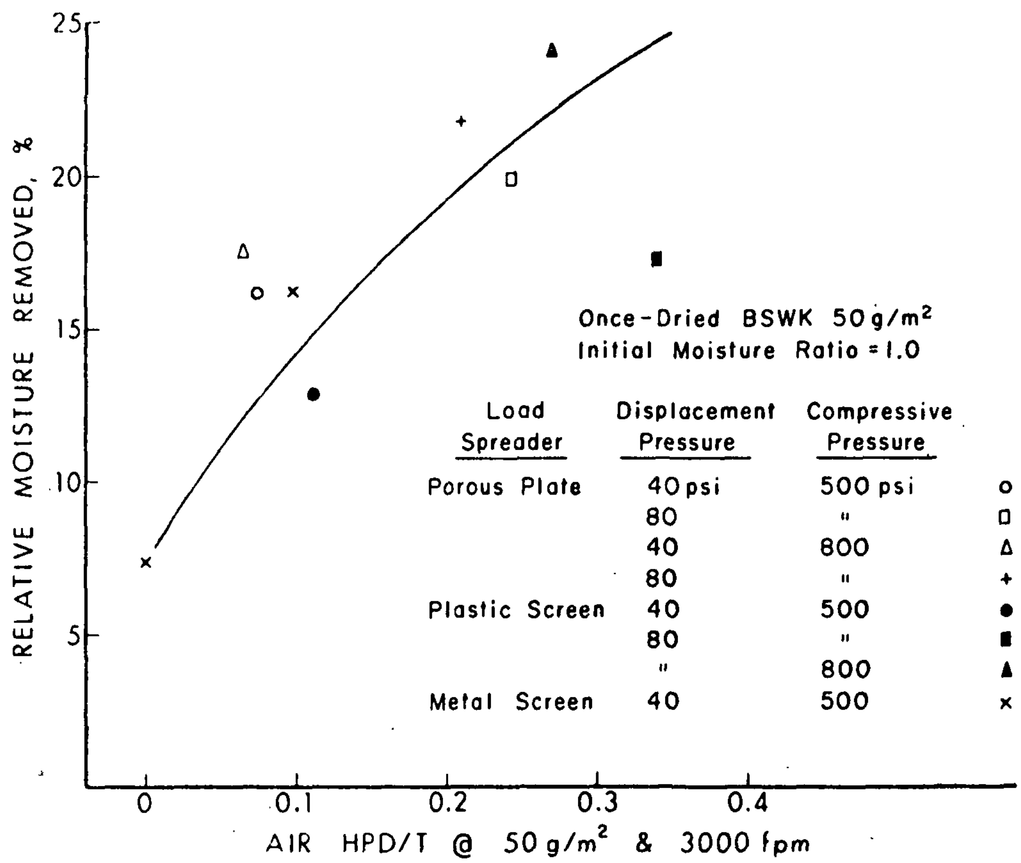

Air horsepower requirements for displacement pressing.

DISPLACEMENT PRESSING

PERFORMANCE

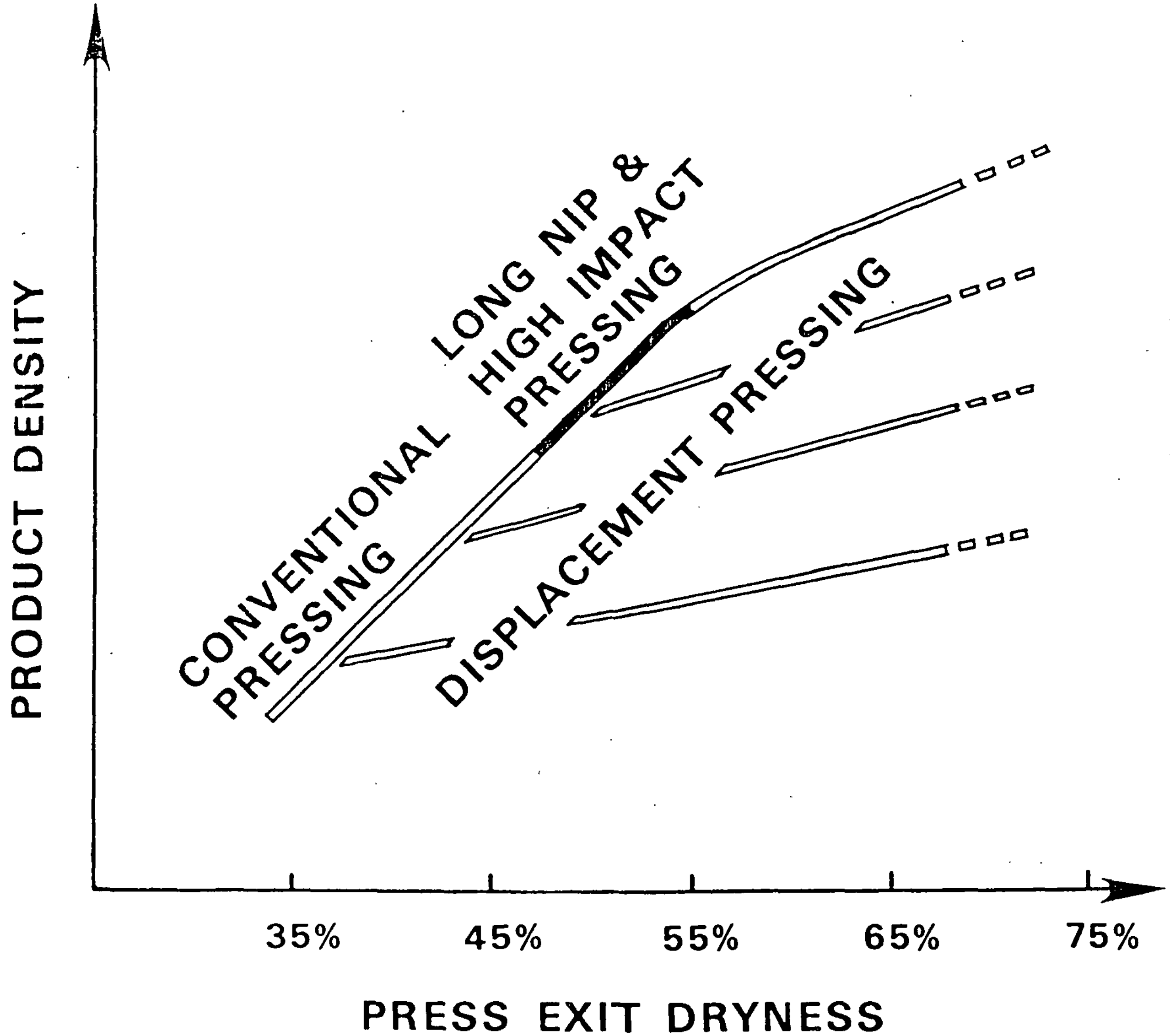

Project 3480/3584

Slide Material

PROJECT 3480/3584

WET PRESSING FUNDAMENTALS

OBJECTIVES: DETERMINE FEASIBILITY AND PERFORMANCE OF DISPLACEMENT PRESSING

DEVELOP A PREDICTIVE MODEL FOR WET PRESSING

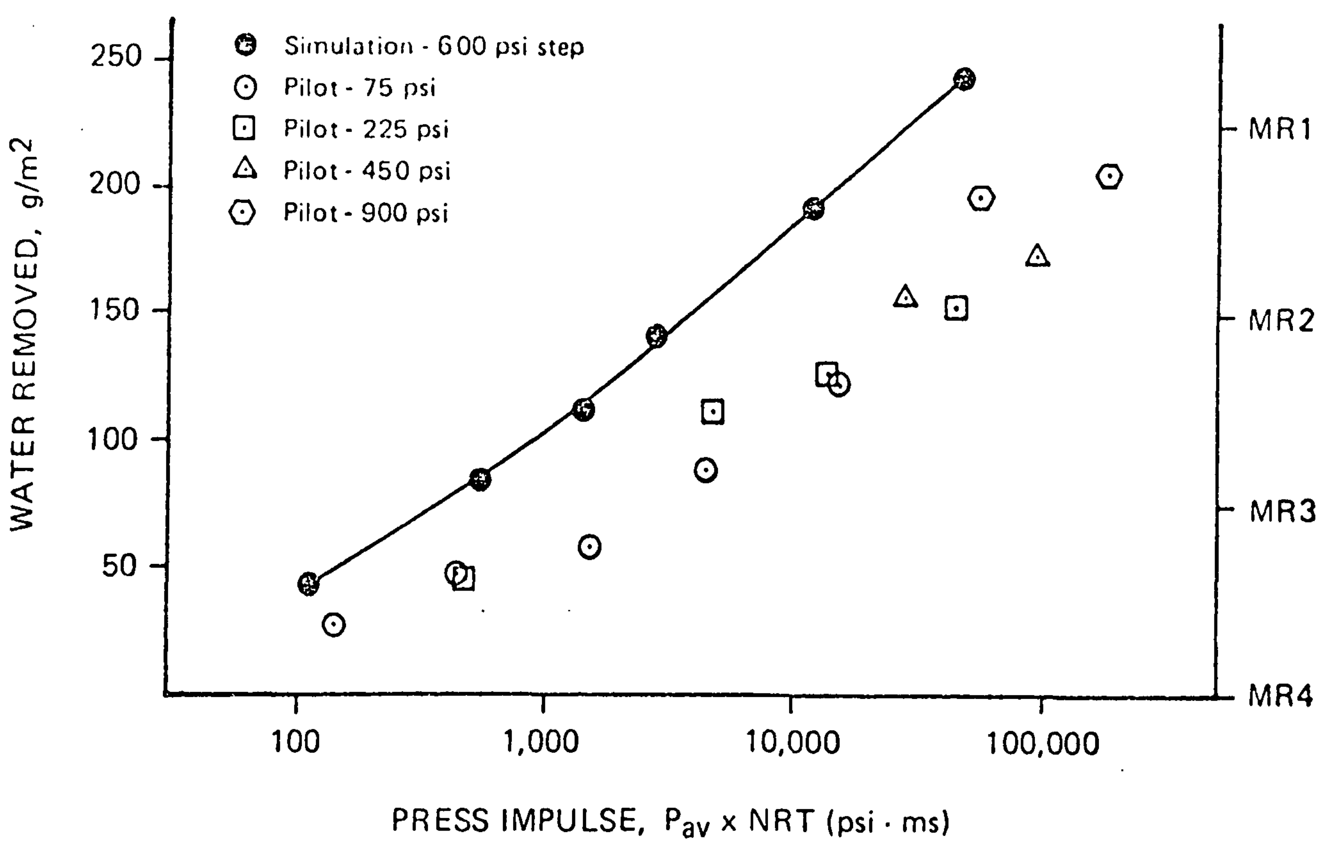

Comparison between pilot and laboratory simulations for 300 CSF bleached softwood kraft, 75 g/m^2.

PILOT PRESS

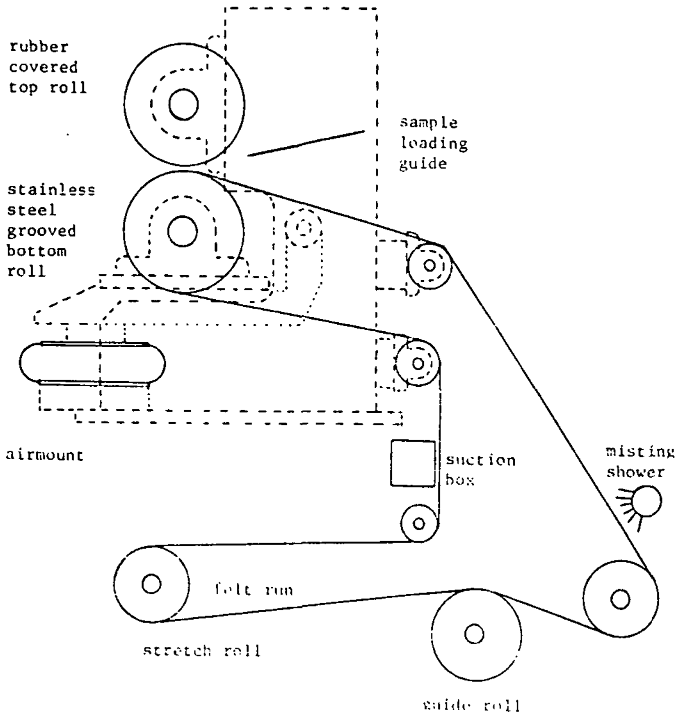

Broken or dotted lines indicate parts of frame or bearings.

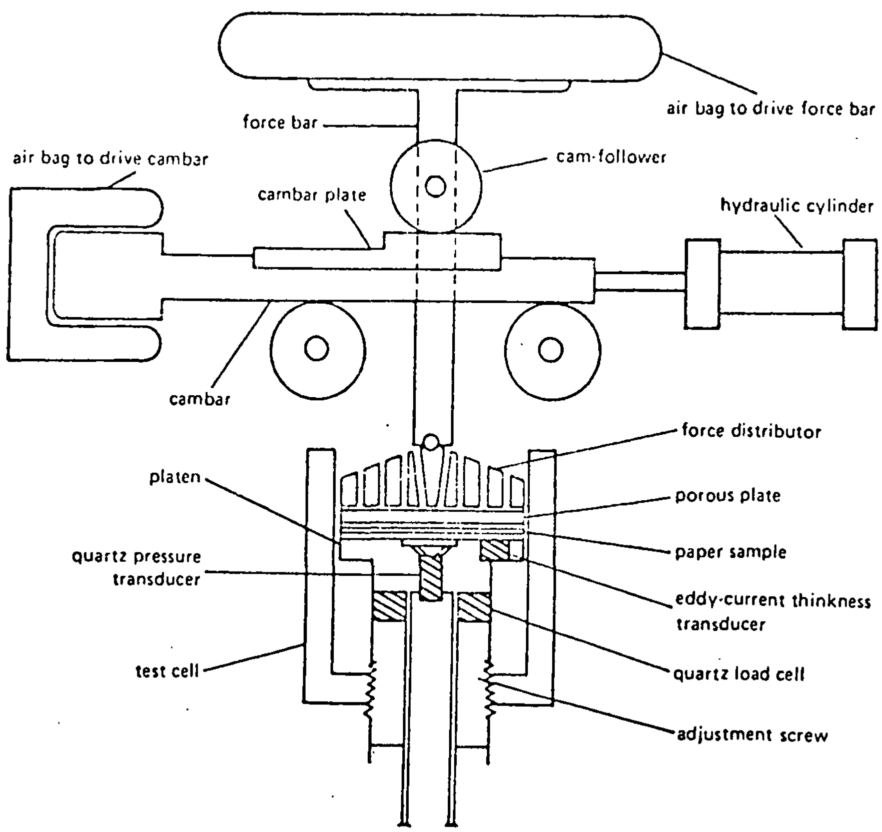

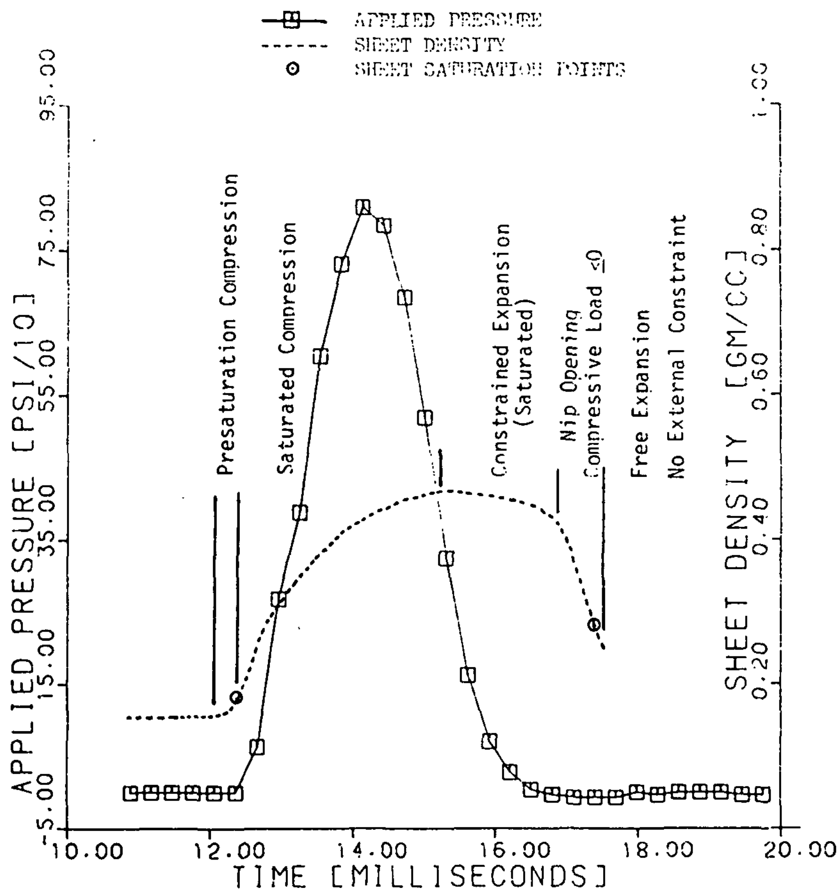

R1L 55.6 GM/SQ-M MR = 4.8
70 F 420 CSF

Instantaneous pressure and density curves for a typical wet pressing cycle.

NIP EFFICIENCY MUST ACCOUNT FOR:

- PRESATURATION COMPRESSION
- CONSTRAINED EXPANSION
- NIP OPENING
- POST-NIP CONTACT
- DIFFERENCES IN WATER RECEIVERS

MODELING OBJECTIVE

DEVELOPMENT OF A MODEL TO PREDICT THE PERFORMANCE OF A WET PRESS, GIVEN BASIC FURNISH PROPERTIES

TASKS

- COMPARATIVE TESTING OF POROUS PLATES/FELTS
- COMPRESSION/EXPANSION MODEL FOR COMPLETE CYCLE
- ADD TRANSPORT PROCESSES TO MODEL
- TREAT NIP OPENING & POST CONTACT

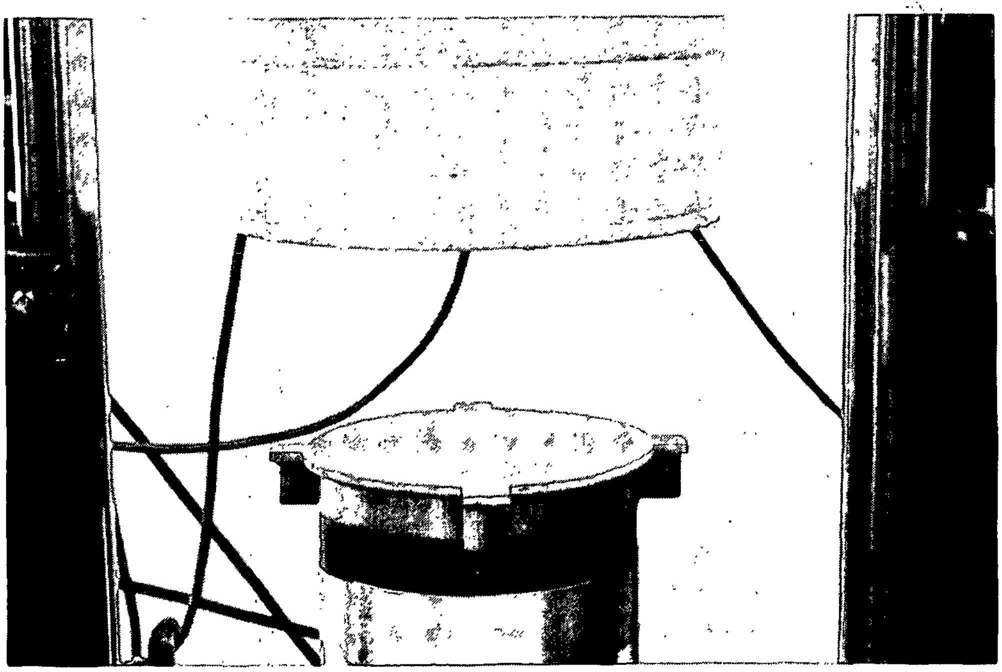

Impulse drying simulator nip. Upper platen is heated, lower platen is water receiver.

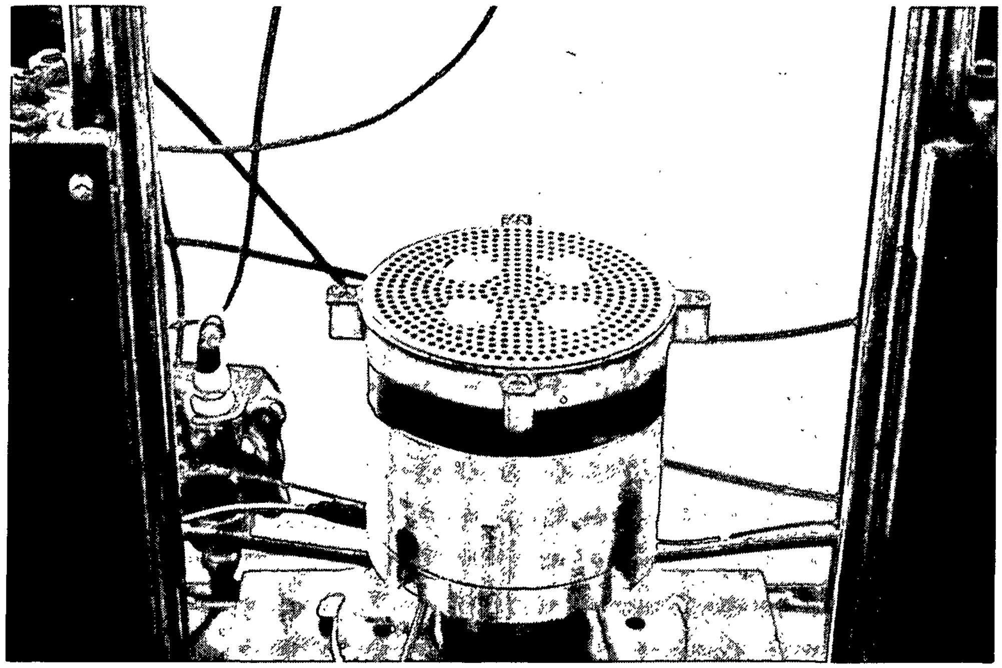

Lower pedestal of impulse drying simulator with ceramic removed revealing displacement transducers and drilled plate.

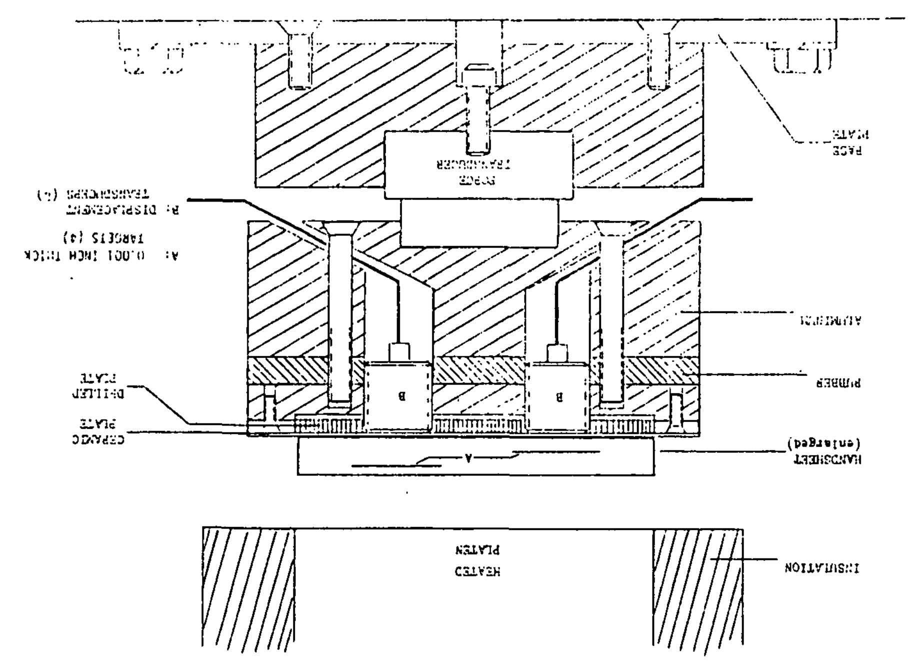

Impulse drying simulator pedestal.

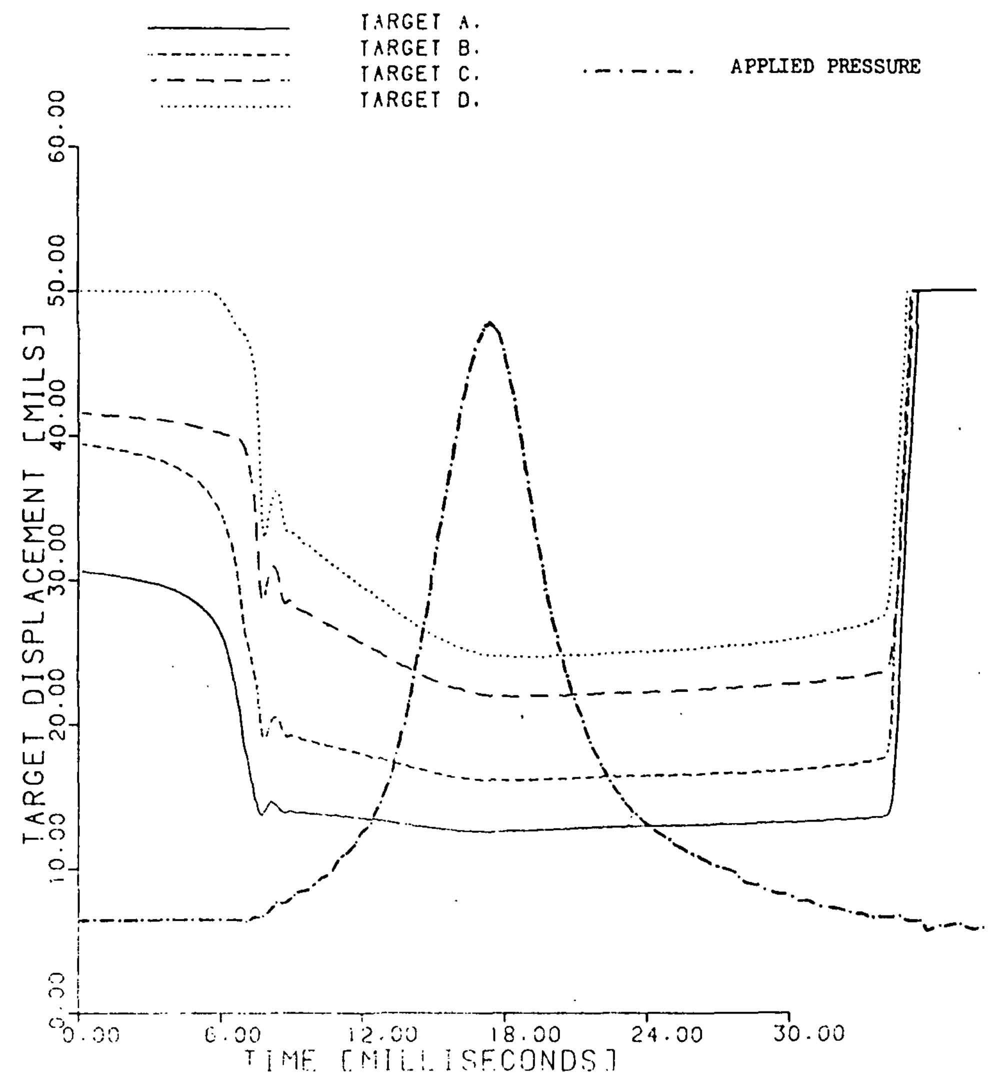

DISPLACEMENT HISTORIES OF FOUR TARGETS PLACED AT DISTINCT POSITIONS WITHIN THE FIBER MAT, WET PRESSED AT ROOM TEMPERATURE, PEAK PRESSURE OF 614 PSI AND A NIP RESIDENCE TIME OF 25 MILLISECONDS. THE HANDSHEET IS A 168 g/m^2 BASIS WEIGHT, 2.3 INITIAL MOISTURE RATIO, 735 CSF.

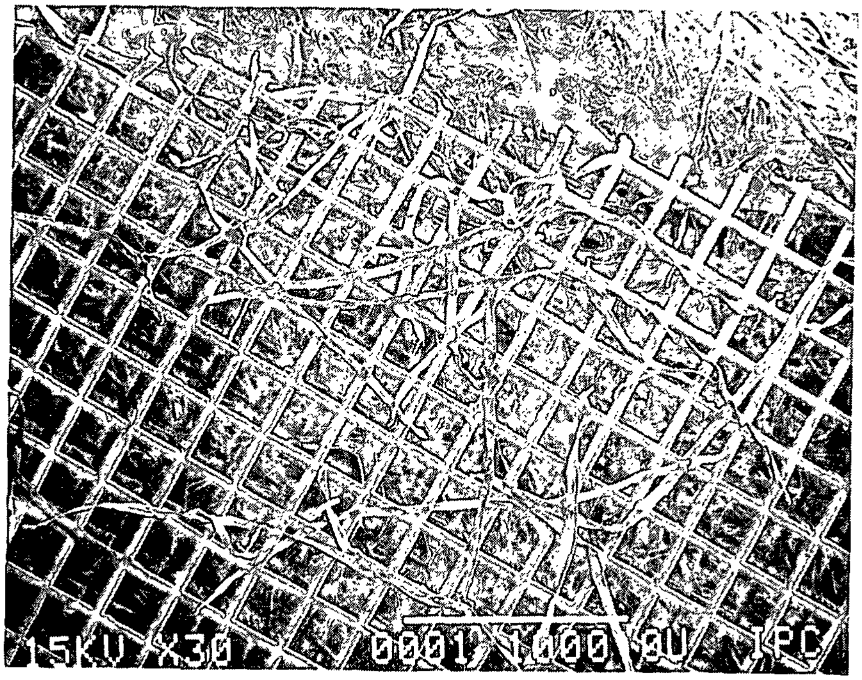

Target material used in thickness measurement - 0.001 inch thick copper mesh.

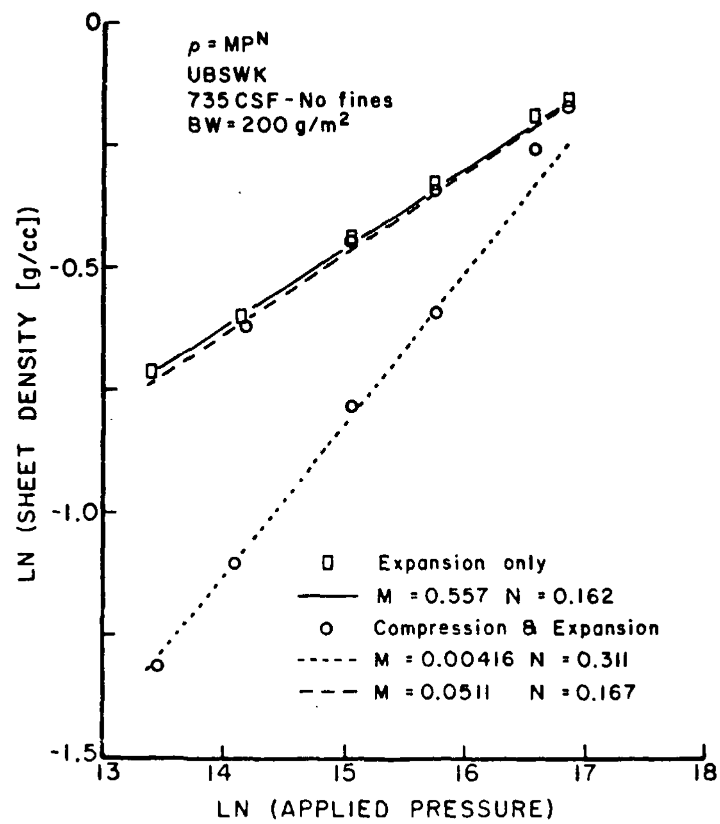

Compression-expansion curves for a "slow" process.

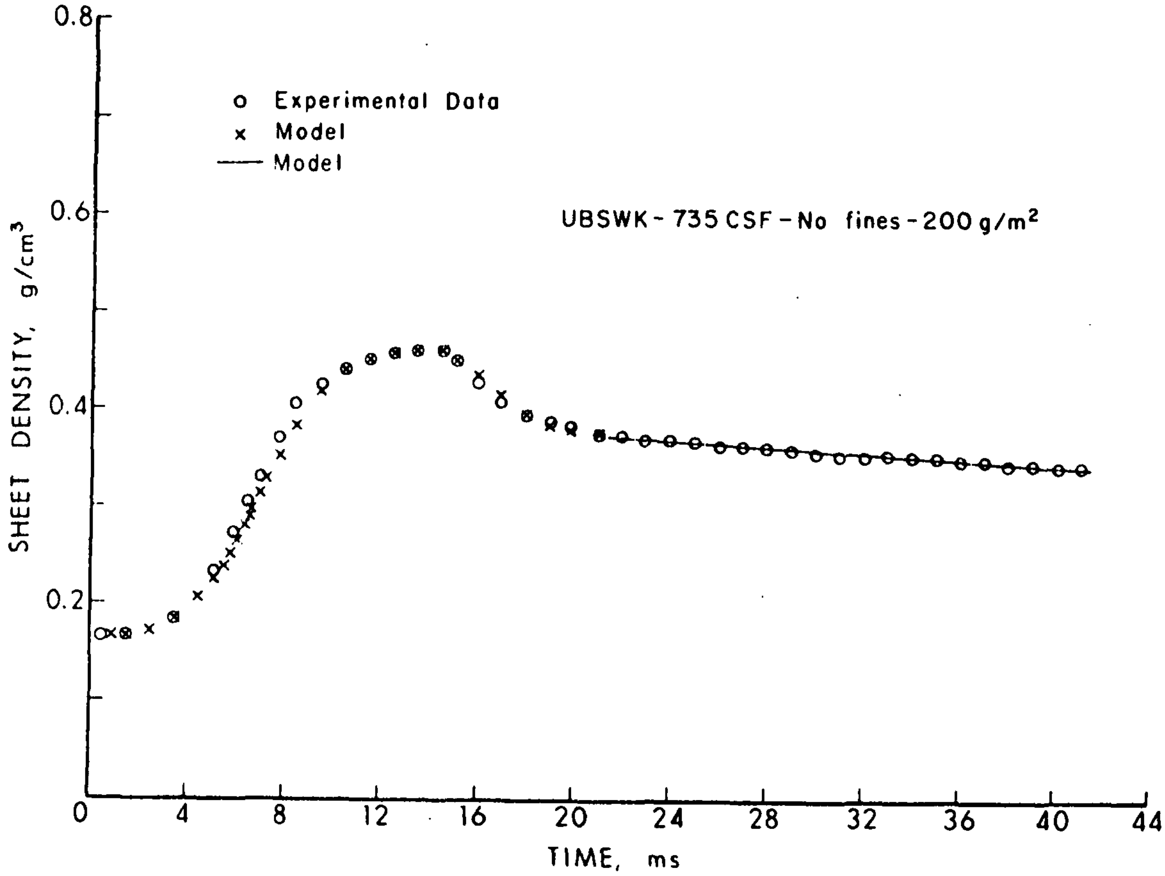

Typical compression-expansion curve including post-nip expansion.

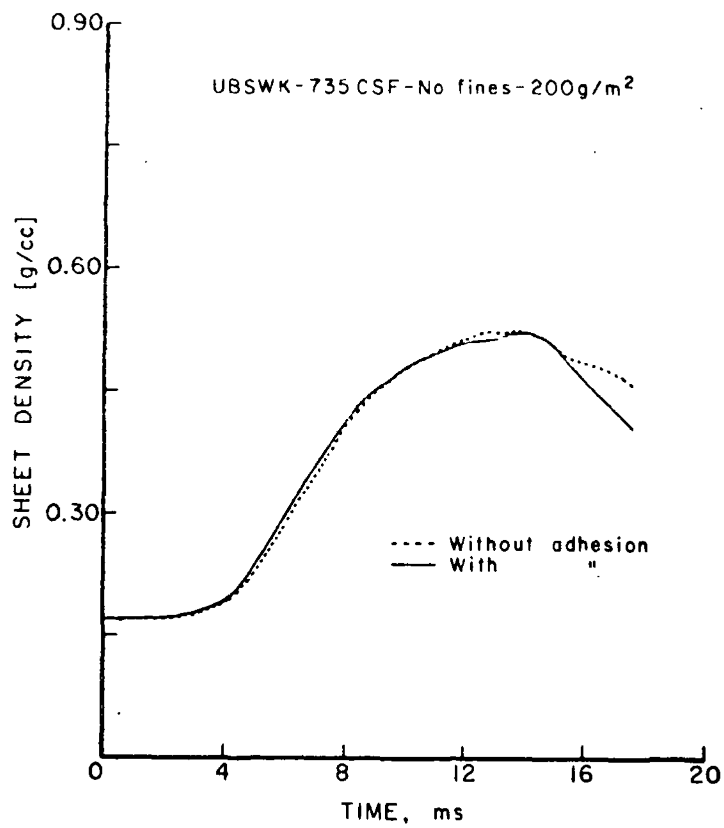

Wet pressing density curve with and without adhesion.

FUTURE WORK

- ° COMPRESSION-EXPANSION MODEL FOR UNSATURATED WEBS
- ° HYDRAULIC PRESSURE MEASUREMENTS FOR SATURATED WEBS
- ° DESCRIBE NIP OPENING PROCESS
- ° COMBINE WITH TRANSPORT EQUATIONS TO COMPLETE MODEL
- ° VERIFY ON NEW LABORATORY ROLL PRESS

Project 3479

HIGHER CONSISTENCY PROCESSING

Clyde Sprague & Ted Farrington

PROJECT 3479: HIGHER CONSISTENCY PROCESSING

OBJECTIVE

DEVELOP THE BACKGROUND AND METHODS FOR PRACTICAL SEPARATION AND FORMING AT ELEVATED CONSISTENCIES.

APPROACH

- SELECT A WORKABLE METHOD FOR ONE PROCESS
- IDENTIFY FUNDAMENTAL LIMITATIONS TO METHOD
- DEVELOP UNDERSTANDING OF FUNDAMENTALS NECESSARY TO REMOVE LIMITATION

SINGLE ROLL WITH AIR DOCTOR

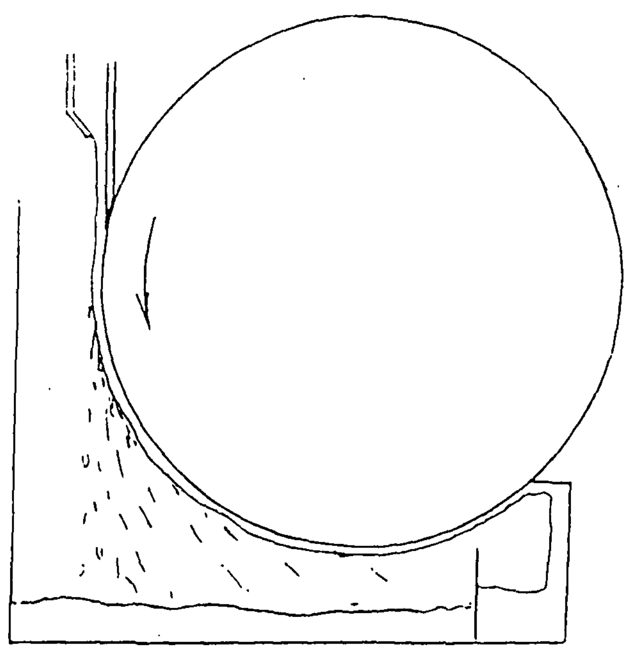

Concept for applying film of slurry to a blade and then to a moving roll.

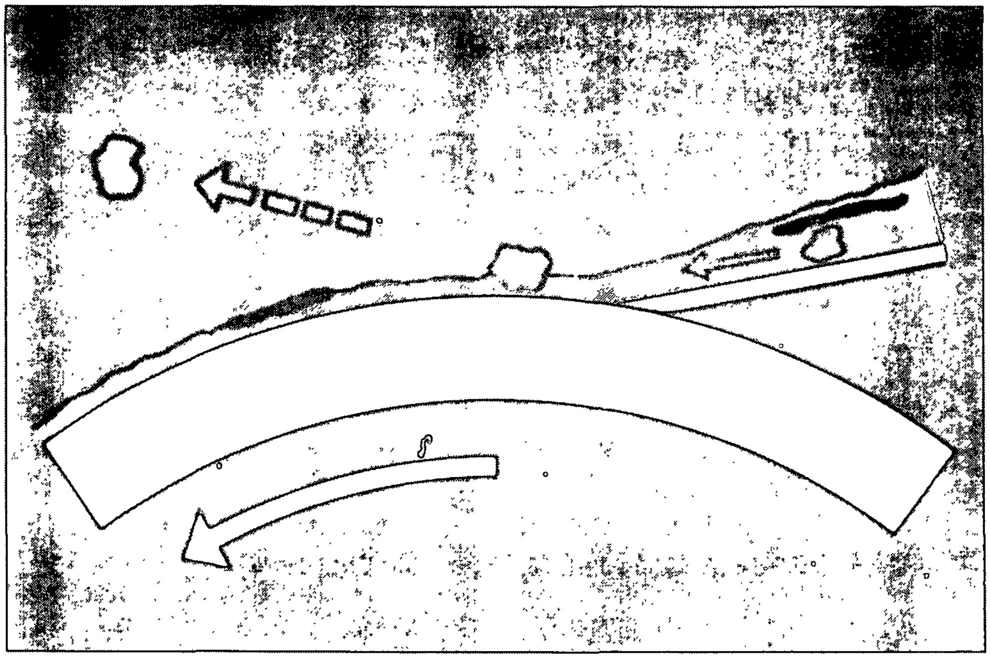

Illustration of particle separation from slurry film on moving roll surface.

$$\frac{v^2}{2\gamma R} = \frac{\cos\theta}{\rho w t}$$

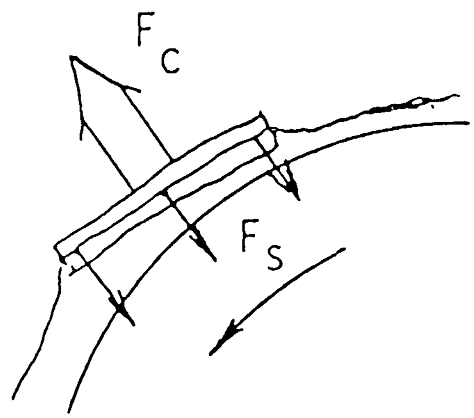

Theoretical basis of separation.

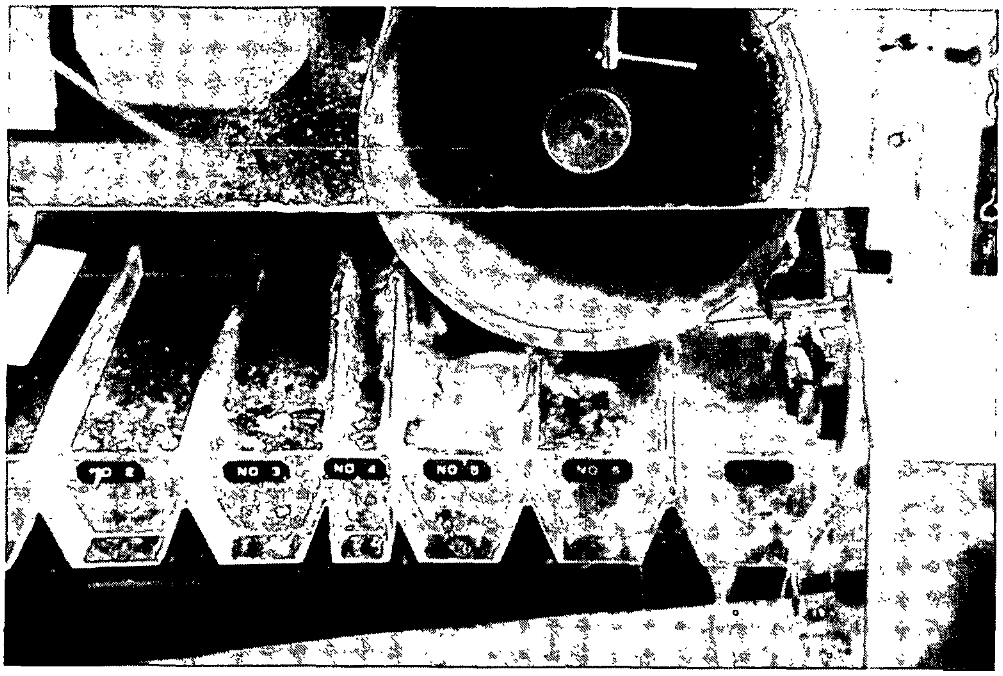

Roll separator operating on 50:50 TMP/kraft pulp.

ROLL SEPARATION OF STICKIES FROM RAFT WRAPPING PAPER STOCK

Feed: 1.29% cons.; 0.59% 6-cut rejects; 0.66% toluene extr.

Roll Speed, ft/min	Reject Rate, %	Percent Removal Efficiency	
		6-cut rejects	Stickies by extn.
3000	5.6	82.9	73.9
	11.6	97.1	78.3
5000	8.0	98.4	75.9
	20.4	99.7	92.6
7000	16.0	98.7	86.0
	25.6	98.5	92.0

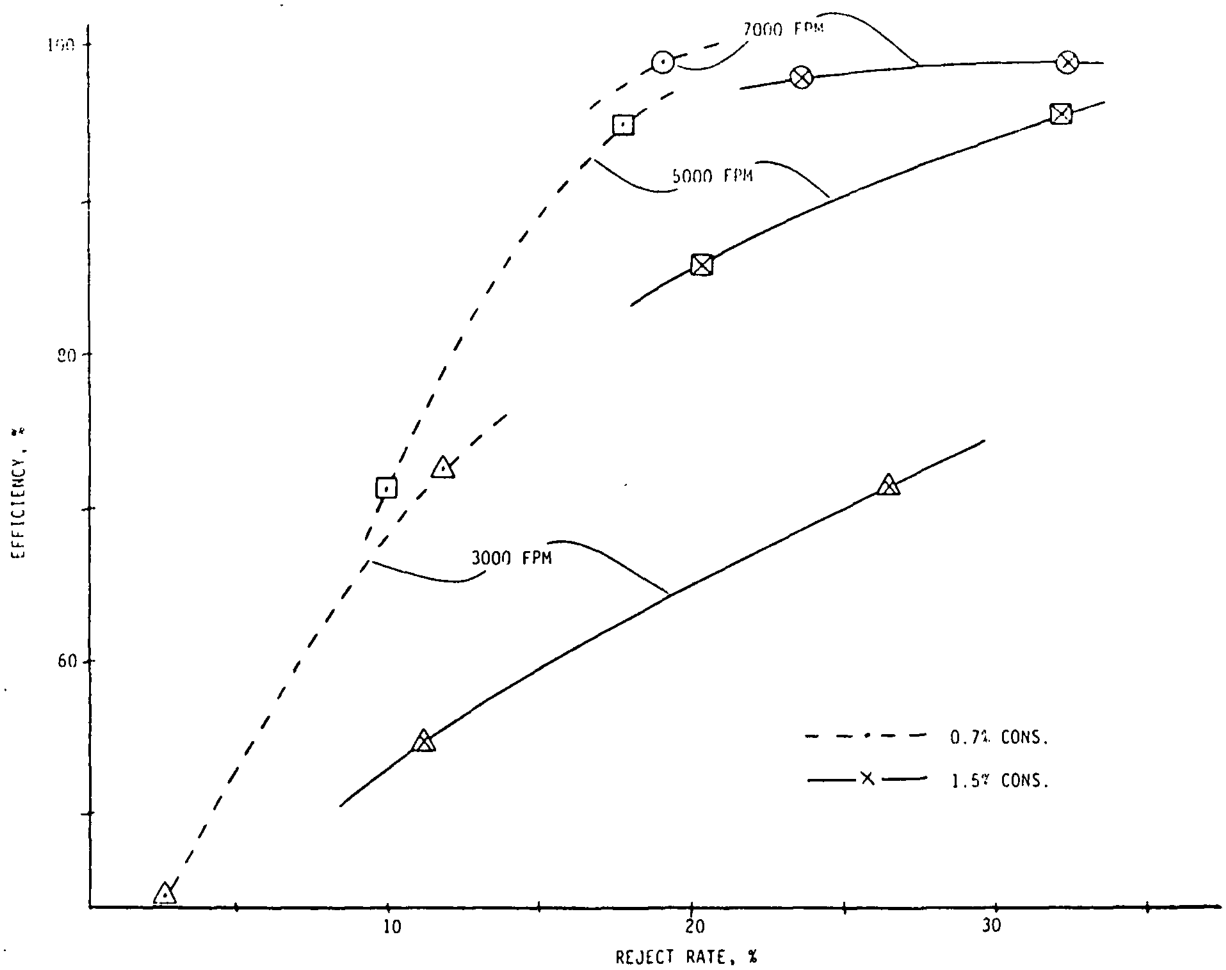

Efficiency of removal of 6-cut shives from 50:50 TMP/kraft mixture, as function of reject rate, roll speed, and consistency.

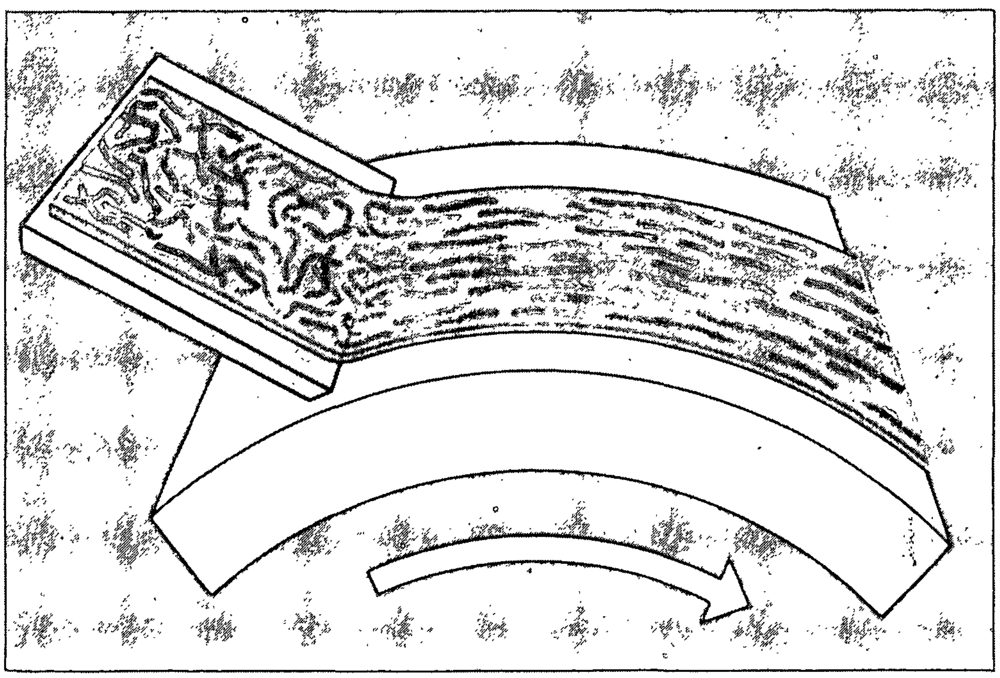

Means for employing shear and acceleration to fiber slurry films, illustrating anticipated fiber orientation effect.

HIGH CONSISTENCY PAPERMAKING

PROJECT 3479

INITIAL PROJECT CONCEPTS

OUTLINE

I. PROBLEM DEFINITION

II. ACTIVITIES THUS FAR

III. INITIAL PROGRAM CONCEPTUALIZATION

IV. POTENTIAL ACTIVITIES

V. TARGETS FOR FIRST YEAR

PROBLEM DEFINITION

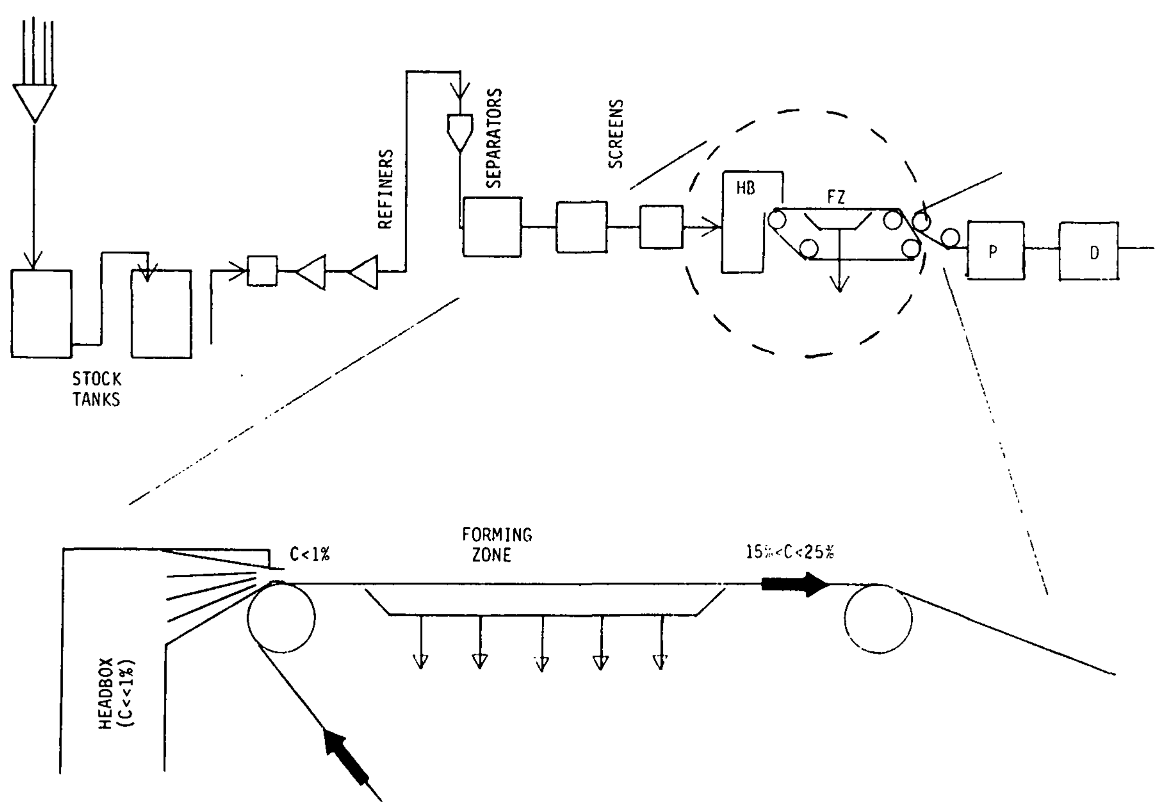

POTENTIAL BENEFITS FROM HIGH CONSISTENCY PAPER MAKING (HCPM)

- REDUCED CAPITAL COSTS
- IMPROVED PAPER QUALITY (REDUCED RAW MATERIAL COSTS)
- IMPROVED FINES RETENTION
- LOWER ENERGY COSTS

ACTIVITIES THUS FAR

I. WHAT'S BEEN DONE?
WHAT'S GOING ON?

A. LITERATURE SURVEYS

1. DOCUMENTED PROBLEMS WITH HCPM
2. COLLOIDAL PROPERTIES
3. RHEOLOGY OF FIBROUS SUSPENSIONS
4. FLOWFIELD - FIBER FLOC INTERACTION
5. FORMATION
6. FLOW THROUGH POROUS MEDIA
7. PATENTS
8. FLOW VISUALIZATION

II. PROJECT DEFINITION AND PLANNING

- RANDOM SURVEY OF PROBLEMS AND POSSIBLE PROJECT ACTIVITIES
- LIST OF REASONABLE PROJECT ACTIVITIES
- SET SOME PRIORITIES
- DEFINE A PLAN OF ATTACK

CONCEPTUAL PROCESS

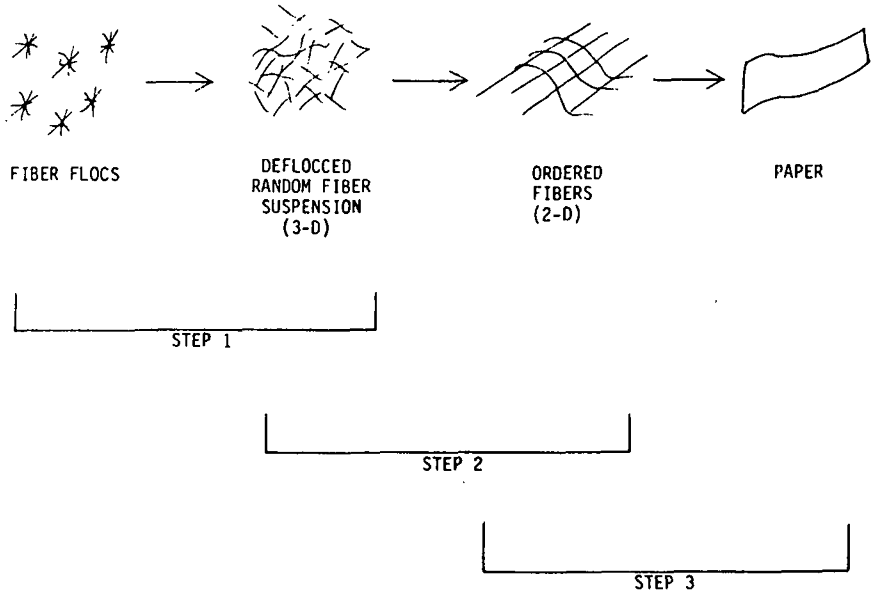

POTENTIAL ACTIVITIES FOR INVESTIGATION OF STEP 1

1. COLLOIDAL BEHAVIOR
   - MAGNITUDE OF ATTRACTIVE FORCES (VDW))
   - ELECTROKINETIC EXPERIMENTS
   - FLOCCULATION EXPERIMENTS
   - FLOCCULATION MODELS (SETTLING, SHEAR)

POTENTIAL ACTIVITIES FOR INVESTIGATION OF STEP 1 (CONTINUED)

2. FIBER FLOC-FLUID DYNAMICS INTERACTION
   - BEHAVIOR OF SINGLE AND MULTIPLE FLOCS IN
     - SHEAR & ELONGATIONAL FLOWS
     - LAMINAR & TURBULENT REGIMES
   - FLOC STABILITY

POTENTIAL ACTIVITIES FOR INVESTIGATION OF STEP 1
(CONTINUED)

3. FUNDAMENTAL FIBER NETWORK PROPERTIES

  ° NETWORK INFLUENCE ON RHEOLOGY

  ° INHERENT NETWORK STRENGTH

POTENTIAL ACTIVITIES FOR INVESTIGATION OF STEPS II AND III

I. CONTROL OF FIBER ORIENTATION

  ° EXPERIMENTAL STUDY OF EFFECT OF VARIOUS FLOW FIELDS ON ORIENTATION
    - SHEAR, ELONGATION, CONVERGING FLOWS

  ° COMPARISON OF RESULTS WITH THEORETICAL PREDICTIONS

II. RELATIONSHIPS BETWEEN FIBER ORIENTATION AT START AND FINISH OF FORMATION PROCESS

  ° FLOW THROUGH POROUS MEDIA

III. PILOT PAPER MACHINE EXPERIMENTS

AND FINALLY:

FLOW VISUALIZATION

OBJECTIVE: TO ASSESS FIBER ORIENTATION DISTRIBUTION IN FIBER SUSPENSIONS FROM <1% to 5% CONCENTRATION

INVESTIGATION POTENTIAL USE OF:

OPTICAL TECHNIQUES

X-RAY WITH TRACER

HOLOGRAPHY

HIGH SPEED MOVIES

ELECTRICAL PROPERTIES

LIST OF ACTIVITIES

COLLOIDAL BEHAVIOR

FIBER FLOC-FLUID INTERACTION

FUNDAMENTAL FIBER NETWORK PROPERTIES

CONTROL OF FIBER ORIENTATION

PILOT PAPER MACHINE STUDIES

FLOW VISUALIZATION

CONCEPTUAL PROCESS

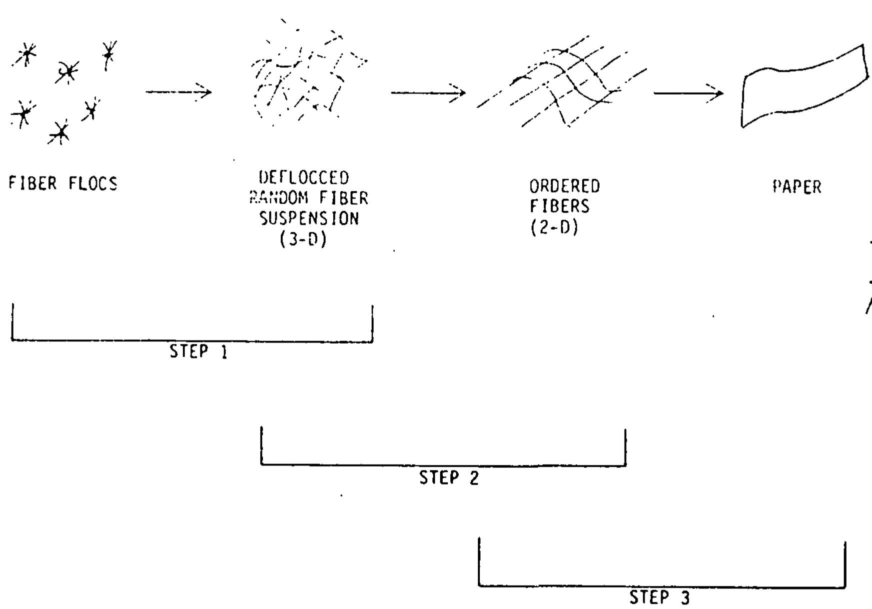

TOP PRIORITIES

1. FLOW VISUALIZATION TECHNIQUE FOR HIGHER CONCENTRATIONS
2. EFFECT OF VARIOUS FLOW FIELDS (SHEAR, ELONGATIONAL, CONVERGING) ON FIBER ORIENTATION AT HIGHER CONCENTRATIONS
3. PILOT MACHINE STUDIES TO QUANTIFY PROBLEM

PROBLEM DEFINITION

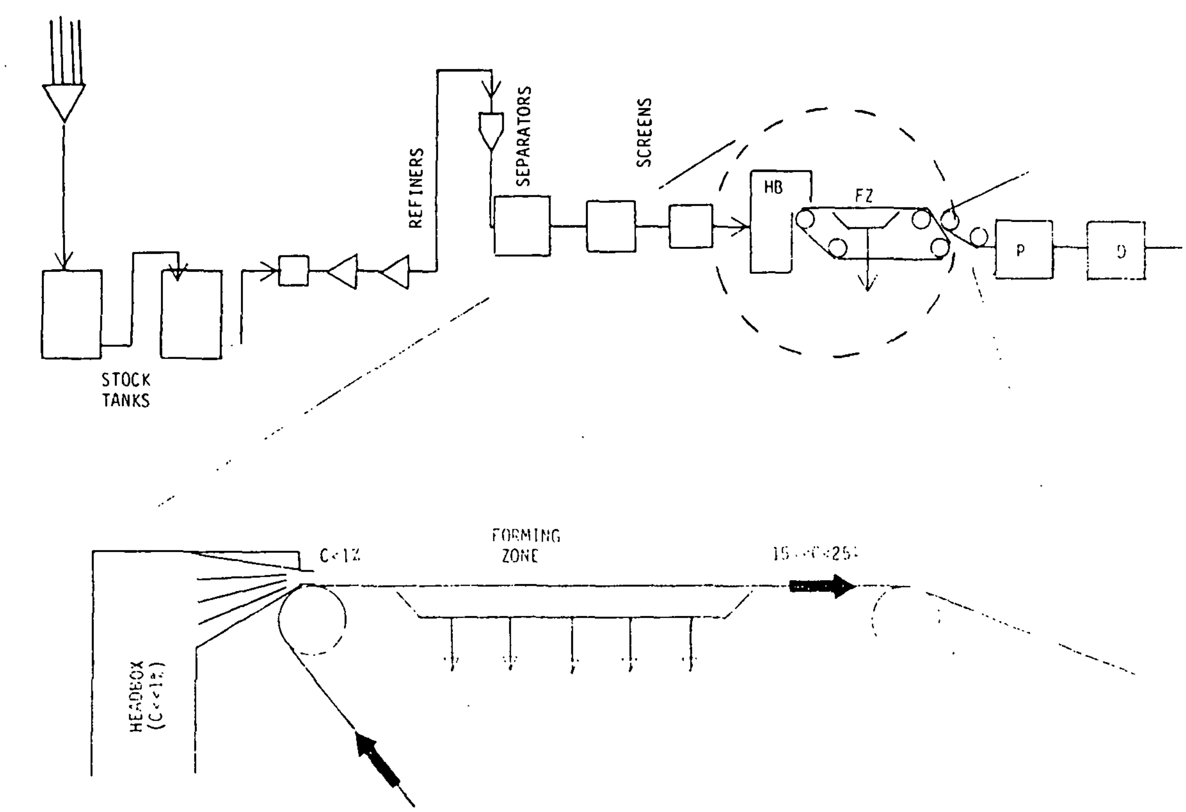

Project 3470

FUNDAMENTALS OF DRYING

Clyde Sprague & Hugh Lavery

PROJECT 3470

FUNDAMENTALS OF DRYING

OBJECTIVE: DEVELOP THE INFORMATION NECESSARY FOR COMMERCIALIZATION OF IMPULSE AND THERMAL/VACUUM DRYING PROCESSES

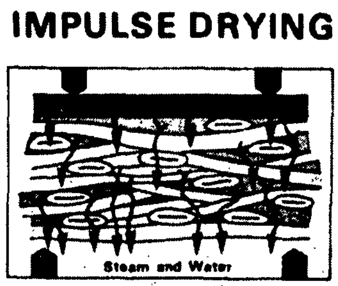

WATER REMOVAL MECHANISMS

- THERMALLY AUGMENTED PRESSING
- HIGH RATE EVAPORATION
- LIQUID PHASE DEWATERING

IMPULSE DRYING GIVES:

- EXTREMELY HIGH DRYING RATES
  - VERY SMALL DRYERS
  - HIGH PRODUCTION RATES
- LIQUID PHASE WATER REMOVAL
  - LESS DRYING ENERGY
- SHEET DENSIFICATION
  - PROPERTY DEVELOPMENT
  - PRESS DRYING EFFECTS

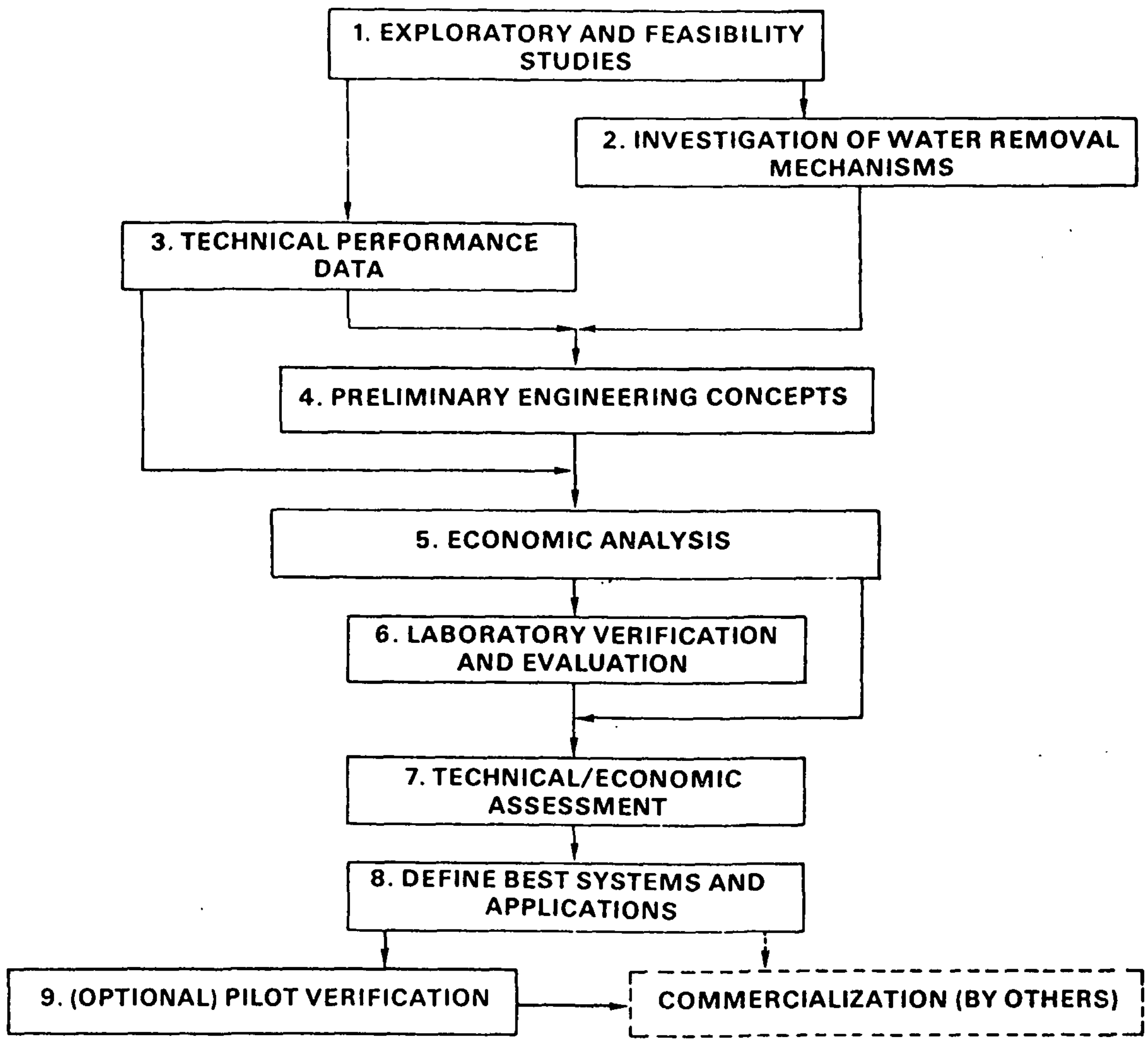

PROJECT PLAN FLOWSHEET.

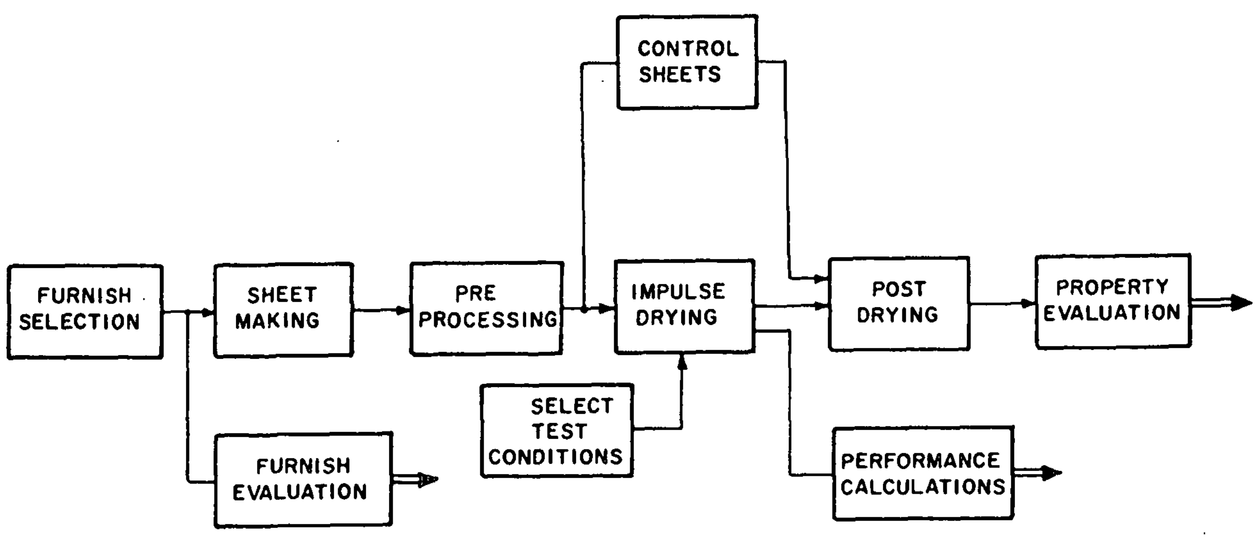

ELEMENTS OF PERFORMANCE EVALUATION.

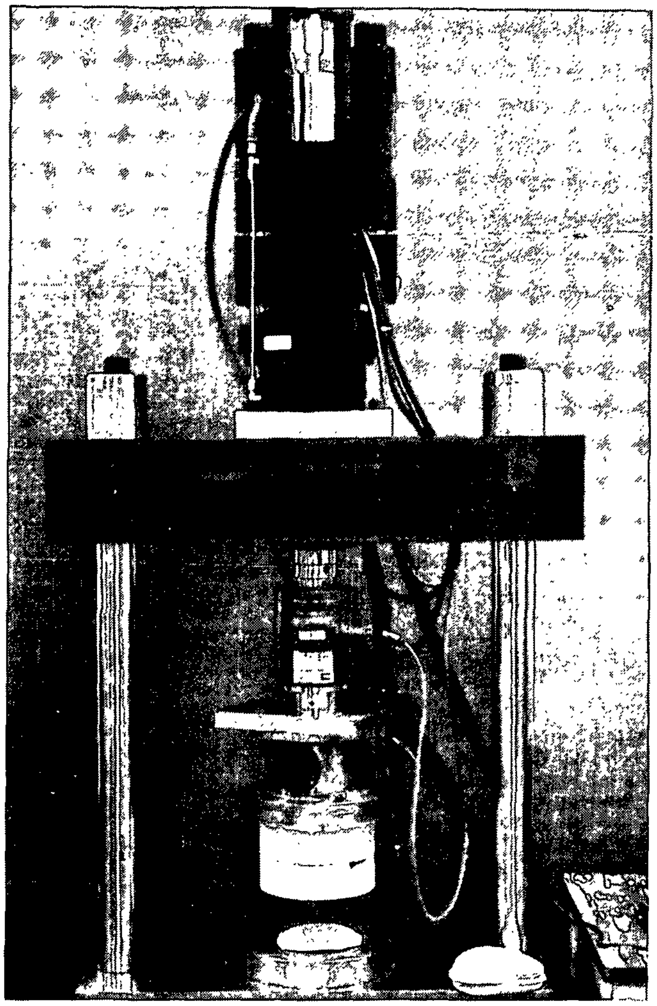

SERVO ACTUATOR AND LOAD FRAME ASSEMBLY.

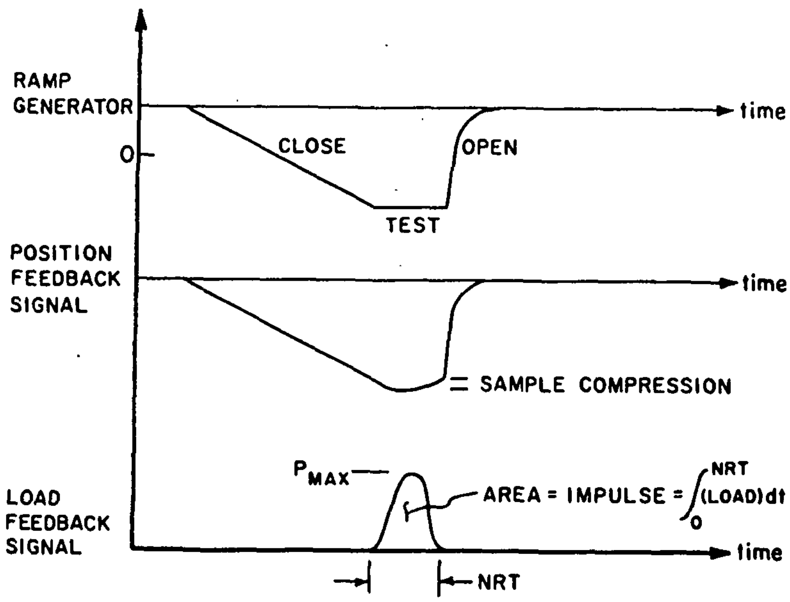

SCHEMATIC REPRESENTATION OF A TEST CYCLE.

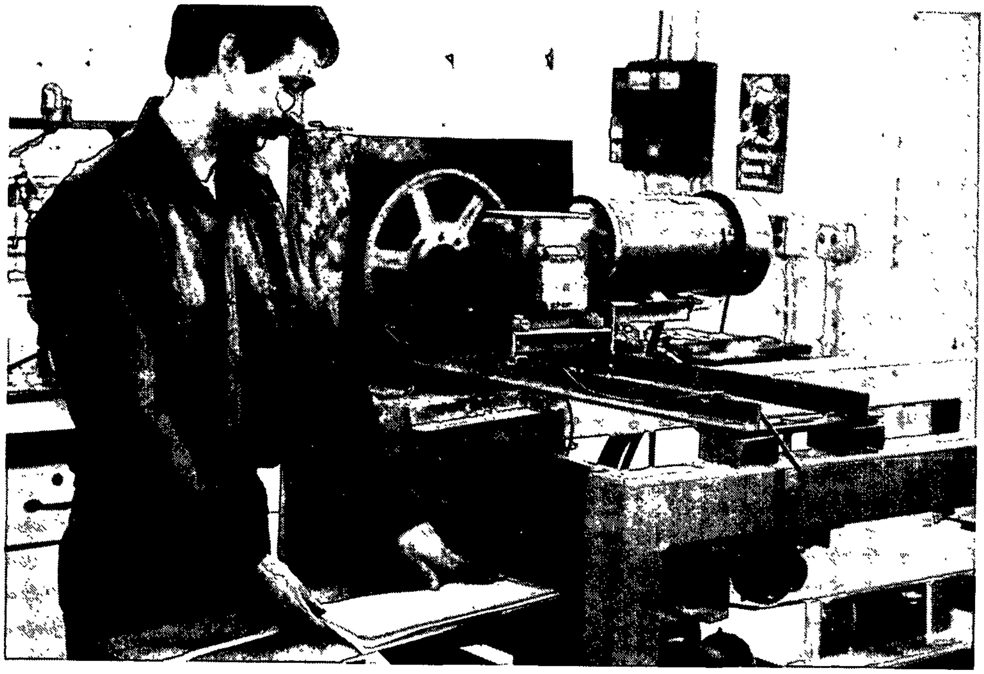

ROLL PRESS FOR PREPRESSING SHEETS.

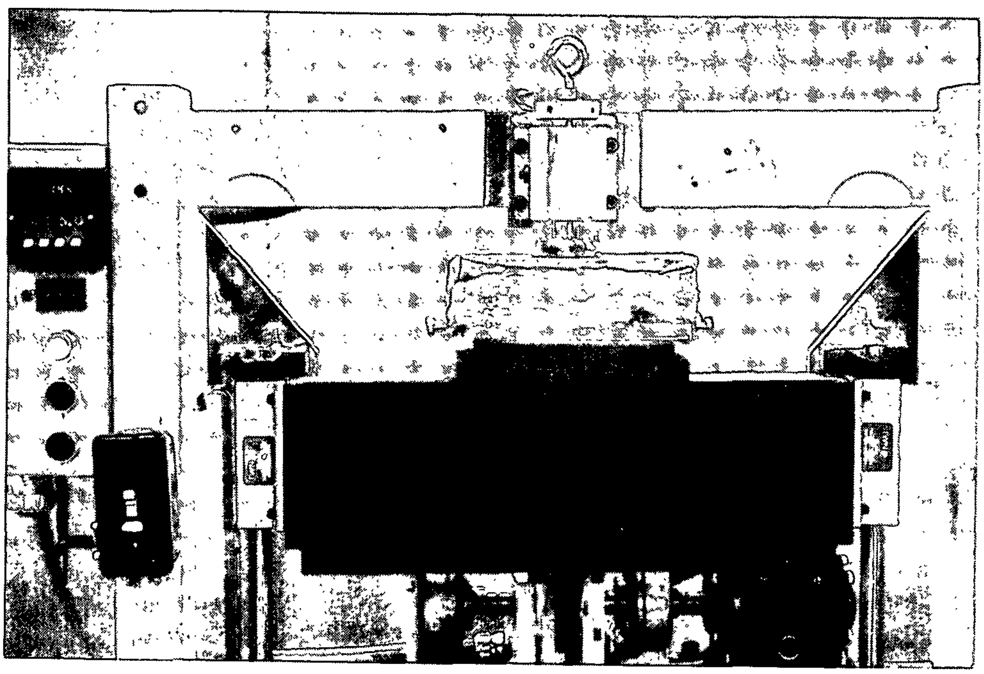

LOW-INTENSITY DRYING SYSTEM.

TEST PROGRAM VARIABLES

- GRADE (FURNISH)
- BASIS WEIGHT
- INITIAL MOISTURE RATIO
- INITIAL SHEET TEMPERATURE
- AMBIENT PRESSURE (ATMOSPHERIC OR VACUUM)
- PEAK APPLIED PRESSURE
- INITIAL HOT SURFACE TEMPERATURE
- RESIDENCE TIME*

GRADES FOR TECHNICAL PERFORMANCE TESTS

		Percent of Total U.S. Production[a]			Percent of Total U.S. Production[a]
1.	Newsprint	7.7	6.	Recycled paperboard	11.6
2.	Uncoated printing or writing paper	13.2	7.	Lightweight coating	- -
3.	Tissue	7.2	8.	Recycled linerboard	- -
4.	Linerboard	23.1	9.	Recycled corrugating medium	- -
5.	Corrugating medium, virgin	7.3	10.	High-yield experimental pulp	- -

[a]Combined paper and board production.

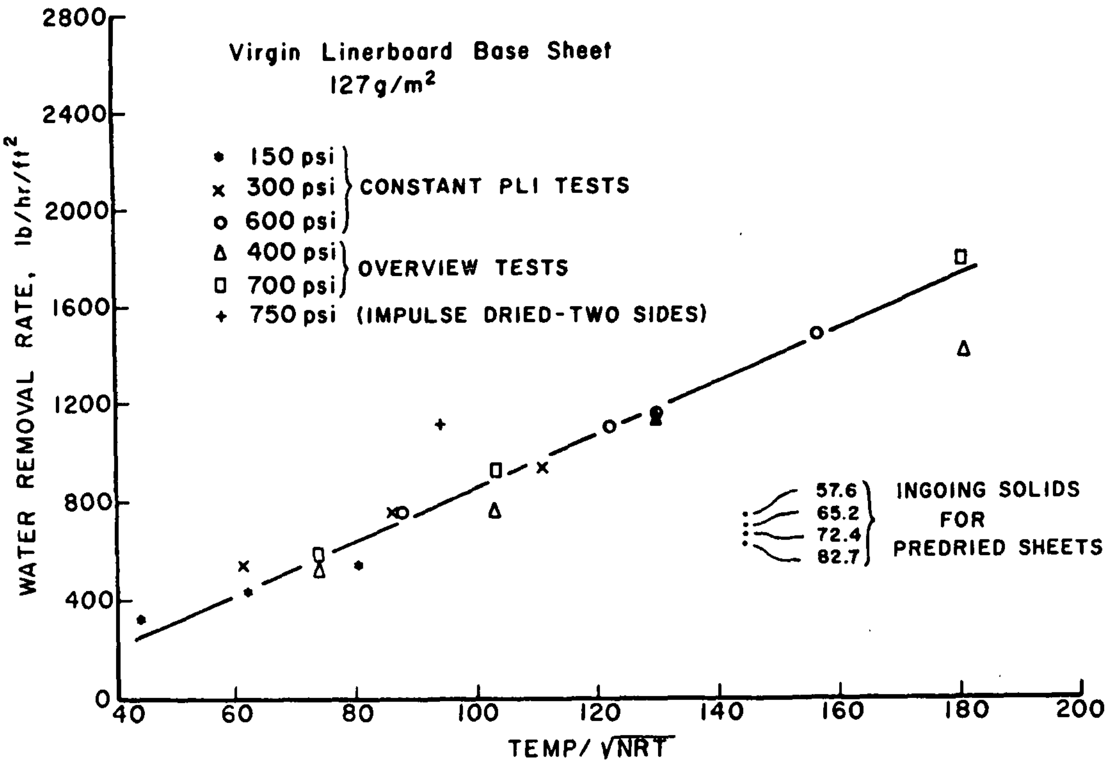

WATER REMOVAL RATES FOR VIRGIN LINERBOARD BASE STOCK.

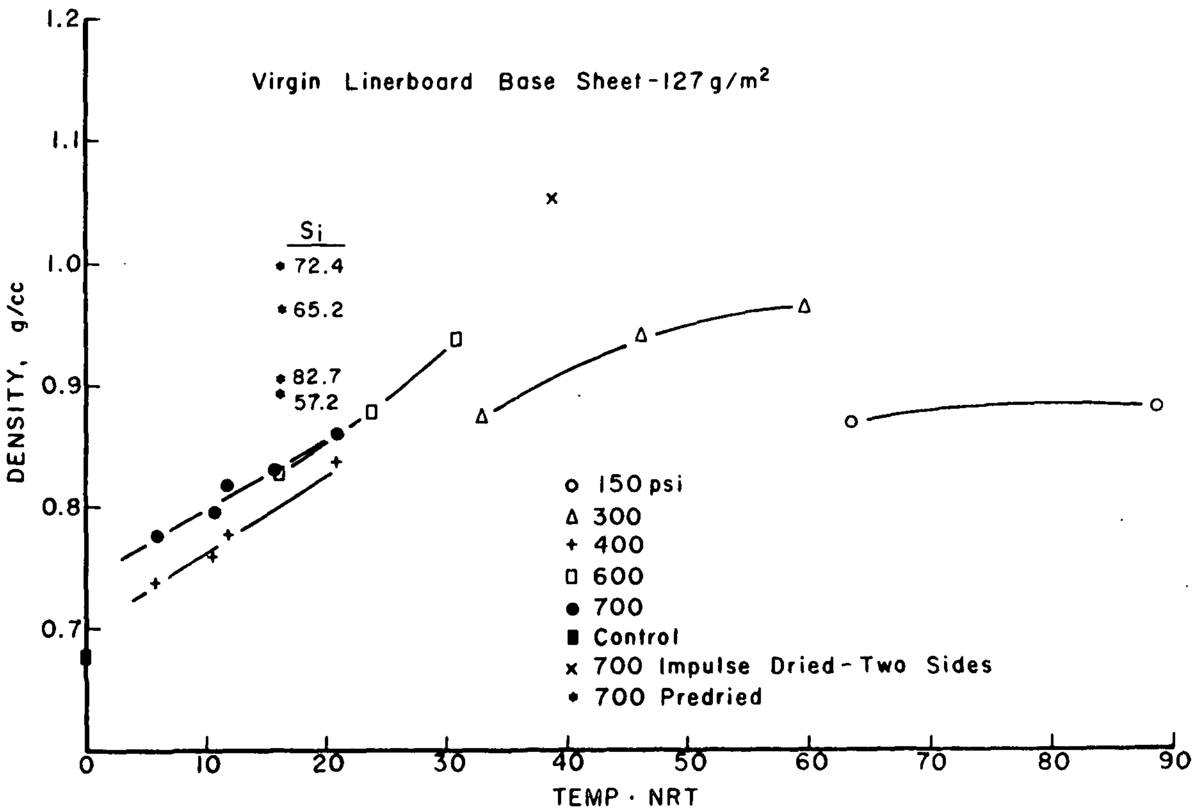

DENSITY DEVELOPMENT FOR VIRGIN LINERBOARD BASE SHEET.

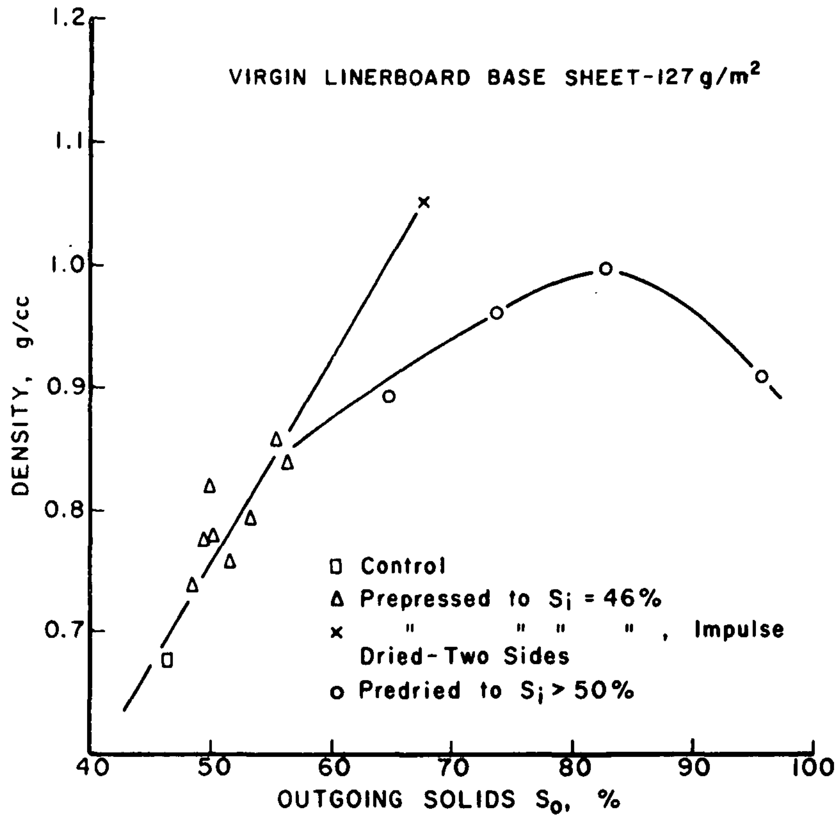

DENSITY DEVELOPMENT WITH DRYNESS FOR VIRGIN LINERBOARD BASE SHEET.

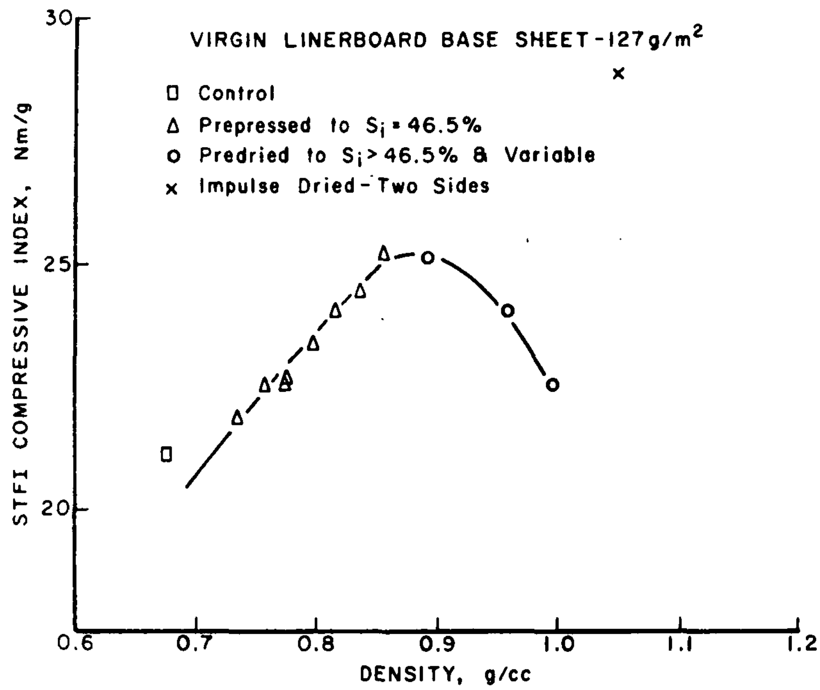

COMPRESSIVE STRENGTH VARIATION WITH DENSITY FOR VIRGIN LINERBOARD BASE STOCK.

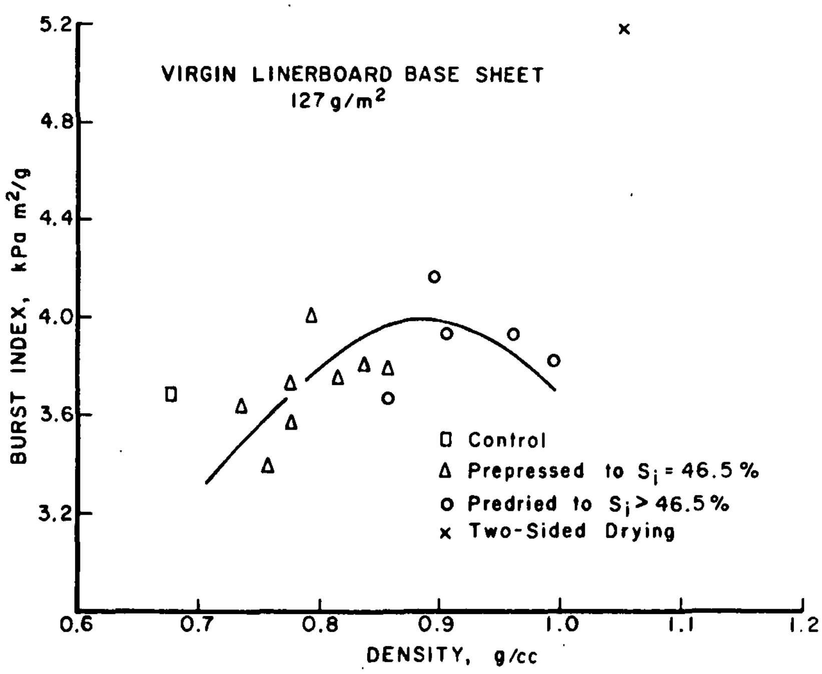

BURST DEVELOPMENT WITH DENSITY FOR VIRGIN LINERBOARD BASE SHEET.

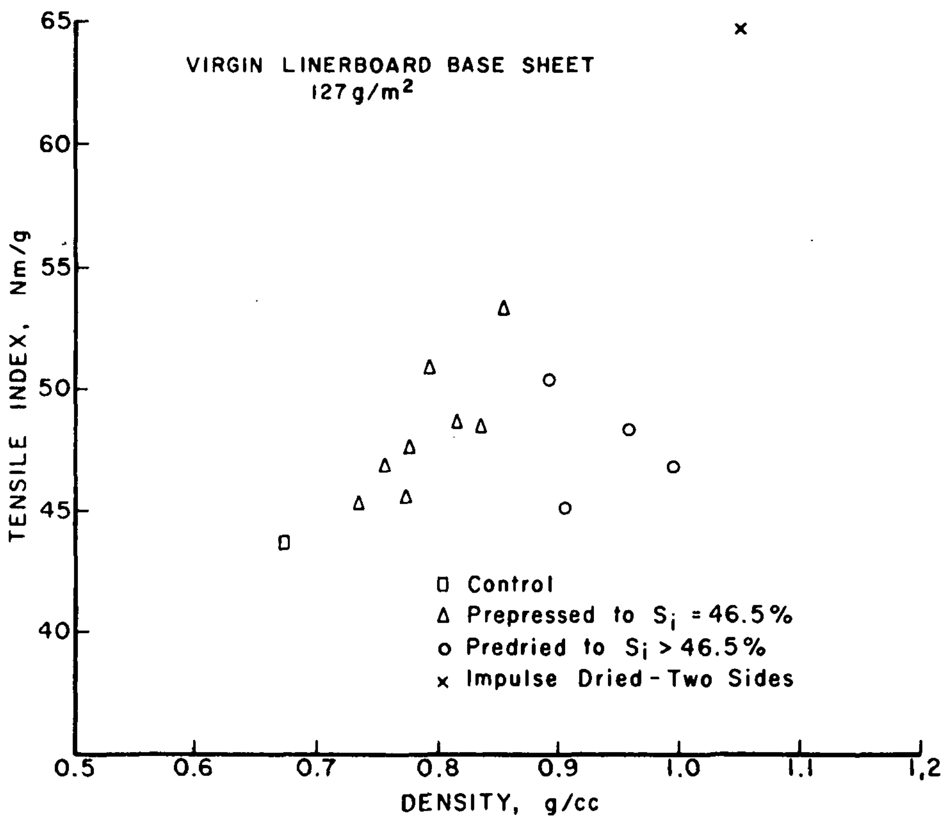

TENSILE STRENGTH DEVELOPMENT WITH DENSITY FOR VIRGIN LINERBOARD BASE SHEET.

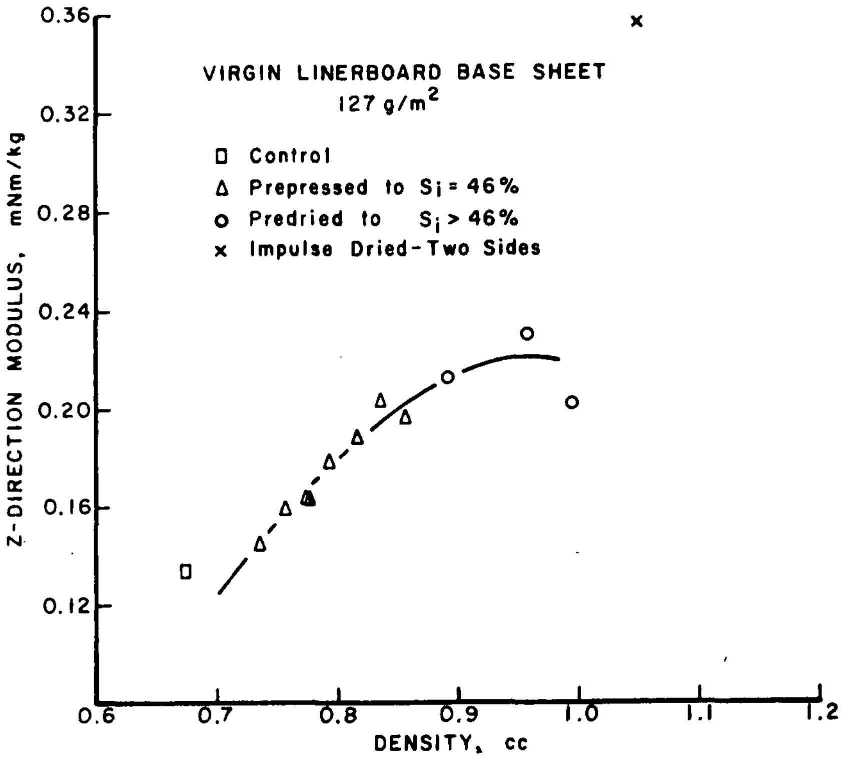

Z-DIRECTION MODULUS VARIATION WITH DENSITY
FOR VIRGIN LINERBOARD BASE SHEET.

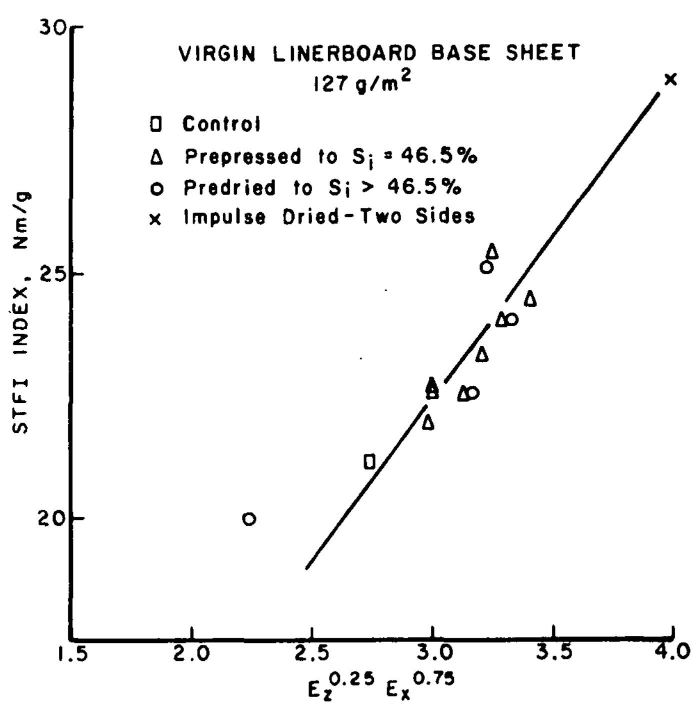

HABEGER-WHITSITT COMPRESSIVE STRENGTH MODEL
FOR VIRGIN LINERBOARD BASE SHEET.

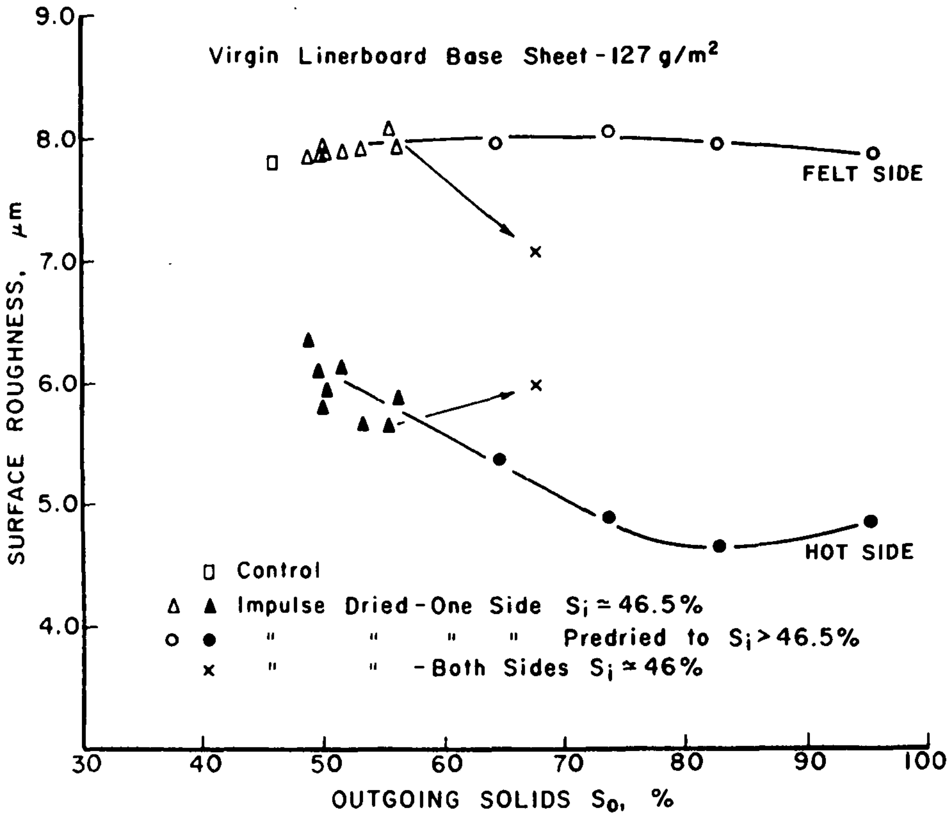

ROUGHNESS CHANGES WITH DRYNESS FOR VIRGIN LINERBOARD BASE SHEET.

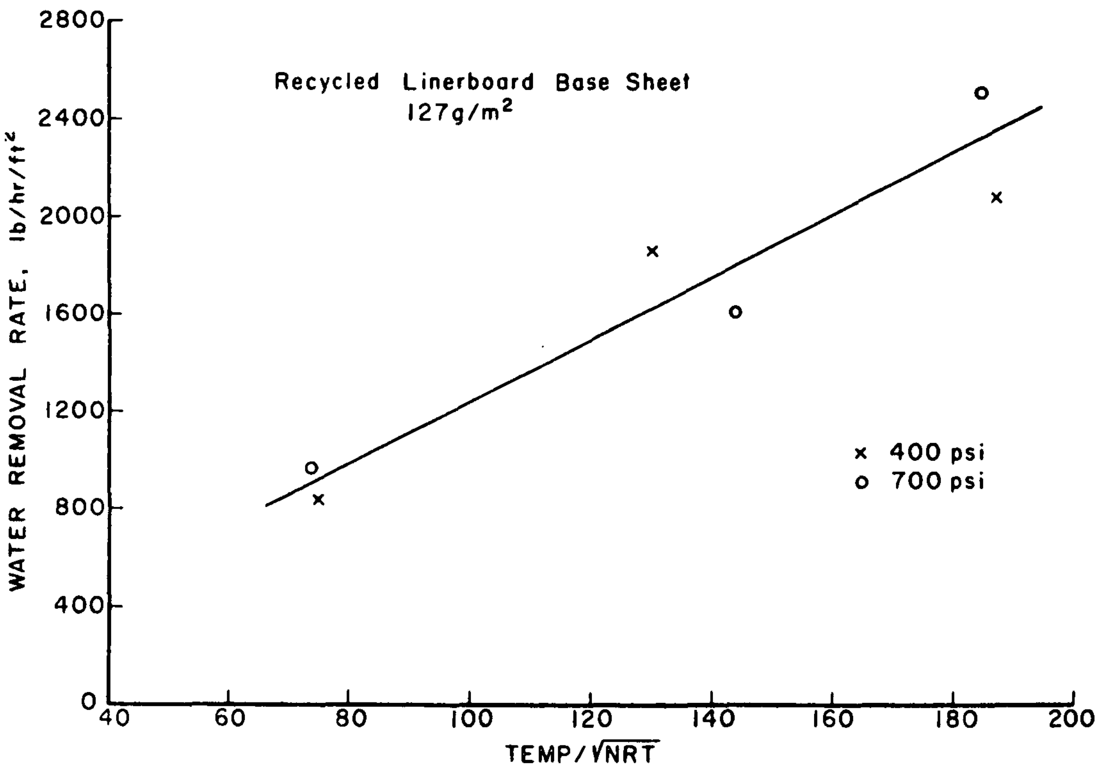

WATER REMOVAL RATES FOR RECYCLED LINERBOARD BASE STOCK.

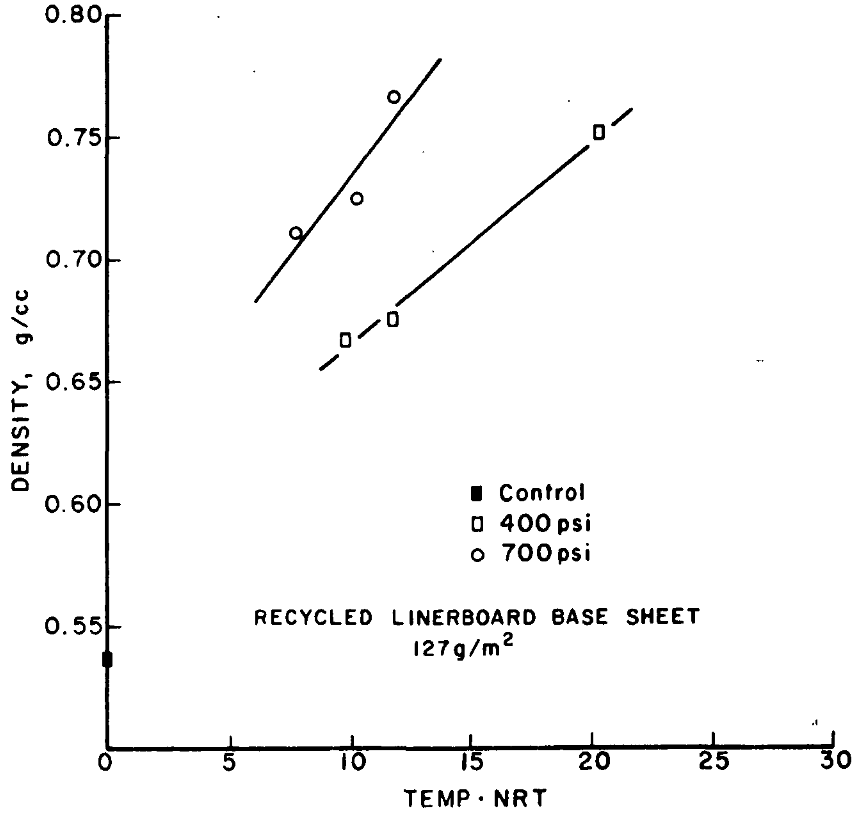

DENSITY DEVELOPMENT FOR RECYCLED LINERBOARD BASE STOCK.

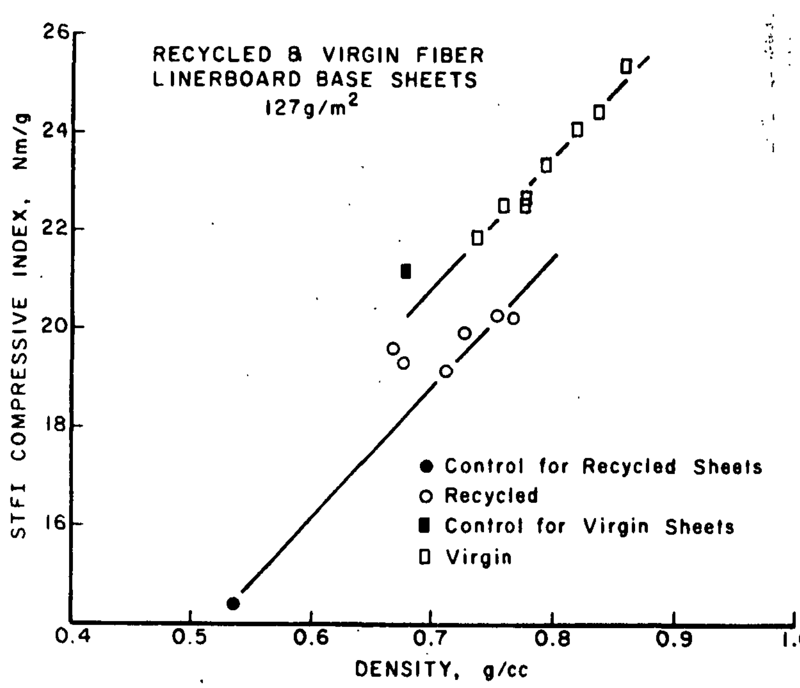

COMPRESSIVE STRENGTH - DENSITY RELATIONSHIPS FOR VIRGIN AND RECYCLED LINERBOARD.

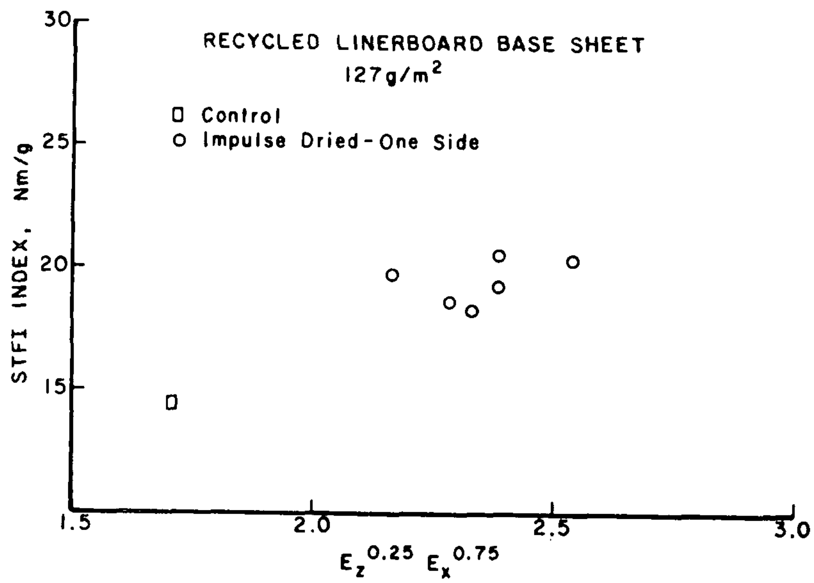

HABEGER-WHITSITT COMPRESSIVE STRENGTH MODEL FOR RECYCLED LINERBOARD BASE SHEET.

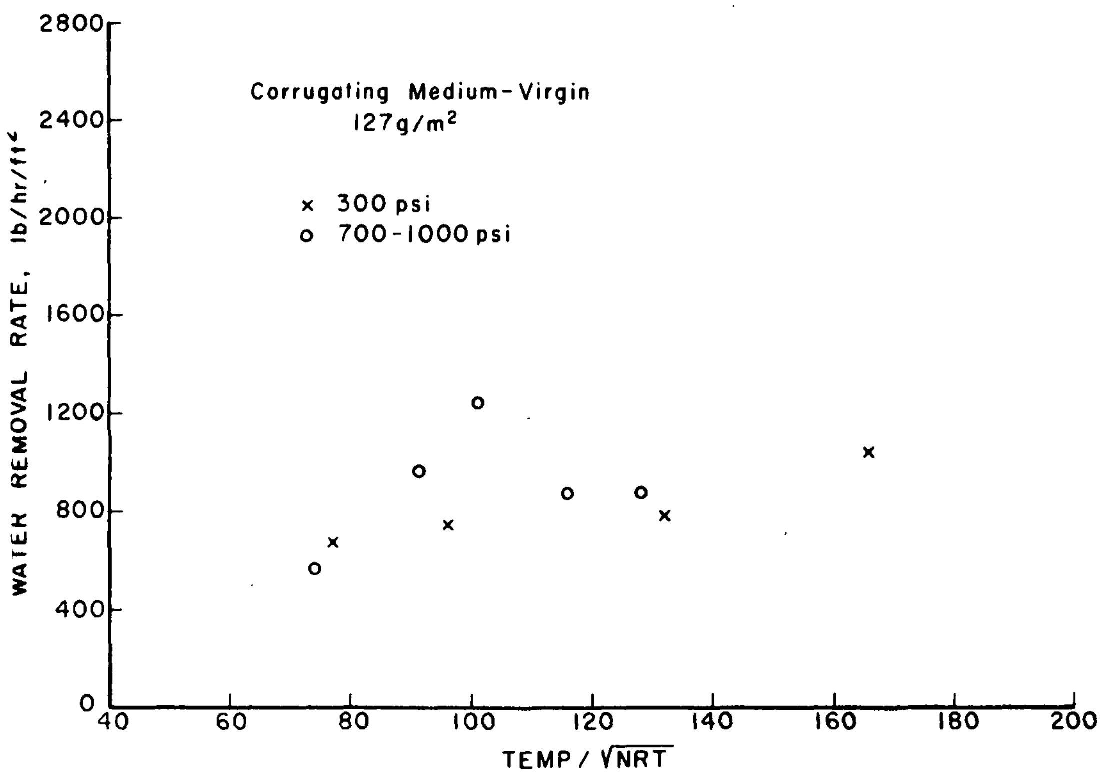

WATER REMOVAL RATES FOR VIRGIN CORRUGATING MEDIUM.

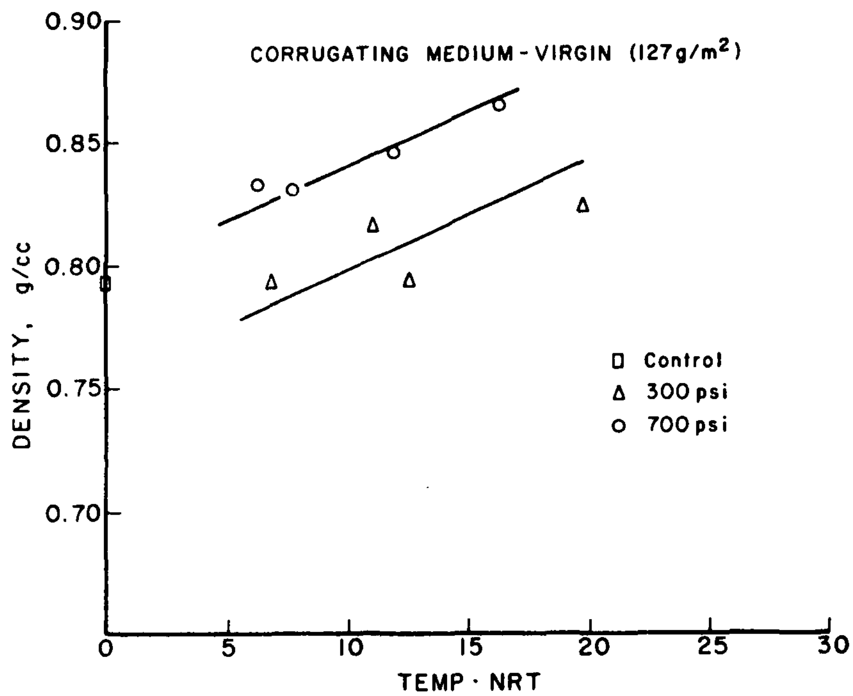

DENSITY DEVELOPMENT FOR CORRUGATING MEDIUM.

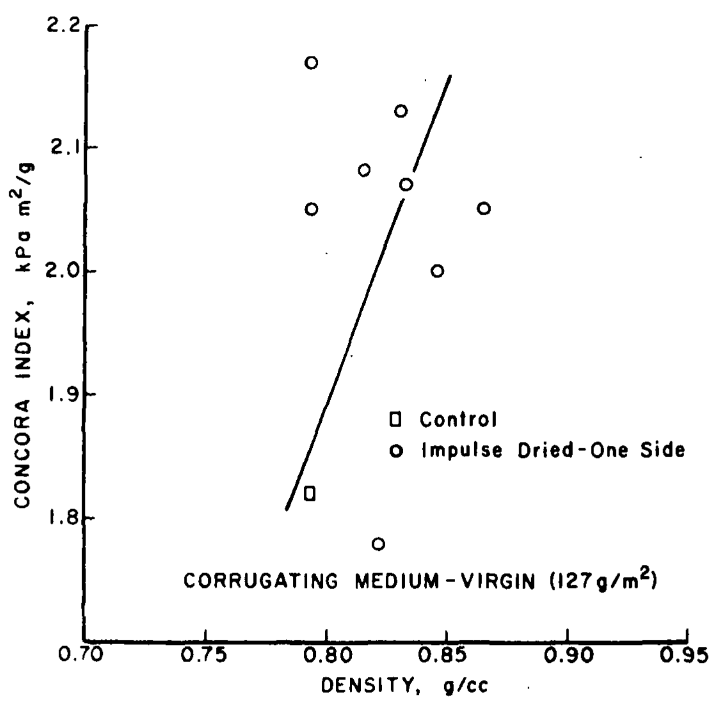

CONCORA VARIATION WITH DENSITY
FOR VIRGIN CORRUGATING MEDIUM.

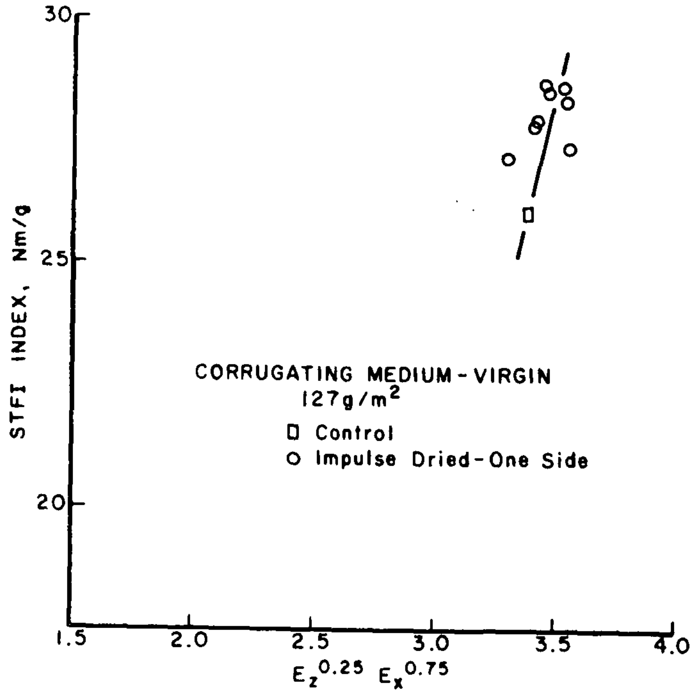

HABEGER-WHITSITT COMPRESSIVE STRENGTH MODEL FOR CORRUGATING MEDIUM.

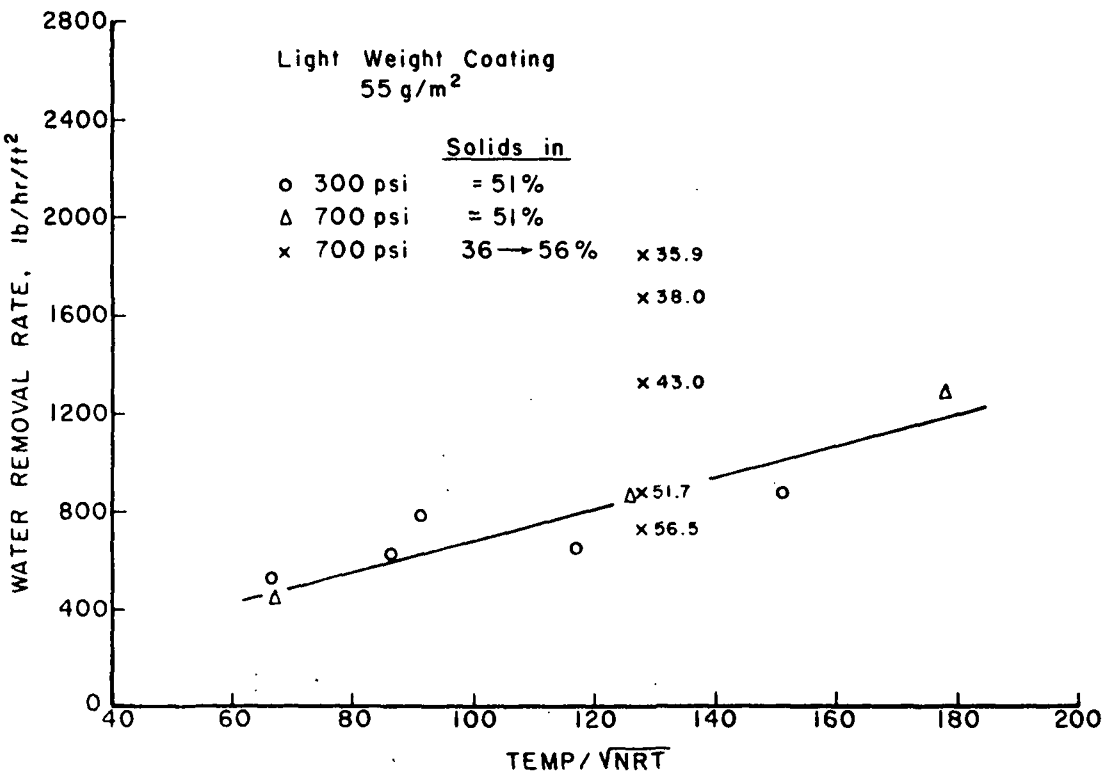

WATER REMOVAL RATES FOR LIGHTWEIGHT COATING PAPER.

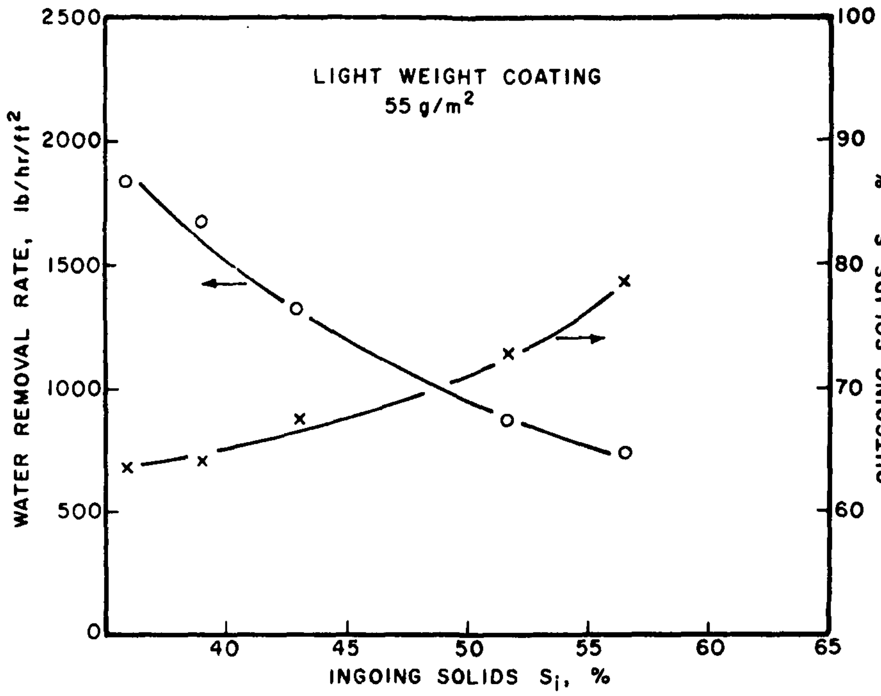

WATER REMOVAL RATE AND OUTGOING SOLIDS VARIATIONS WITH PREPRESSING LEVEL FOR LIGHTWEIGHT COATING PAPER.

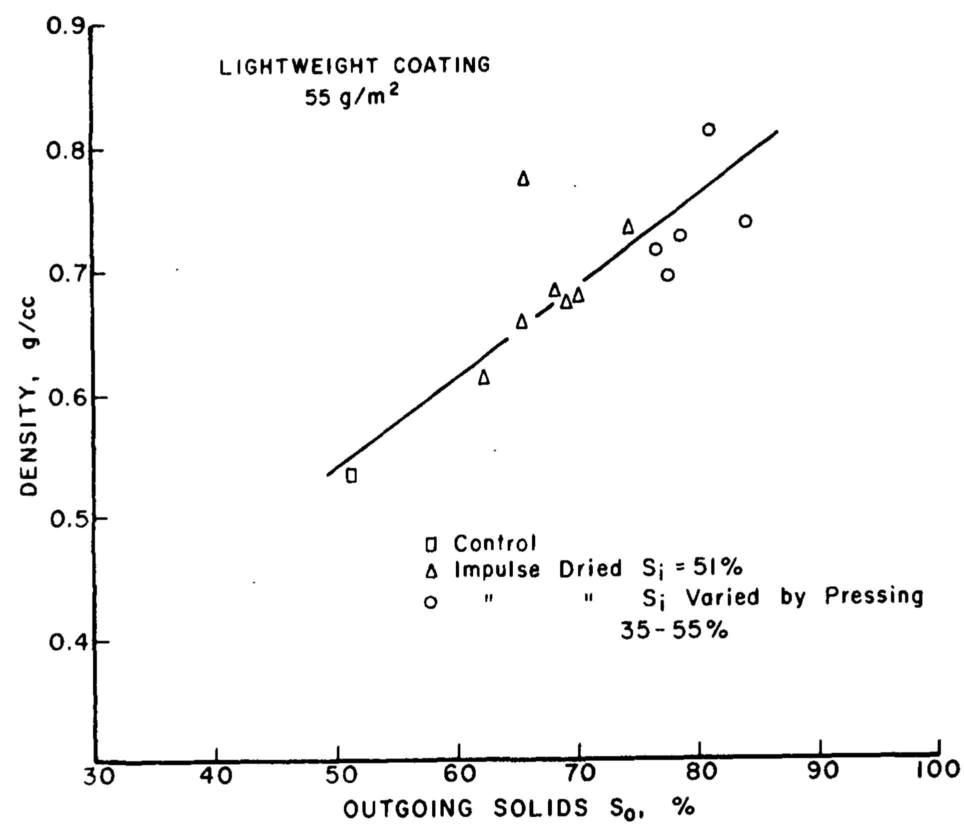

DENSITY DEVELOPMENT WITH DRYNESS FOR LIGHTWEIGHT COATING GRADE.

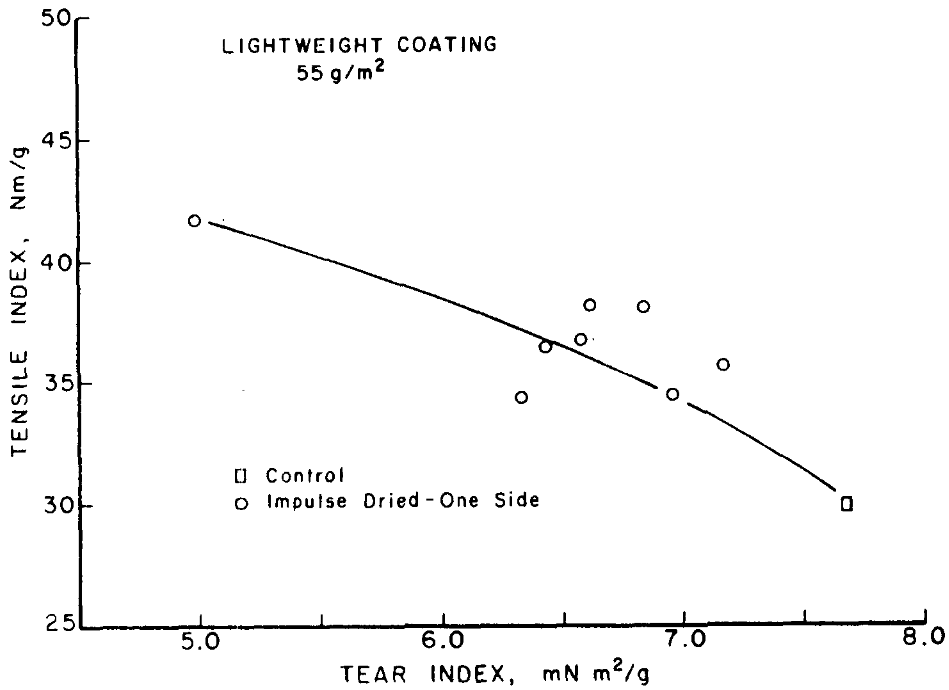

TENSILE-TEAR RELATIONSHIP FOR LIGHTWEIGHT COATING GRADE.

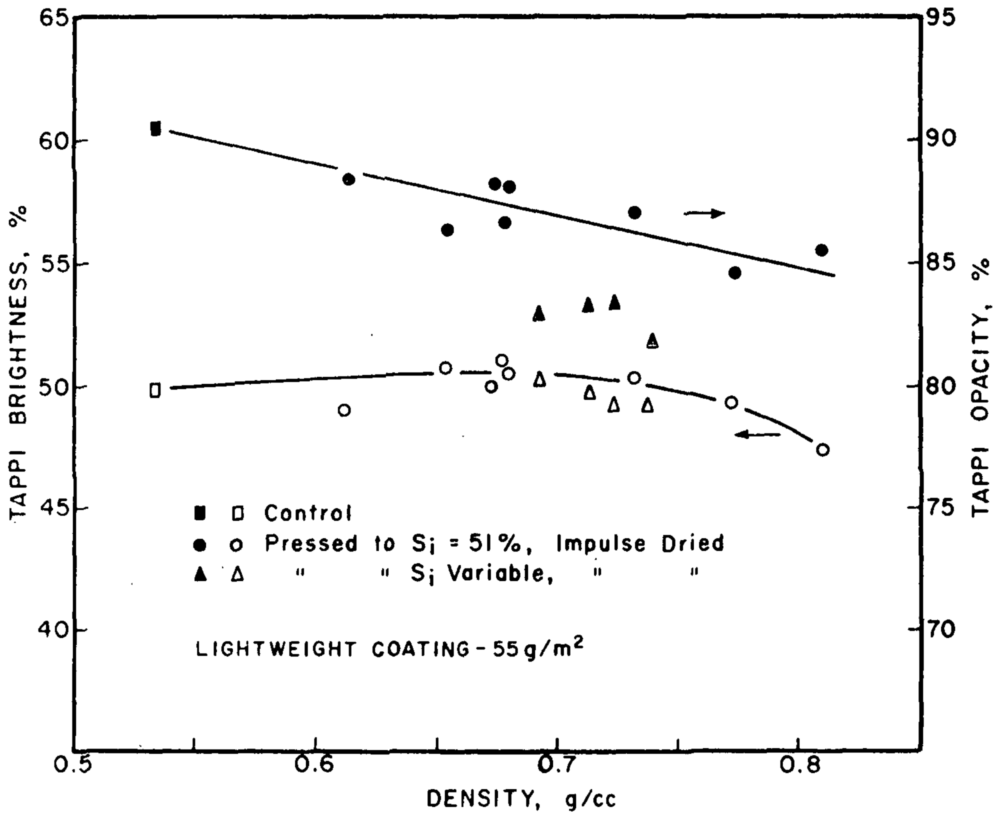

BRIGHTNESS AND OPACITY CHANGES WITH DENSITY
FOR LIGHTWEIGHT COATING PAPER.

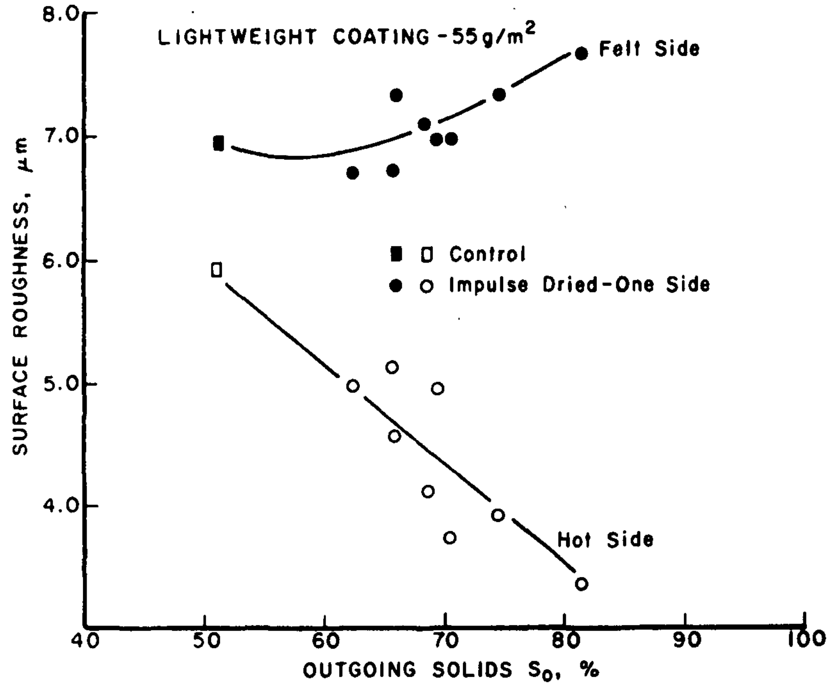

ROUGHNESS CHANGES WITH DRYNESS FOR LIGHTWEIGHT COATING PAPER.

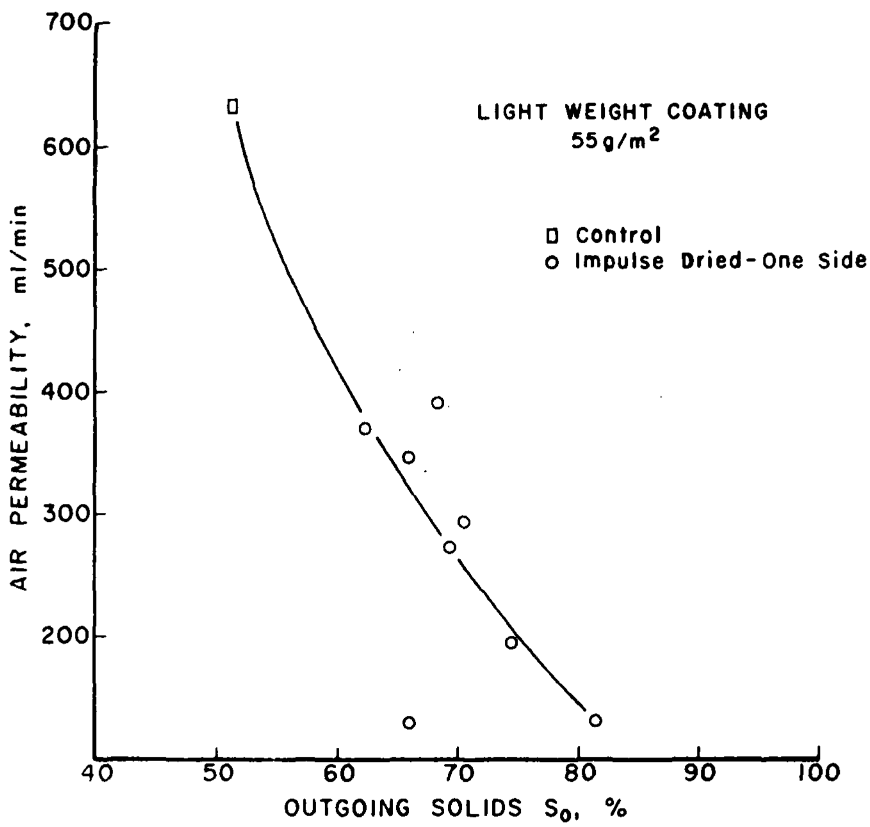

AIR PERMEABILITY VARIATIONS WITH OUTGOING SOLIDS FOR LIGHTWEIGHT COATING PAPER.

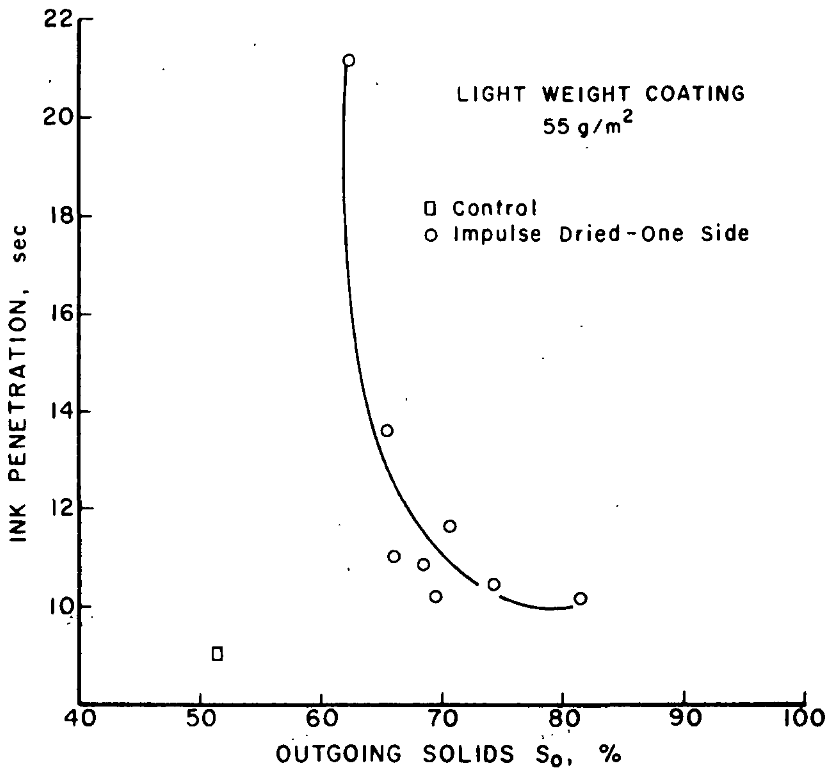

INK PENETRATION VARIATION WITH OUTGOING SOLIDS FOR LIGHTWEIGHT COATING PAPER.

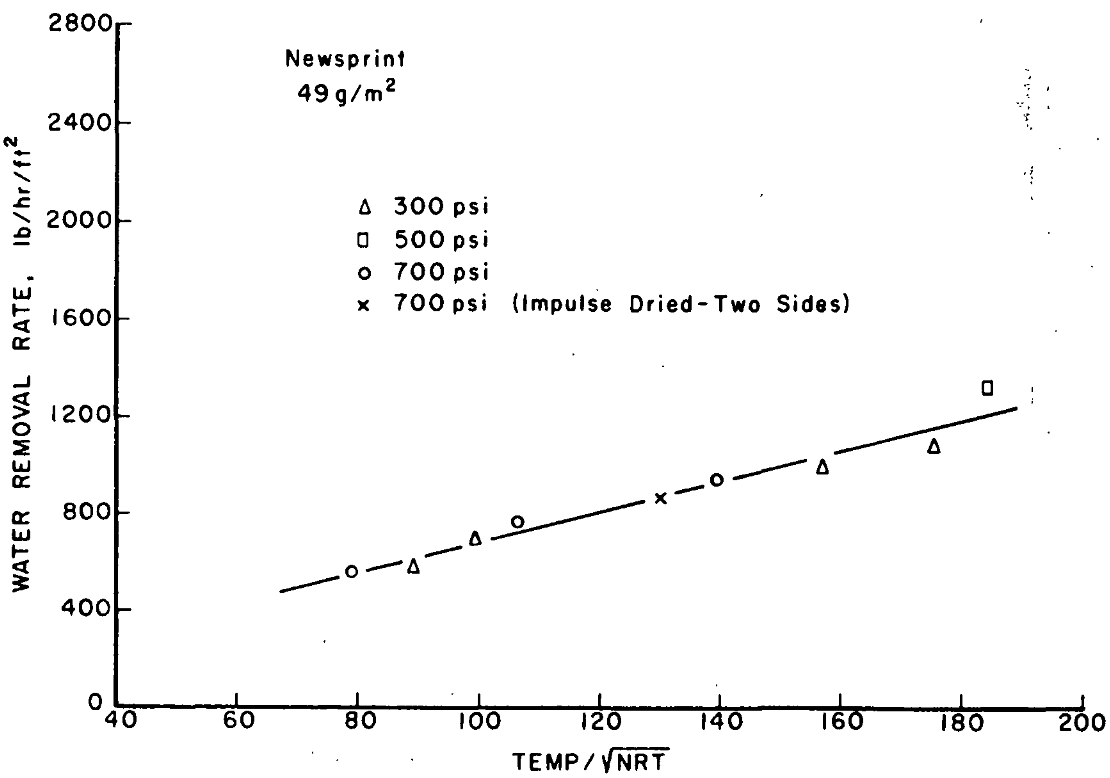

WATER REMOVAL RATES FOR NEWSPRINT.

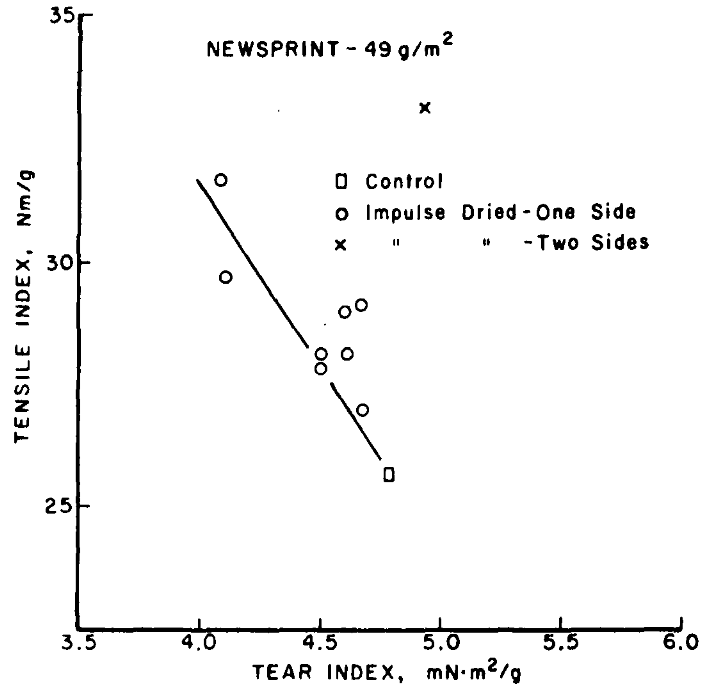

TENSILE-TEAR RELATIONSHIP FOR NEWSPRINT.

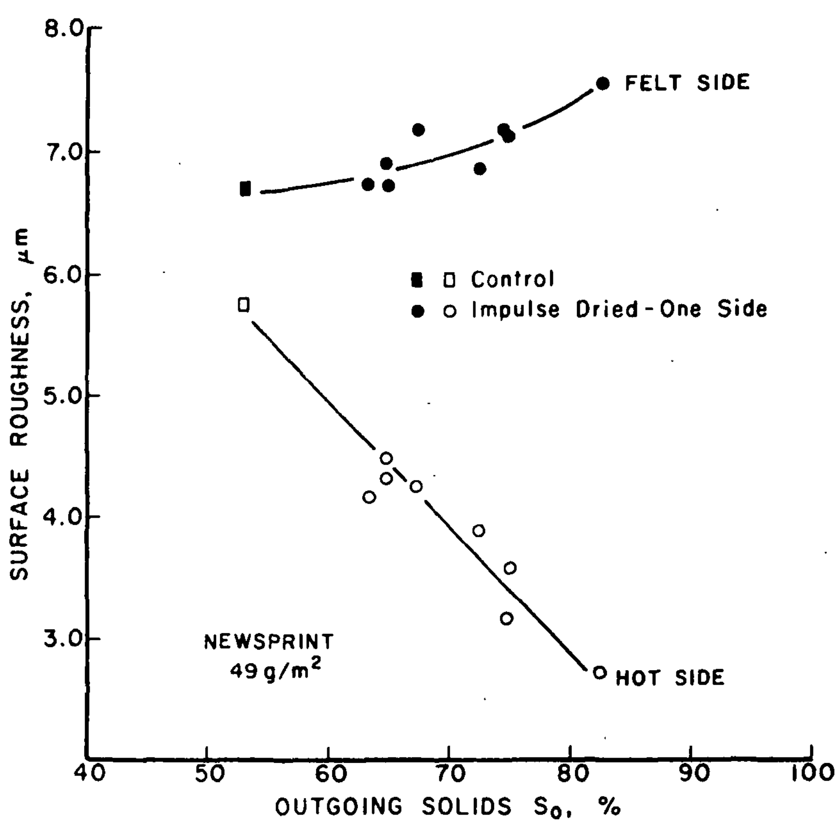

ROUGHNESS CHANGES WITH DRYNESS FOR NEWSPRINT.

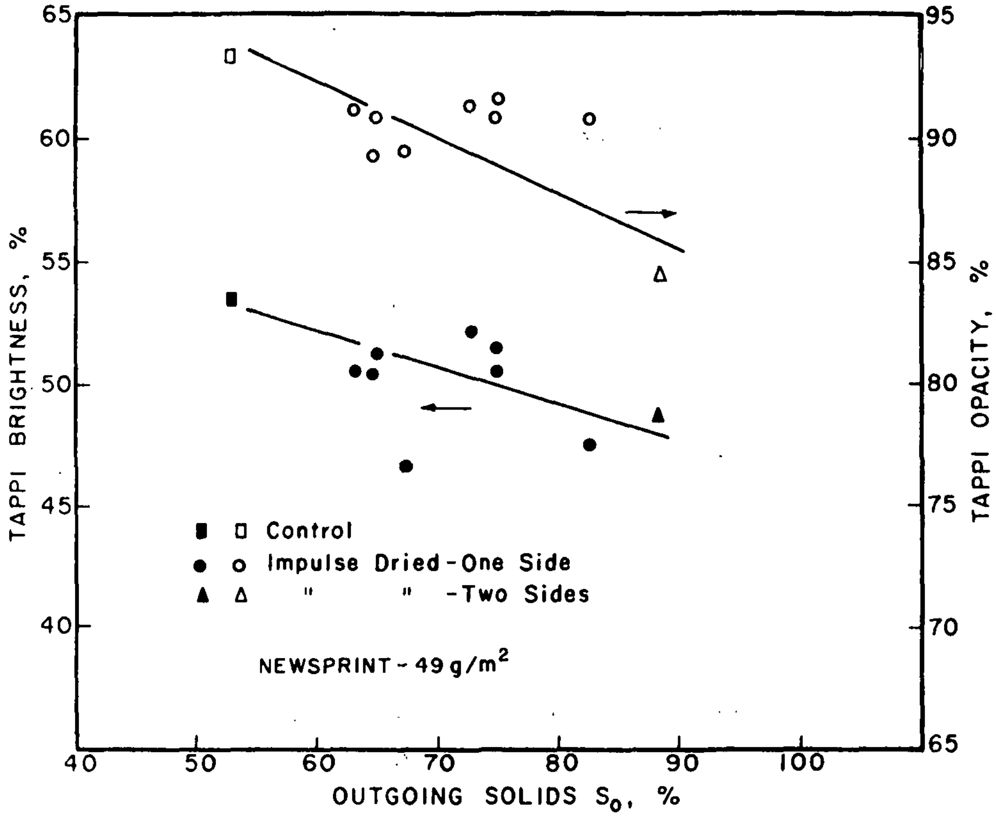

BRIGHTNESS AND OPACITY CHANGES WITH DRYNESS FOR NEWSPRINT.

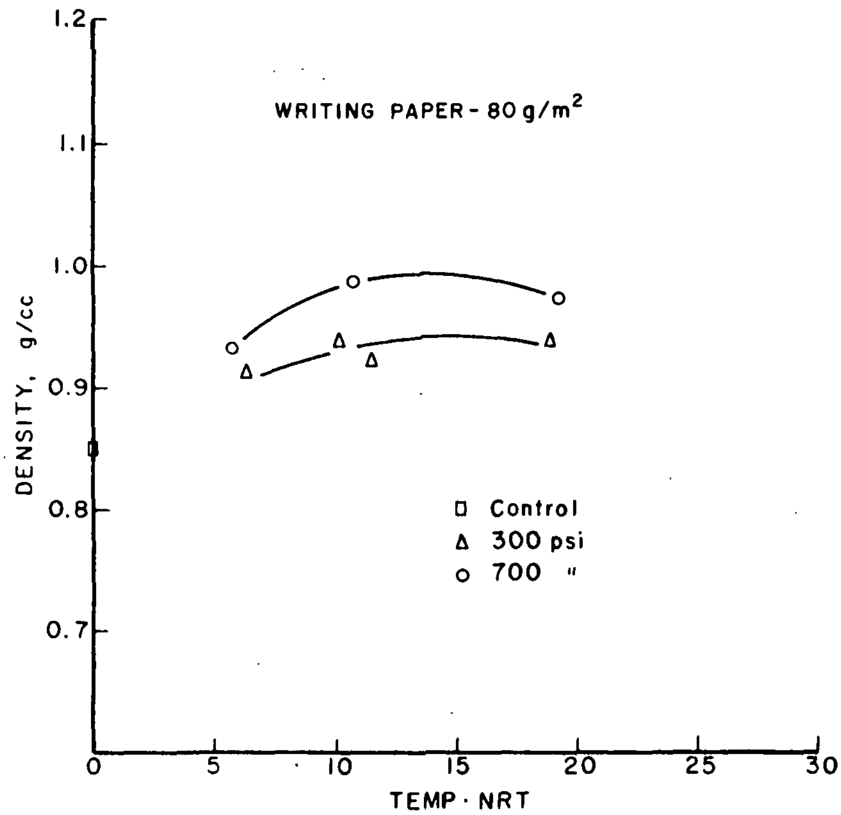

DENSITY DEVELOPMENT FOR WRITING PAPER.

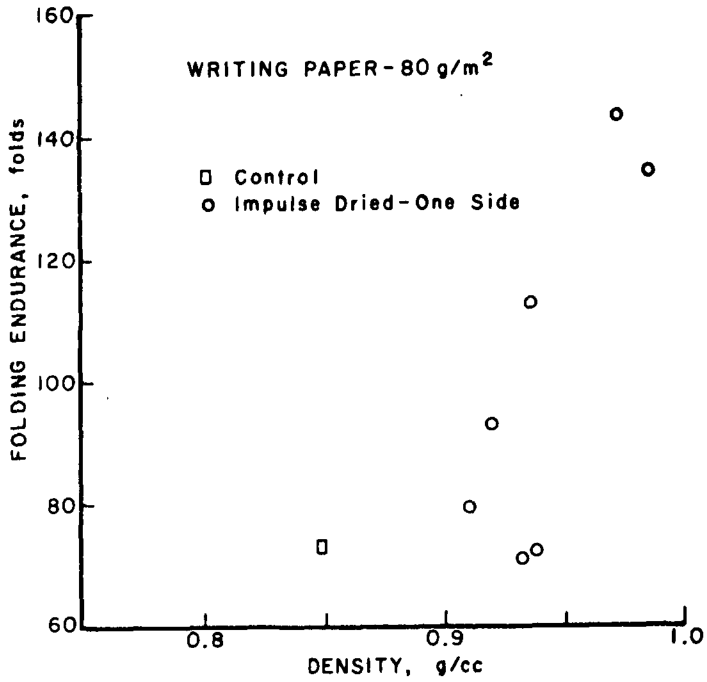

FOLD ENDURANCE VARIATIONS WITH
DENSITY FOR WRITING PAPER.

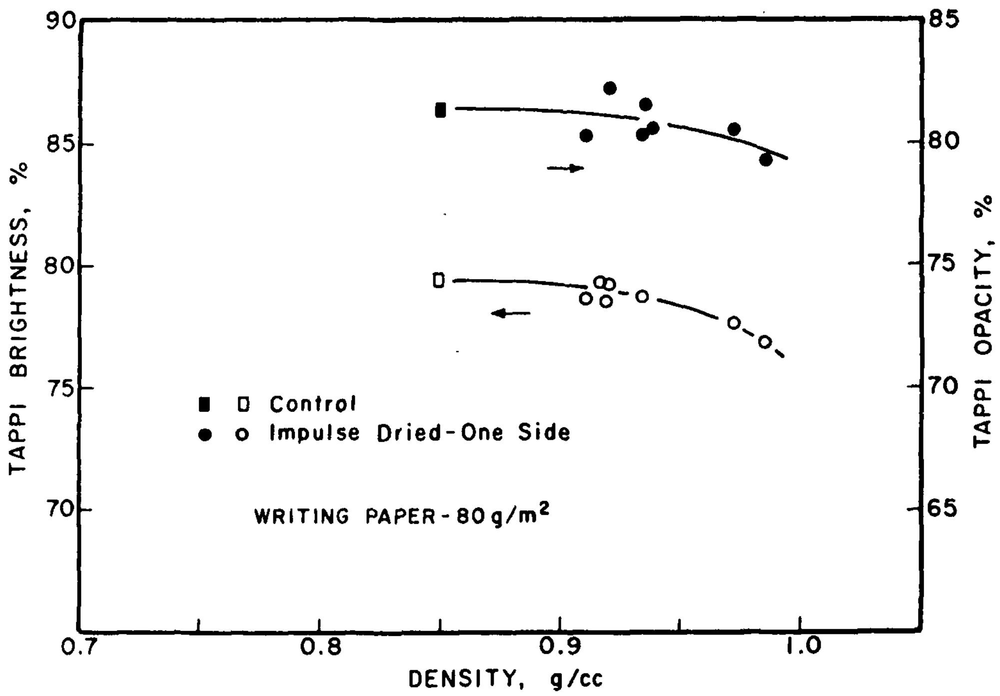

BRIGHTNESS AND OPACITY CHANGES
WITH DENSITY FOR WRITING PAPER.

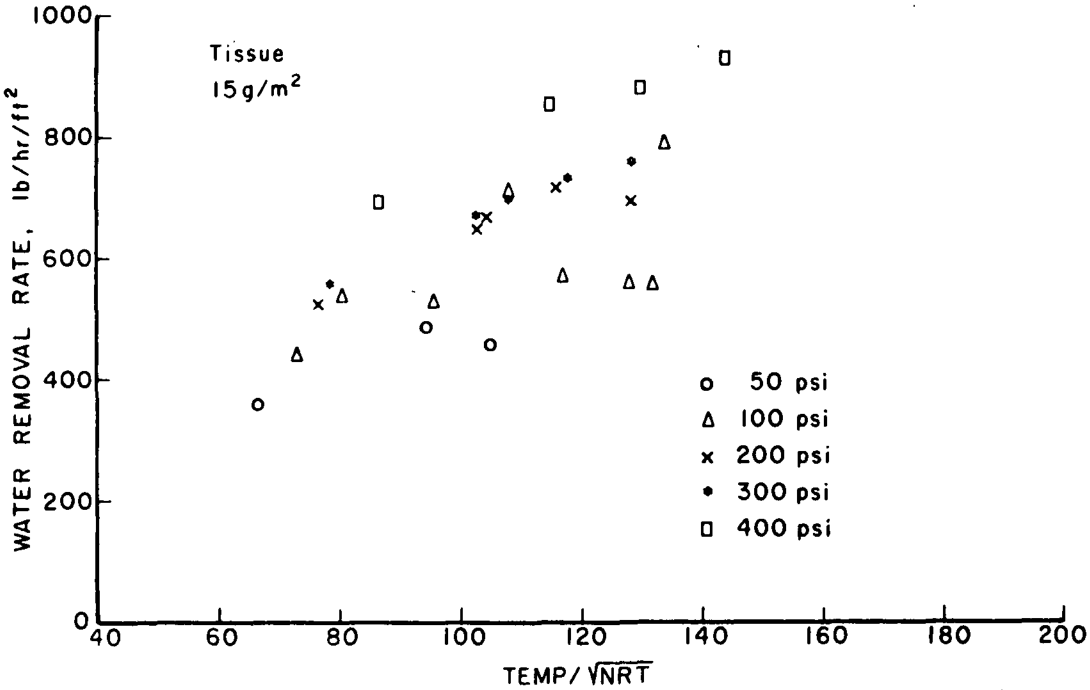

WATER REMOVAL RATES FOR TISSUE.

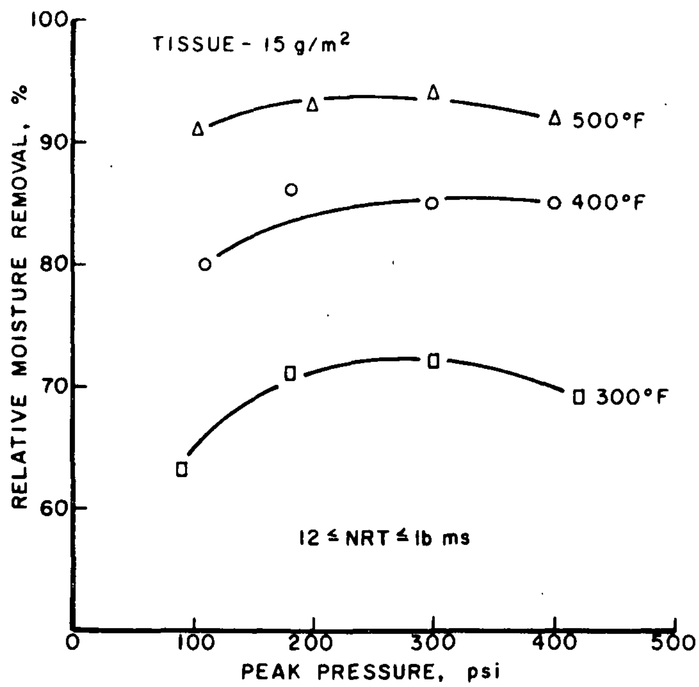

VARIATION OF RELATIVE MOISTURE
REMOVAL WITH PRESSURE FOR TISSUE.

WATER REMOVAL RATE CORRELATIONS - IMPULSE DRYING

GENERAL FORM: $WRR = A + B \cdot P + C \cdot TEMP/\sqrt{NRT}$

GRADE	A	B	C	R^2	BW
VIRGIN LINER	-397	0.407	0.308	0.97	127
RECYCLED LINER	-151	0.306	0.389	0.90	127
CORRUGATING MEDIUM	290	0.314	0.115	0.32	127
WRITING PAPER	-116	0.494	0.232	0.81	80
LWC	-98.9	0.350	0.183	0.80	55
NEWSPRINT	-55.5	0.163	0.204	0.96	49

DENSITY CORRELATIONS - IMPULSE DRYING

GENERAL FORM: $\rho = D + E \cdot P + F \cdot TEMP \cdot NRT$

GRADE	D	E	F	R^2	BW
VIRGIN LINER	0.643	0.0001	0.0066	0.98	127
RECYCLED LINER	0.483	0.0003	0.0080	0.98	127
CORRUGATING MEDIUM	0.747	0.00008	0.0029	0.78	127
WRITING PAPER	0.870	0.0001	0.0019	0.78	80
LWC	0.502	0.0002	0.0088	0.93	55
NEWSPRINT	0.540	0.0001	0.0088	0.79	49

OBSERVATIONS 1

- WRR & TWR VERY HIGH TEMP NRT P
- DENSITY VERY HIGH TEMP·NRT P
- STRENGTH USUALLY INCREASES WITH DENSITY
- COMPRESSIVE STRENGTH FOLLOWS HW MODEL

OBSERVATIONS 2

- LARGE SMOOTHNESS INCREASES
- LARGE ABSORBENCY DECREASES
- LARGE AIR PERMEABILITY DECREASES
- LARGE PICK RESISTANCE INCREASES

OBSERVATIONS 3

- SMALL BRIGHTNESS DECREASES
- SMALL OPACITY DECREASES

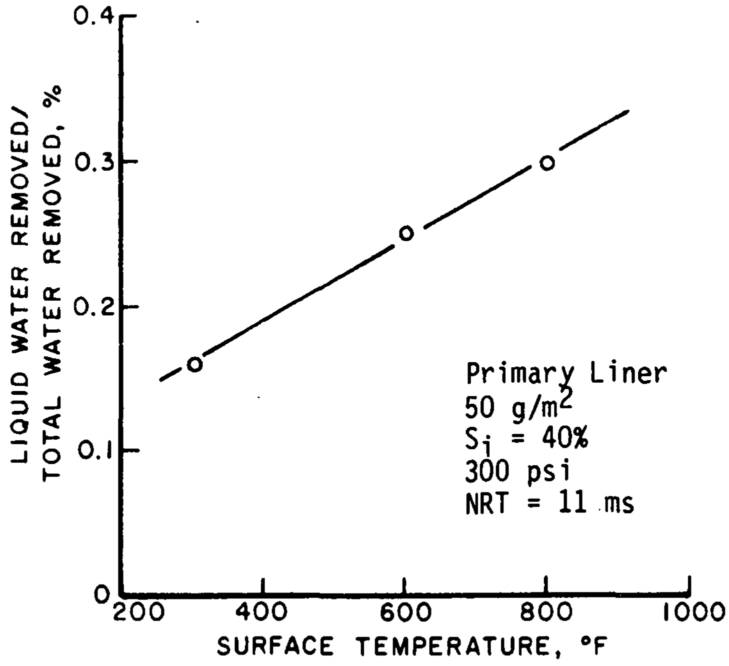

LIQUID WATER REMOVAL IN IMPULSE DRYING.

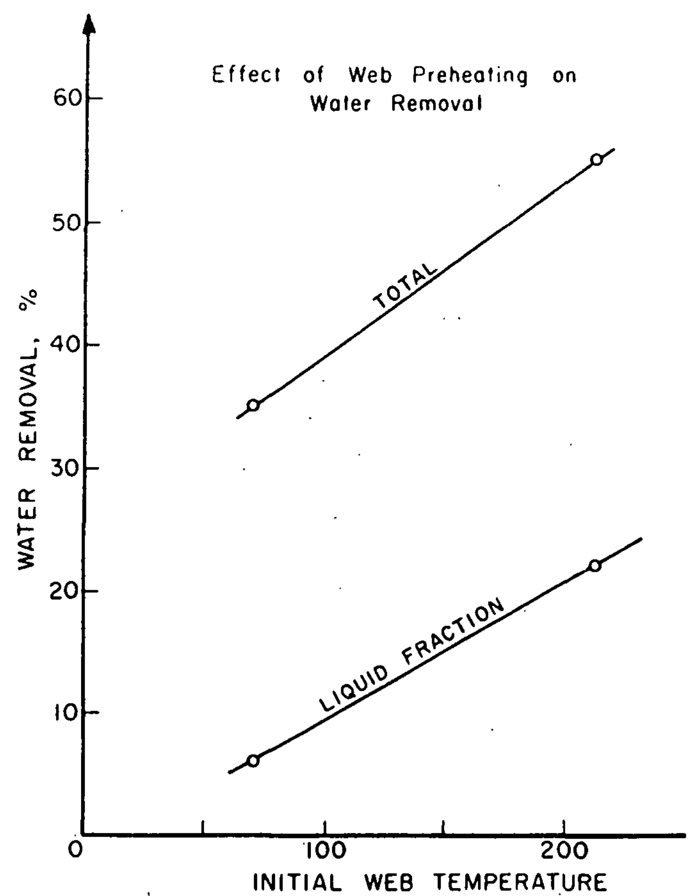

EFFECT OF WEB PREHEATING
IN LIQUID WATER REMOVAL.

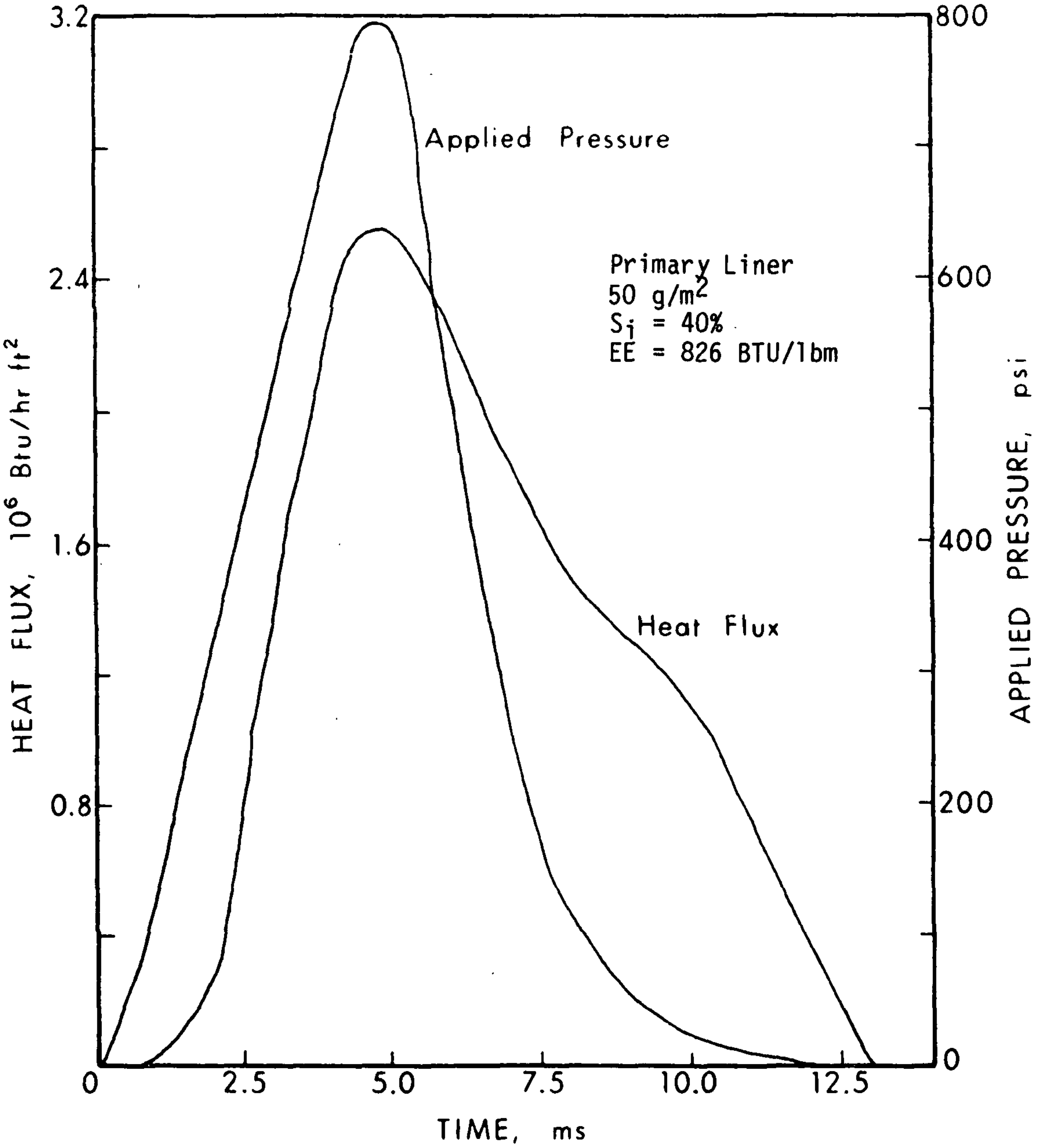

INSTANTANEOUS HEAT FLUX IN IMPULSE DRYING.
ROOM TEMPERATURE WEB.

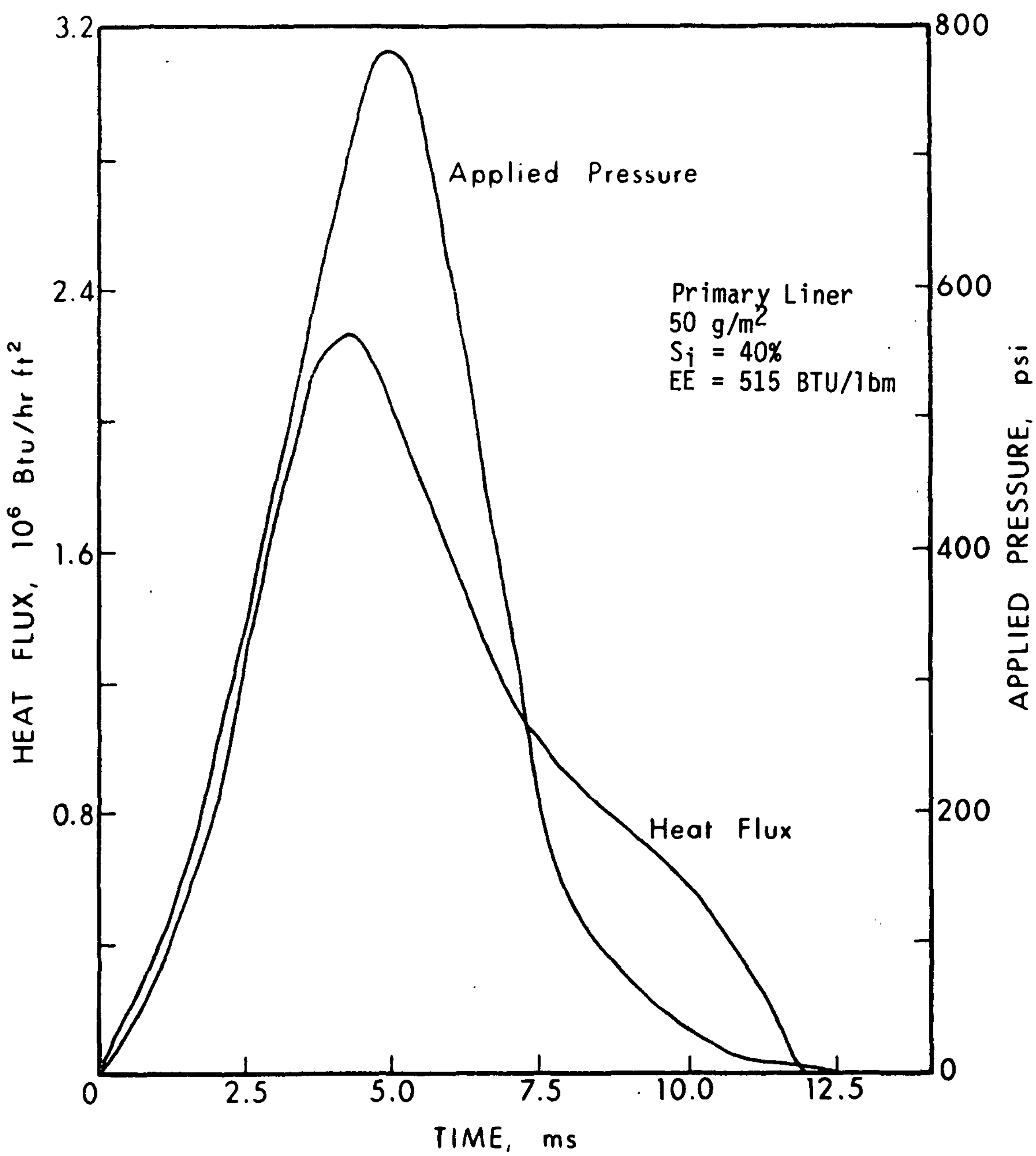

INSTANTANEOUS HEAT FLUX IN IMPULSE DRYING.
PREHEATED WEB.

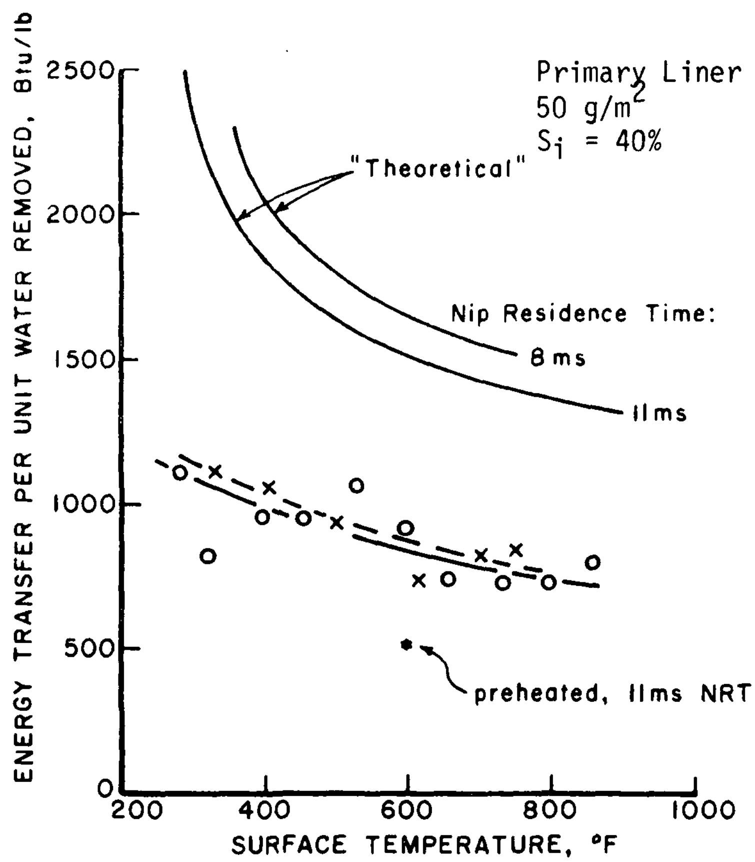

THEORETICAL HEAT INPUT FOR PURE EVAPORATION PROCESS AND ACTUAL HEAT INPUT FOR IMPULSE DRYING.

VALUE TO THE INDUSTRY

- PROPERTY DEVELOPMENT/CONTROL
- PRODUCTIVITY
- DRYER SIZE/CAPITAL COST
- MOISTURE & PROPERTY PROFILE LEVELING
- NEW PRODUCT PROPERTIES
- LESS DRYING ENERGY

IMPULSE DRYING

Plans for the coming period

Hugh P. Lavery

Topics for Discussion:

-Overview of research questions

-Priorities

-Six-month Deliverables

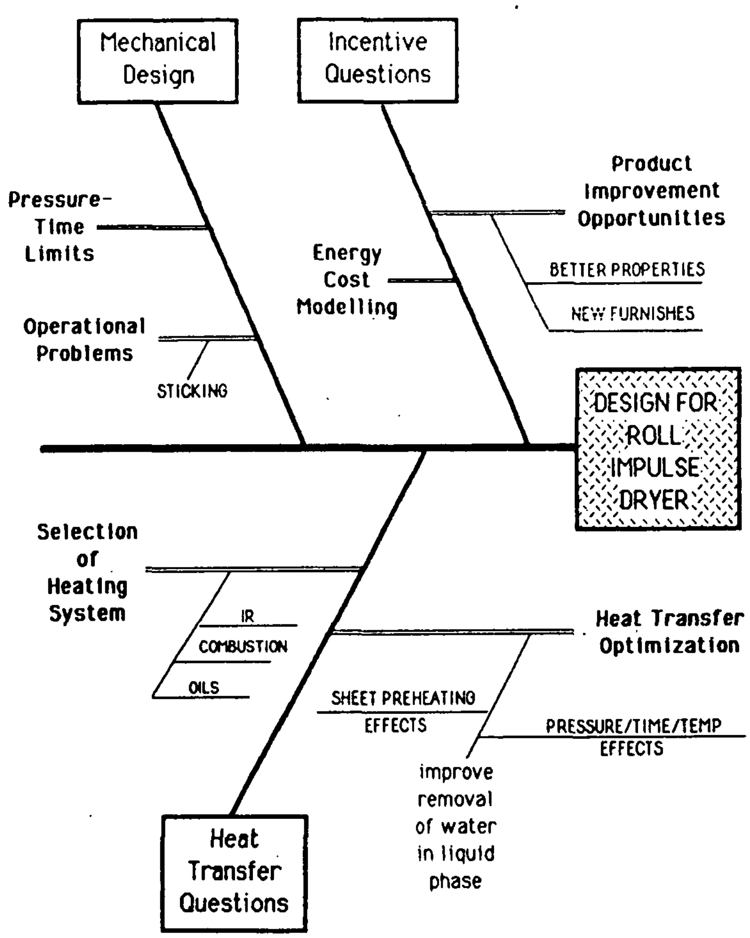

Impulse Drying

Priorities for coming period:

- To complete work to determine how to maximize liquid water removal in an impulse dryer

- To complete the heat transfer and mechanical systems designs for a pilot roll impulse dryer

- To complete the studies in progress on product improvement incentives with both conventional and alternative low-cost furnishes

Maximizing liquid water removal is essential to impulse dryer design.

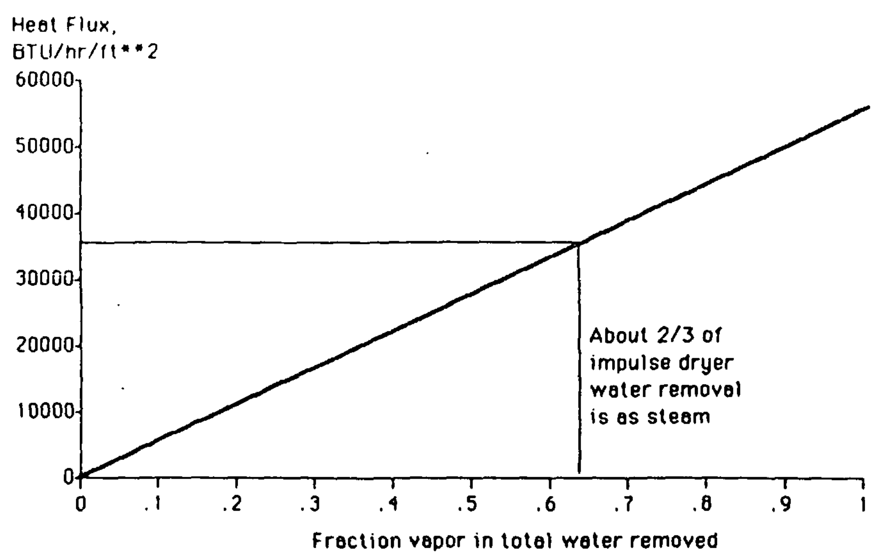

Curve was calculated assuming a 3 foot diameter roll, and a heater covering 3/4 of the roll surface.

Optimization of water removal in liquid phase

Plans: To complete analysis of past data and to perform additional experiments as needed.

Essential data includes heat flux through the nip and liquid water removal as measured by the LiCl tracer technique

IMPORTANT VARIABLES

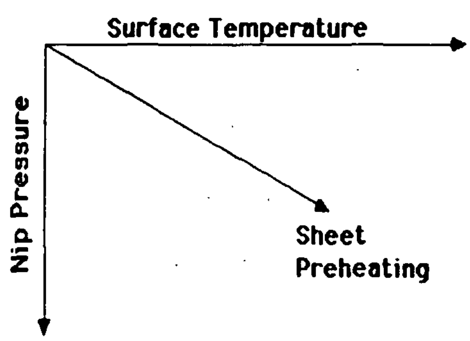

Heat fluxes correspond to reasonable heater temperatures

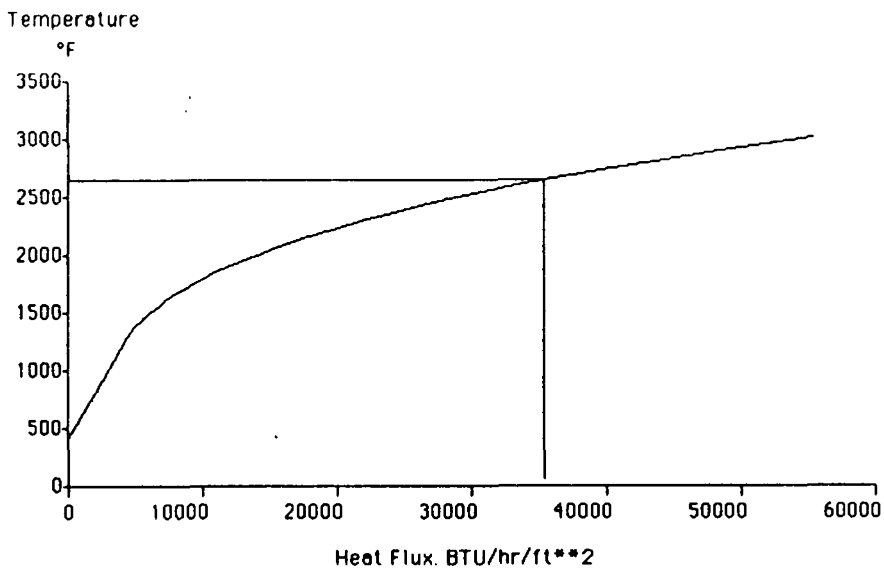

Calculated for a 400°F roll
surface temperature with
a heater emissivity of 0.8
and a roll emissivity of 0.3.
Assumed no participating gases.

Incentives:
Product improvement
and
Furnish Cost Reduction

Plans: To complete and summarize experiments on improved strength properties from conventional furnishes.

To complete the 2-level factorial experiments in P, T, and NRT on lower-cost furnishes

- -TMP
- -High recycle linerboard

IMPULSE DRYING
Six-Month Deliverables

- Complete design for pilot impulse dryer
- Data to optimize liquid water removal
- Data on furnish incentives
- Pilot dryer experimental plans

IMPULSE DRYING

WATER REMOVAL IN A HIGH TEMPERATURE PRESS NIP

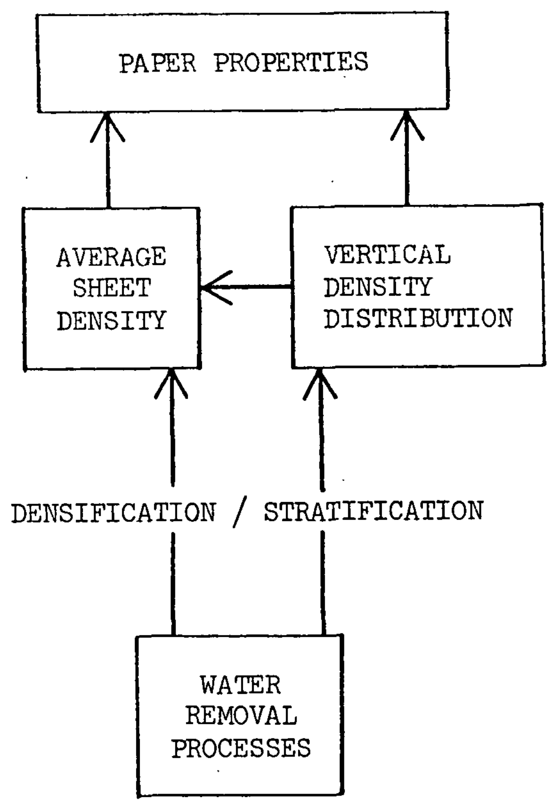

IMPULSE DRYING MECHANISMS

- ENHANCED WET PRESSING MECHANISMS
- HEAT TRANSFER/CONTACT COEFFICIENT
- THERMAL SOFTENING/INCREASED COMPRESSIBILITY
- VAPOR - INDUCED FLOW

THESIS TITLE

AN INVESTIGATION OF DYNAMIC DENSIFICATION UNDER IMPULSE DRYING CONDITIONS

PRIMARY THESIS OBJECTIVES

TO OBTAIN A FUNDAMENTAL UNDERSTANDING, BASED ON PHYSICAL PRINCIPLES, OF THE DYNAMIC DENSIFICATION PROCESS WHICH OCCURS DURING IMPULSE DRYING AND ITS INFLUENCE ON PAPER PROPERTY DEVELOPMENT.

SPECIFIC OBJECTIVES

- TESTING OF PROPOSED HYPOTHESES
- INVESTIGATE INTERRELATIONSHIPS BETWEEN WATER REMOVAL AND DENSIFICATION MECHANISMS
- UTILIZE AND/OR EXTEND EXISTING MATHEMATICAL MODELS OF SHEET COMPRESSION

RESEARCH PLAN

- "DYNAMIC" DENSITY DISTRIBUTION STUDY
- SHEET TEMPERATURE DISTRIBUTION STUDY
- MICROSCOPIC SHEET STRUCTURE EVALUATION
- MATHEMATICAL MODELING OF PROCESS

STATUS

COMPLETED WORK:

- DYNAMIC DENSIFICATION STUDY
- TEMPERATURE DISTRIBUTION STUDY
- SHEET STRUCTURE EVALUATION

  VARIABLES: TEMPERATURE
  PRESSURE
  TIME
  MOISTURE
  BASIS WEIGHT
  REFINING

WORK IN PROGRESS:

- MATHEMATICAL MODEL

IMPULSE · DRYING SIMULATOR
"DATA COLLECTION CAPABILITIES"

- DISPLACEMENT MEASUREMENT SYSTEM
- HOT SURFACE TEMPERATURE
- APPLIED MECHANICAL PRESSURE
- HOT SURFACE VAPOR PRESSURE
- INTERNAL SHEET TEMPERATURES

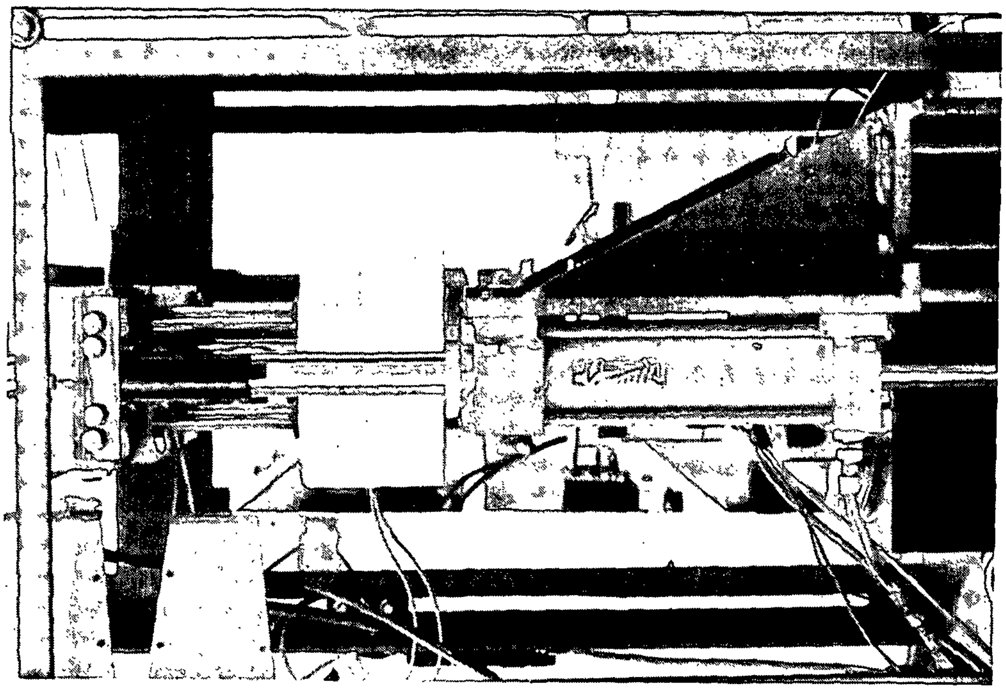

IMPULSE DRYING SIMULATOR BRAKING SYSTEM - SIDE VIEW.

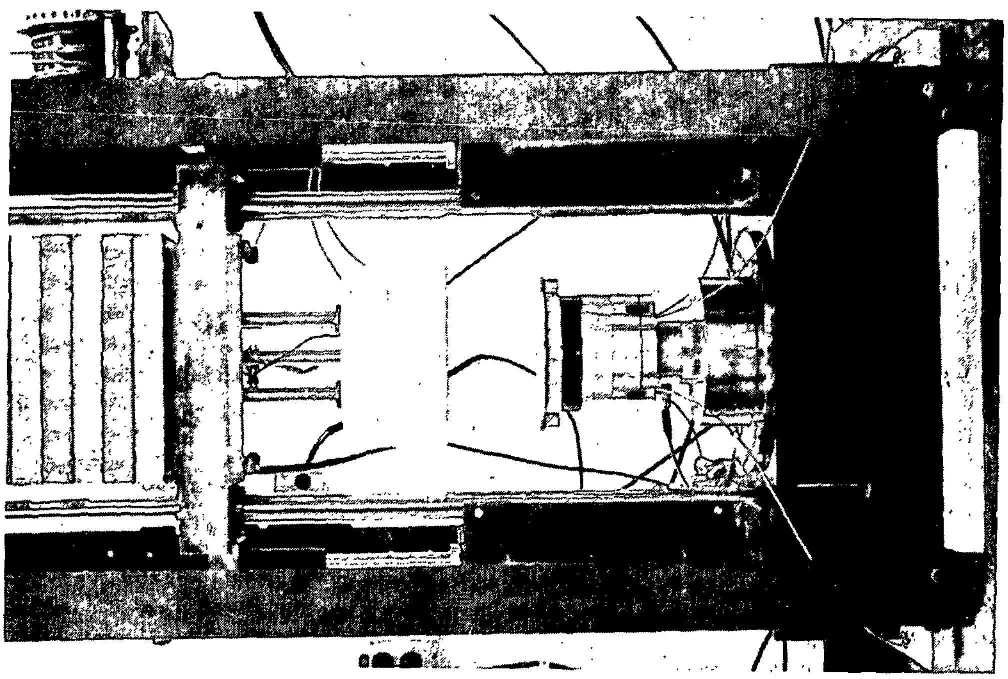

IMPULSE DRYING SIMULATOR - FRONT VIEW.

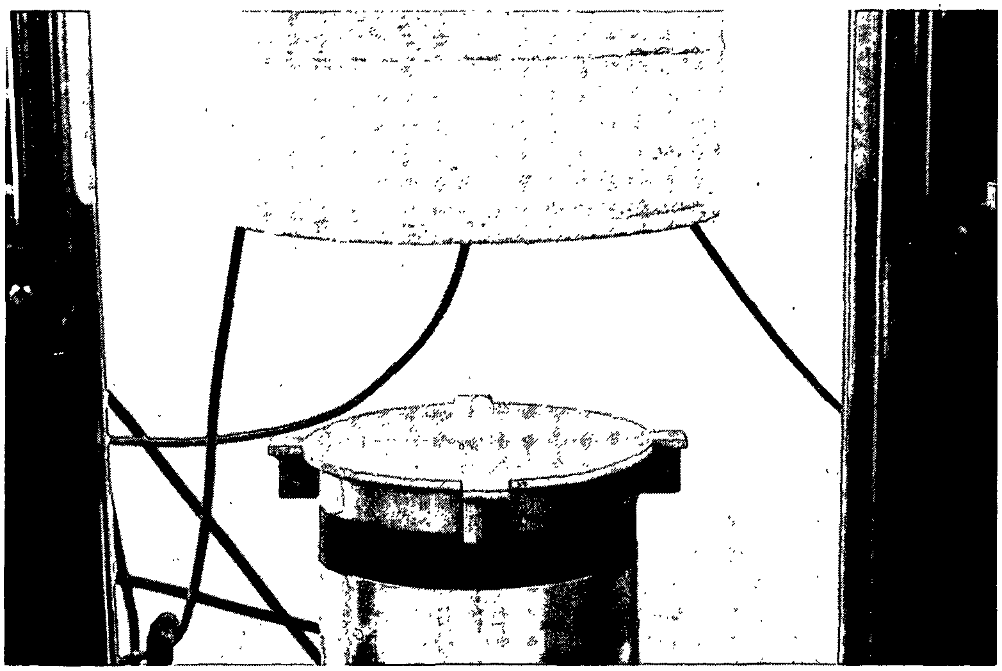

IMPULSE DRYING SIMULATOR NIP
UPPER PLATEN IS HEATED, LOWER PLATEN IS WATER RECEIVER

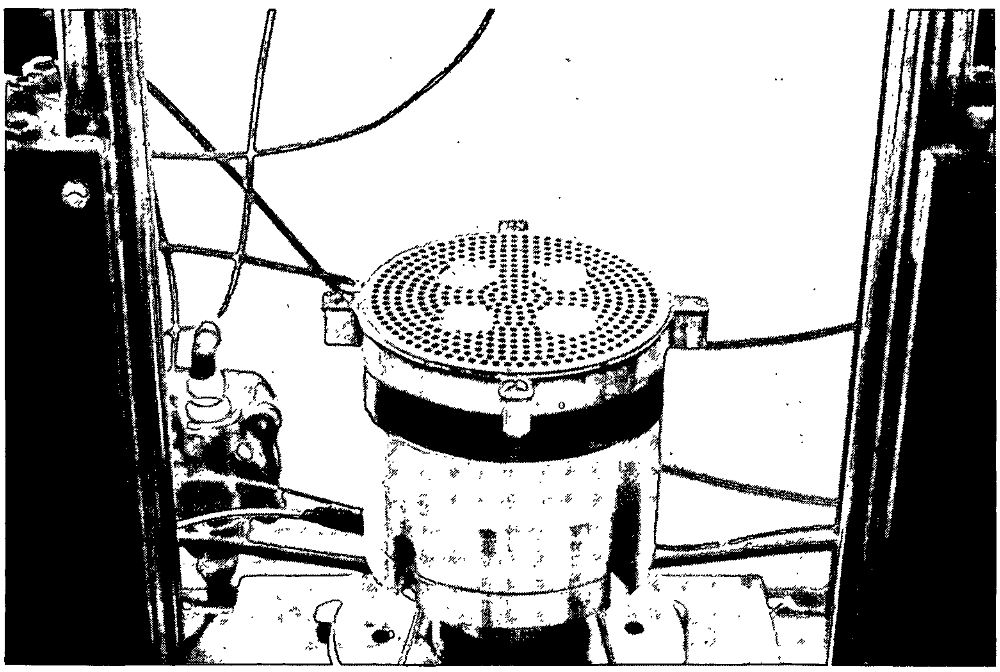

LOWER PEDESTAL OF IMPULSE DRYING SIMULATOR WITH CERAMIC REMOVED
REVEALING DISPLACEMENT TRANSDUCERS AND DRILLED PLATE

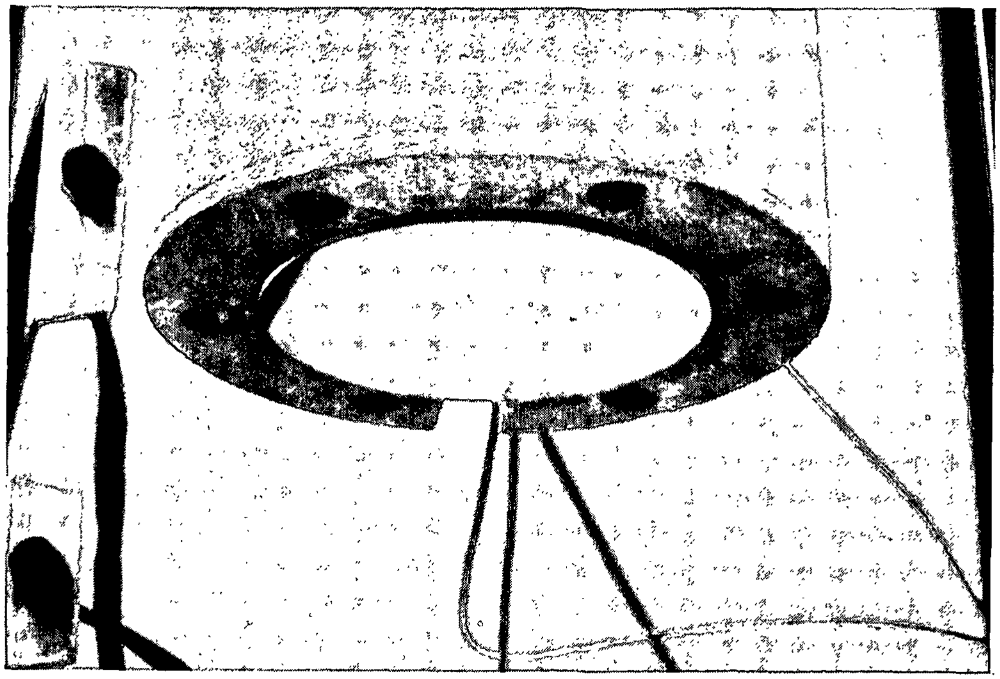

UPPER HEATED PLATEN OF IMPULSE DRYING SIMULATOR

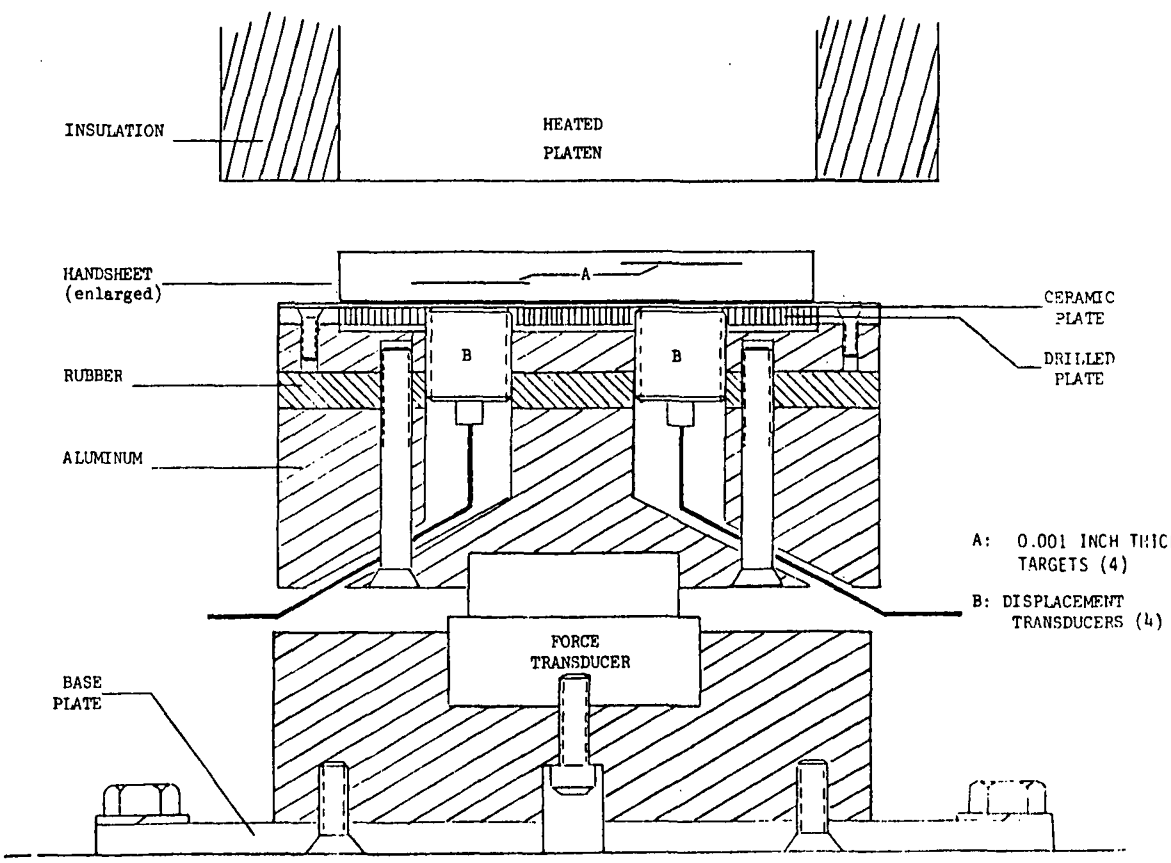

IMPULSE DRYING SIMULATOR PEDESTAL

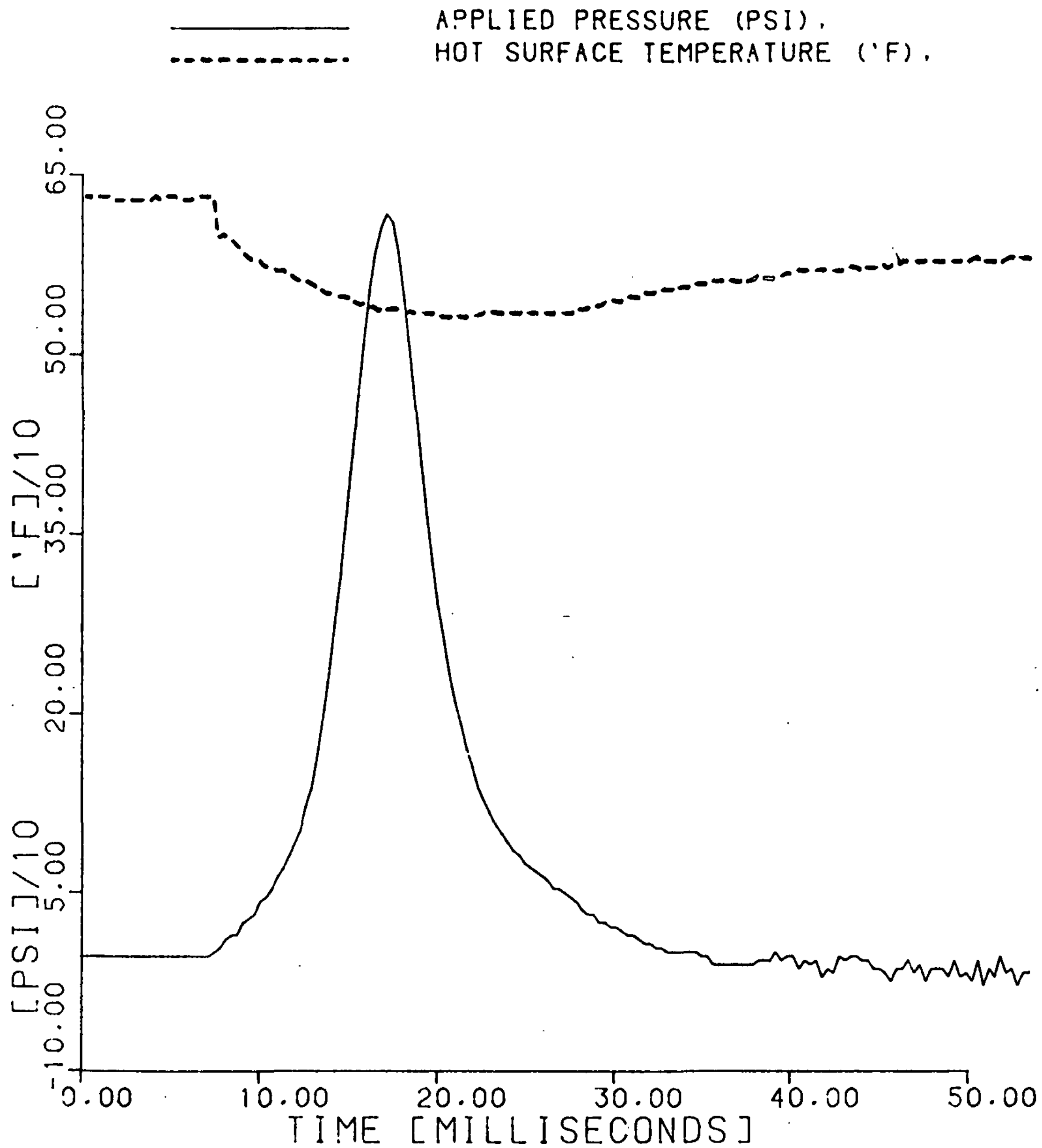

APPLIED MECHANICAL PRESSURE AND HOT SURFACE TEMPERATURE FOR AN UNBLEACHED SOFTWOOD KRAFT HANDSHEET, 166 g/m^2 BASIS WEIGHT, 2.2 INITIAL MOISTURE RATIO, 735 CSF.

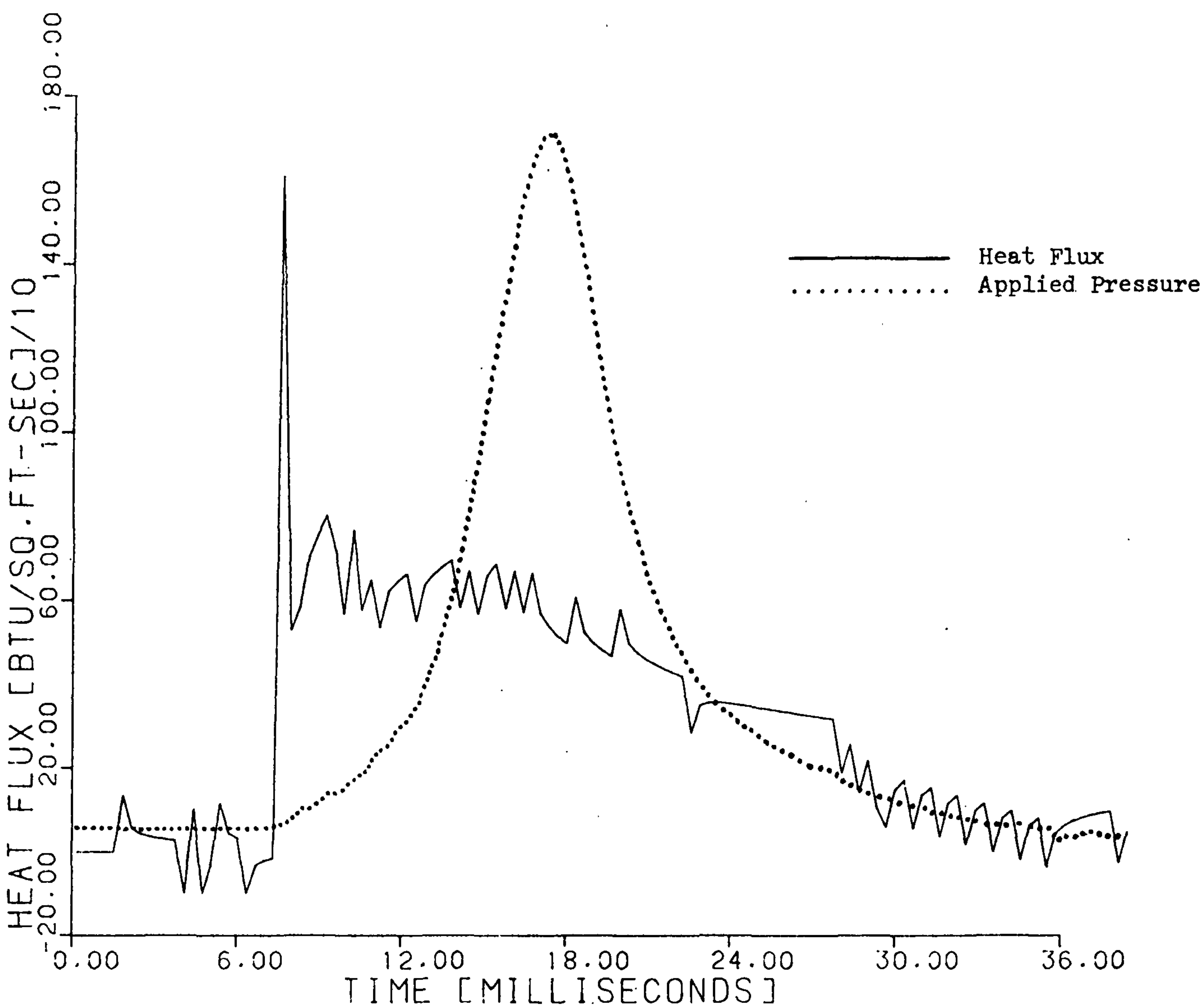

INSTANTANEOUS HEAT FLUX CALCULATED FROM THE HOT SURFACE TEMPERATURE. APPLIED MECHANICAL PRESSURE PULSE INCLUDED FOR REFERENCE.

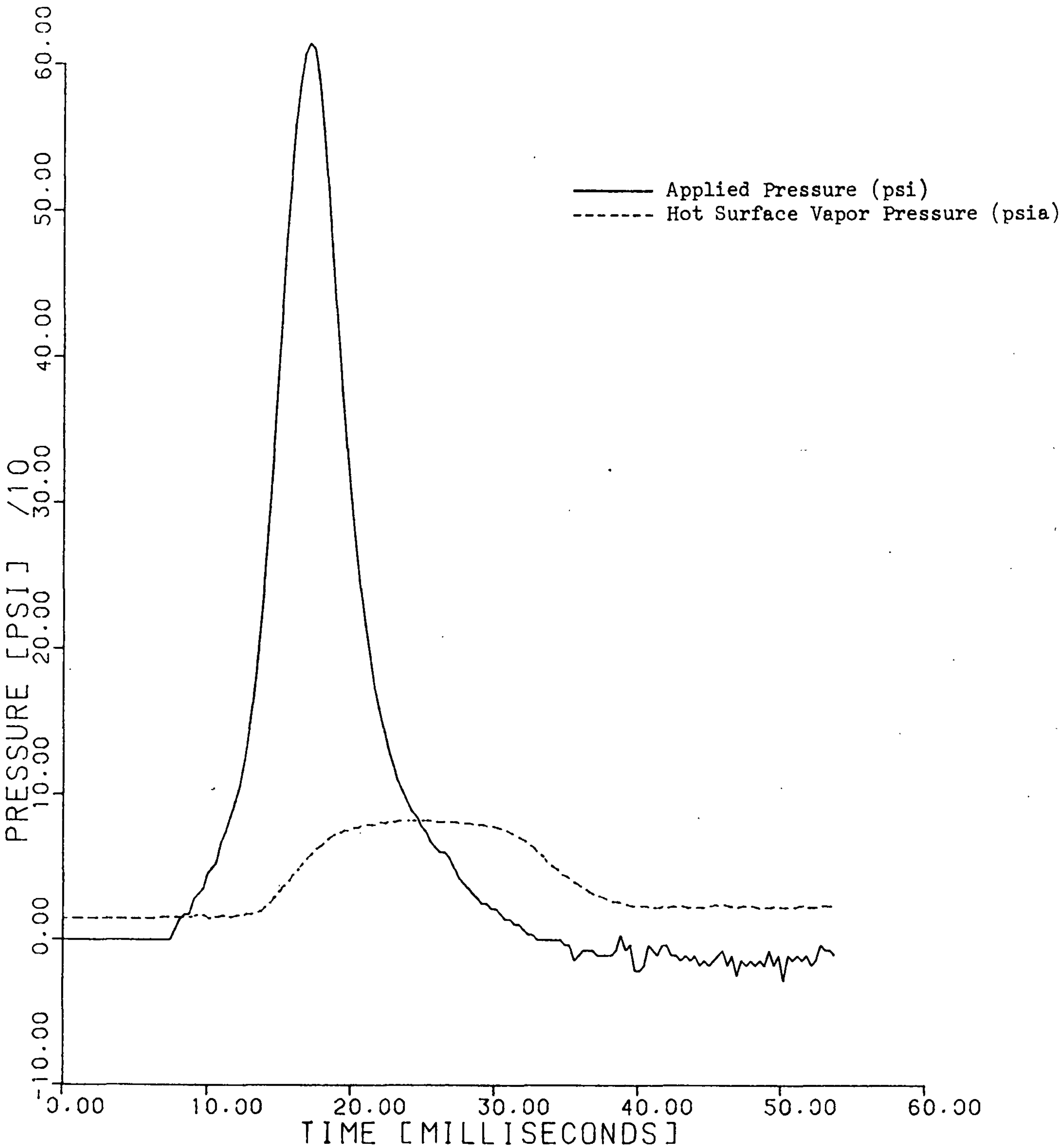

APPLIED MECHANICAL PRESSURE AND HOT SURFACE VAPOR PRESSURE FOR AN UNBLEACHED SOFTWOOD KRAFT HANDSHEET IMPULSE DRIED AT 630°F HOT SURFACE TEMPERATURE; 166 g/m^2 BASIS WEIGHT, 2.2 INITIAL MOISTURE RATIO, 735 CSF.

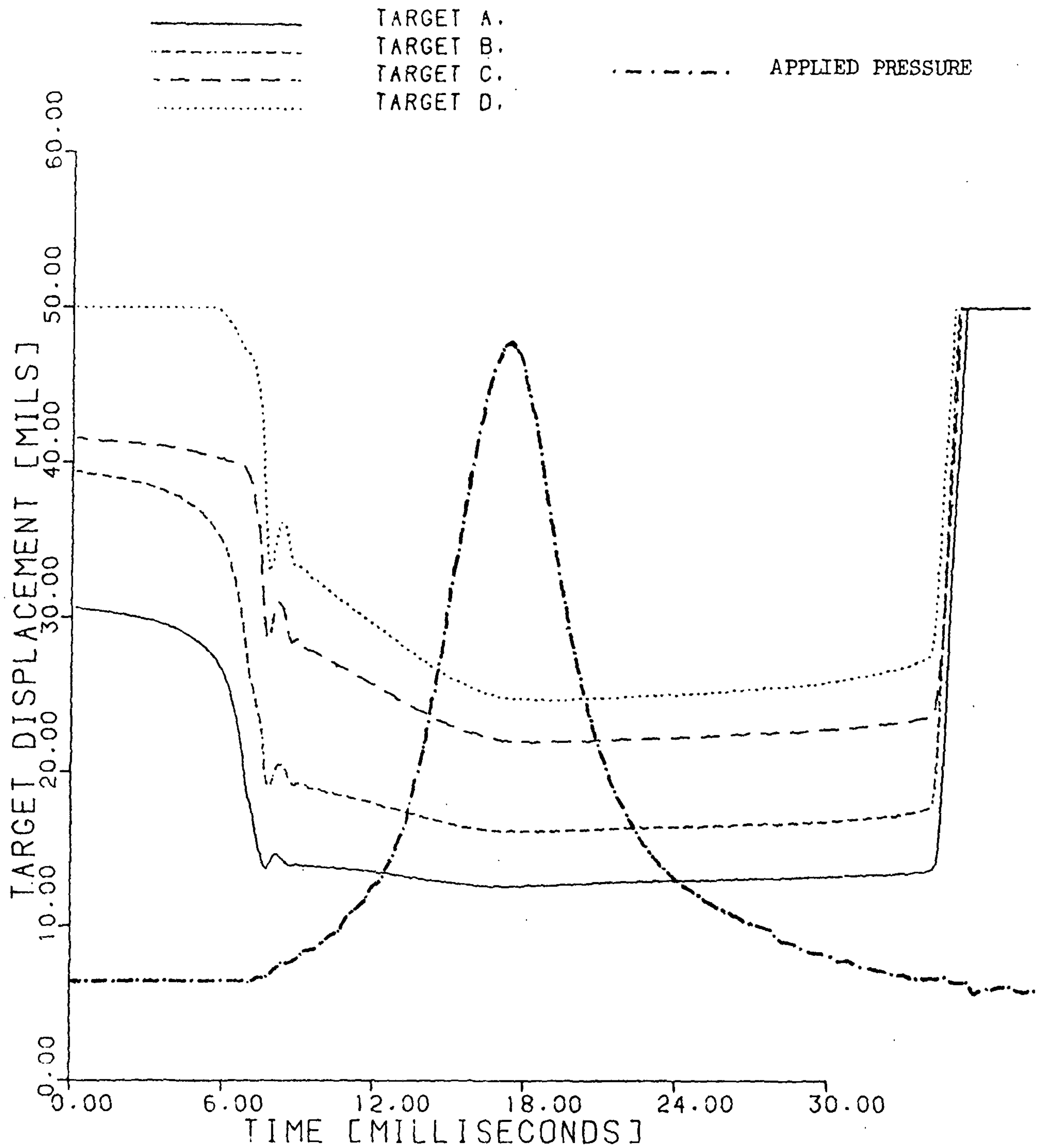

DISPLACEMENT HISTORIES OF FOUR TARGETS PLACED AT DISTINCT POSITIONS WITHIN THE FIBER MAT, WET PRESSED AT ROOM TEMPERATURE, PEAK PRESSURE OF 614 PSI AND A NIP RESIDENCE TIME OF 25 MILLISECONDS. THE HANDSHEET IS A 168 g/m^2 BASIS WEIGHT, 2.3 INITIAL MOISTURE RATIO, 735 CSF.

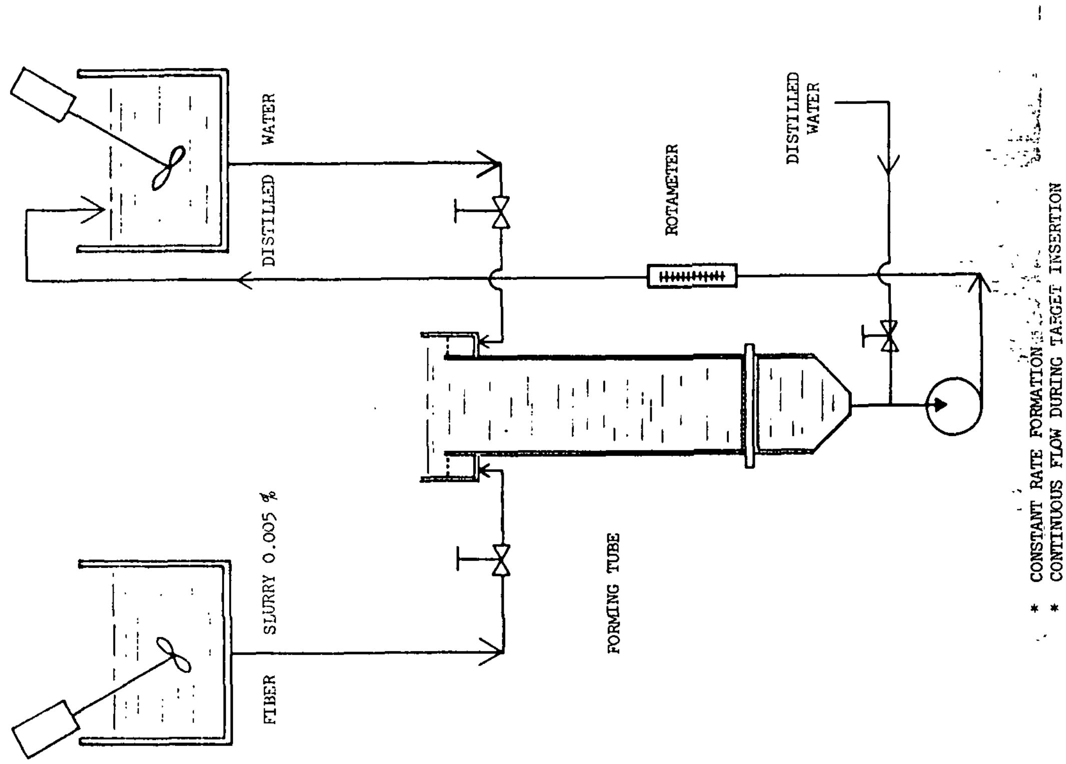

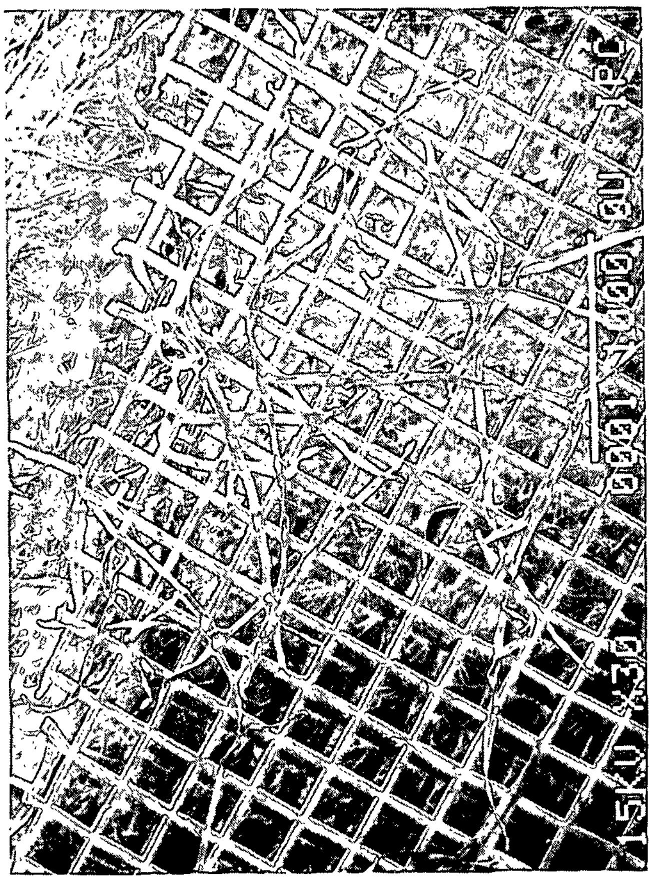

TARGET MATERIAL USED IN THICKNESS MEASUREMENT
0.001 INCH THICK COOPER MESH

METHODS USED FOR DETERMINING
Z-DIRECTIONAL DENSITY DISTRIBUTION

- SHEET GRINDING
- GOLD MAPPING TECHNIQUE
- DYNAMIC DENSIFICATION MEASUREMENTS

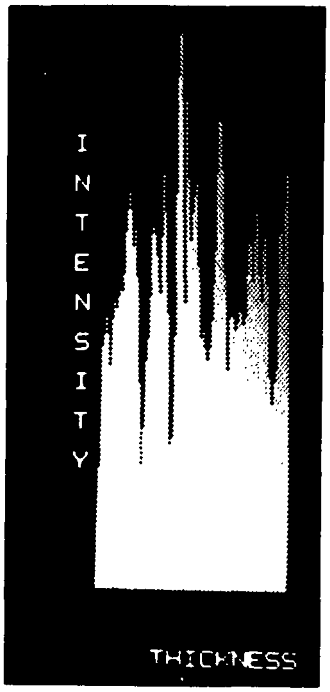

Control 70°F

300°F

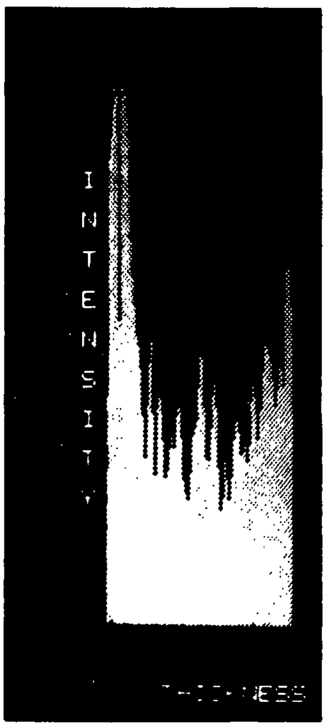

450°F

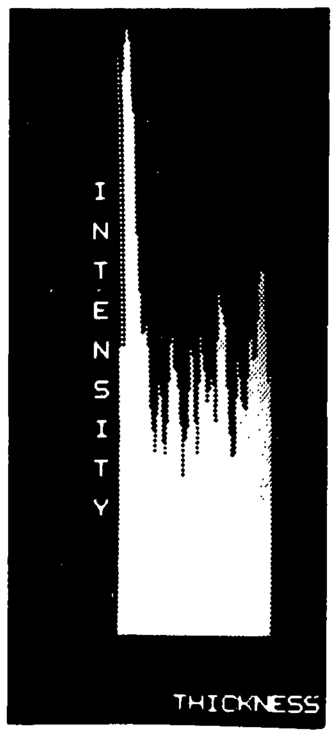

600°F

SCANNING ELECTRON MICROSCOPE MAPPINGS OF THE INTENSITY OF GOLD COUNTS (Y AXIS) VERSUS SHEET THICKNESS (X AXIS). INTENSITY IS A RELATIVE MEASURE OF THE APPARENT DENSITY OF THE WEB.

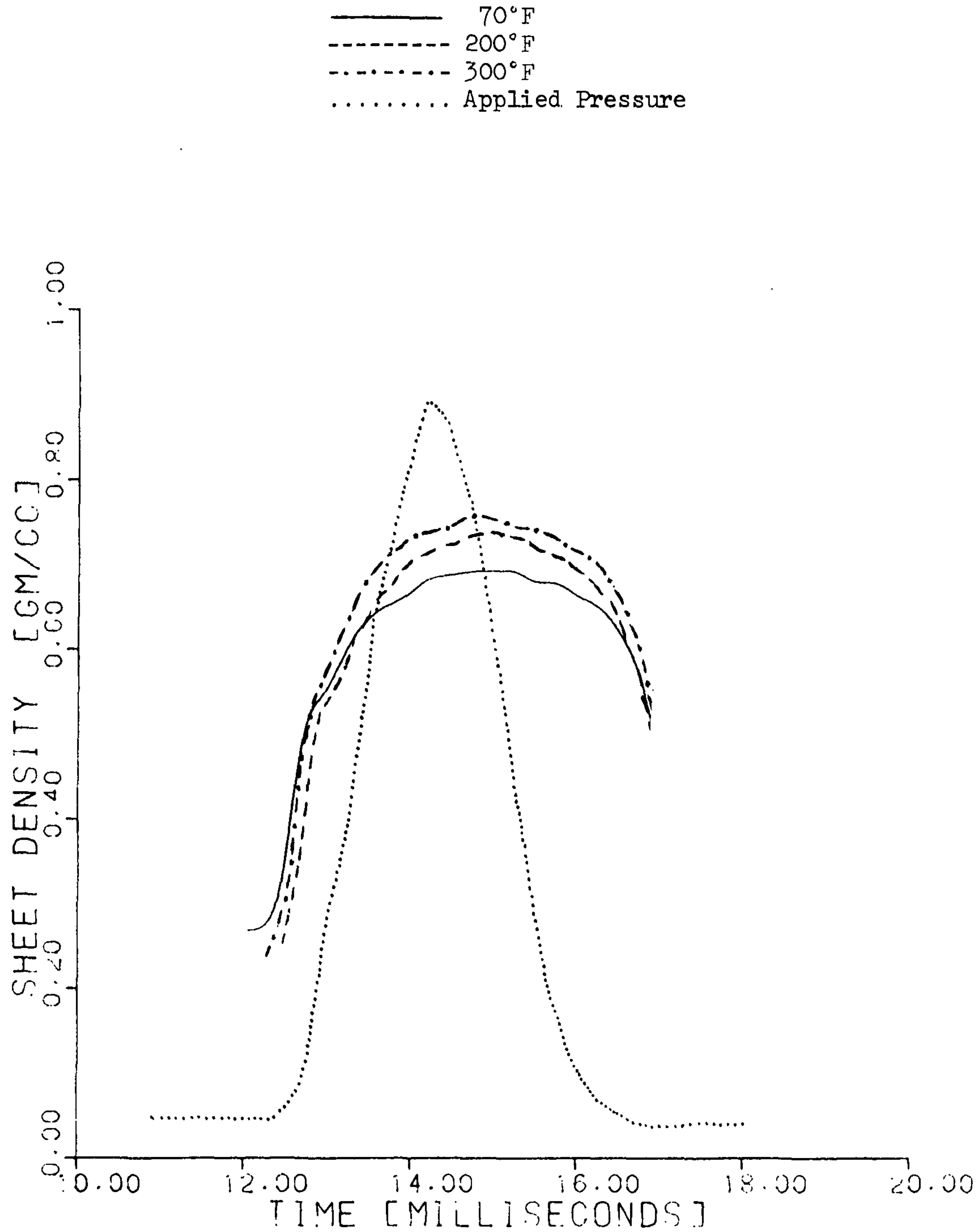

SHEET DENSITY VERSUS TIME FOR VARYING HOT SURFACE TEMPERATURES (70°F, 200°F, AND 300°F). EACH CURVE REPRESENTS A SINGLE RUN. BASIS WEIGHT 50 g/sq.m., 800 PSI PEAK APPLIED PRESSURE, 4.5 MSEC NIP RESIDENCE TIME, 735 CSF FREENESS, 1.2 INITIAL MOISTURE RATIO.

SHEET DENSITY VERSUS TIME FOR VARYING HOT SURFACE TEMPERATURES (400°F, 500°F, AND 700°F). EACH CURVE REPRESENTS A SINGLE RUN. BASIS WEIGHT 50 g/sq.m., 800 PSI PEAK APPLIED PRESSURE, 4.5 MSEC NIP RESIDENCE TIME, 420 CSF FREENESS, 1.2 INITIAL MOISTURE RATIO.

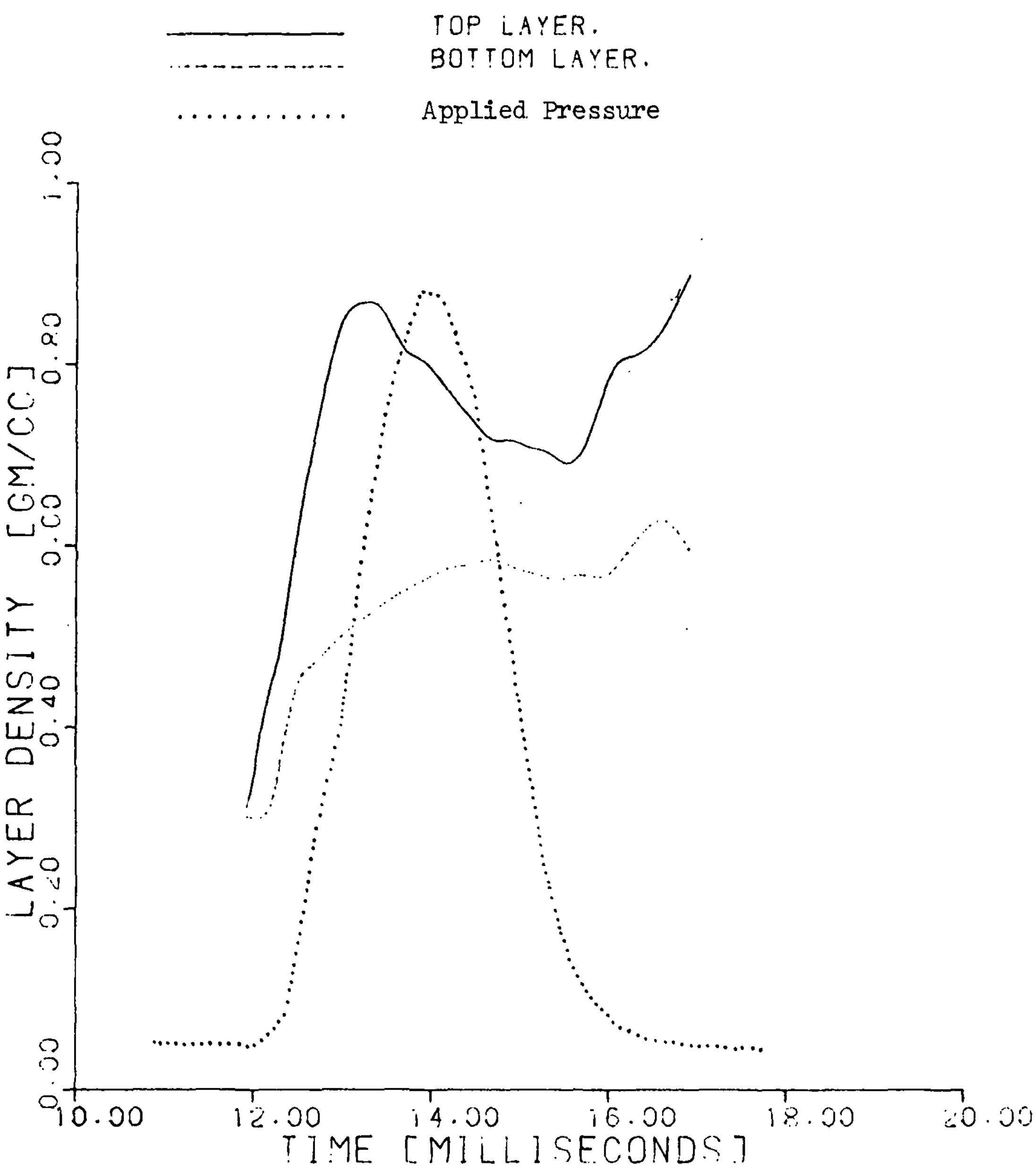

LAYER DENSITIES VERSUS TIME FOR AN IMPULSE DRIED 50 g/sq.m. BASIS WEIGHT SHEET OF 420 CSF FREENESS. 800 PSI PEAK APPLIED PRESSURE, 4.5 MSEC NIP RESIDENCE TIME, 700°F HOT SURFACE TEMPERATURE, 1.2 INITIAL MOISTURE RATIO.

EACH LAYER REPRESENTS 25 g/sq.m. BASIS WEIGHT. THE TOP LAYER IS NEXT TO THE HOT SURFACE.

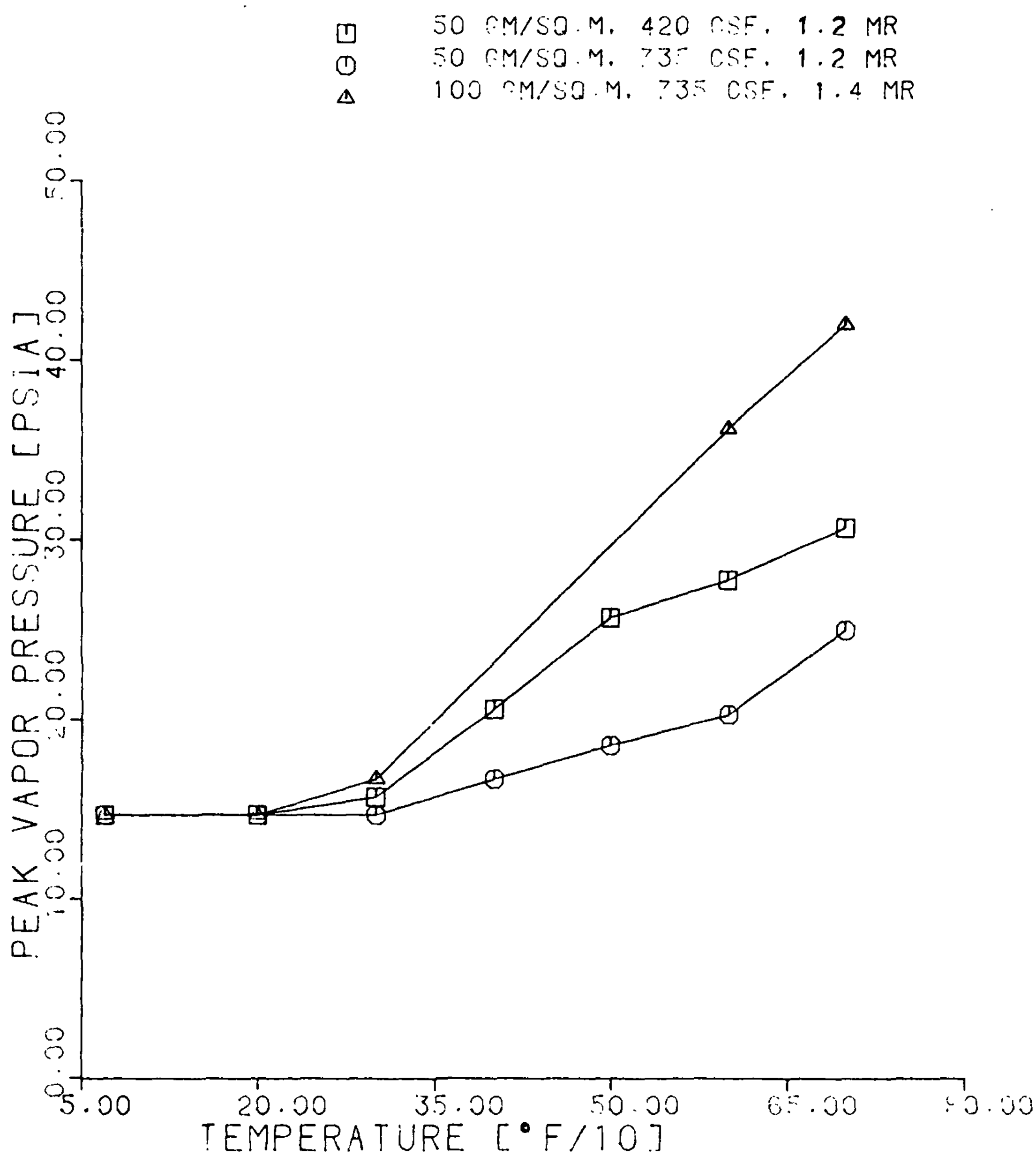

PEAK VAPOR PRESSURES AS A FUNCTION OF HOT SURFACE TEMPERATURE FOR AN 800 PSI PEAK PRESSURE, 4.5 MSEC NIP RESIDENCE TIME. BASIS WEIGHT OF 50 TO 100 g/sq.m. AND FREENESS VALUES OF 420 AND 735 CSF.

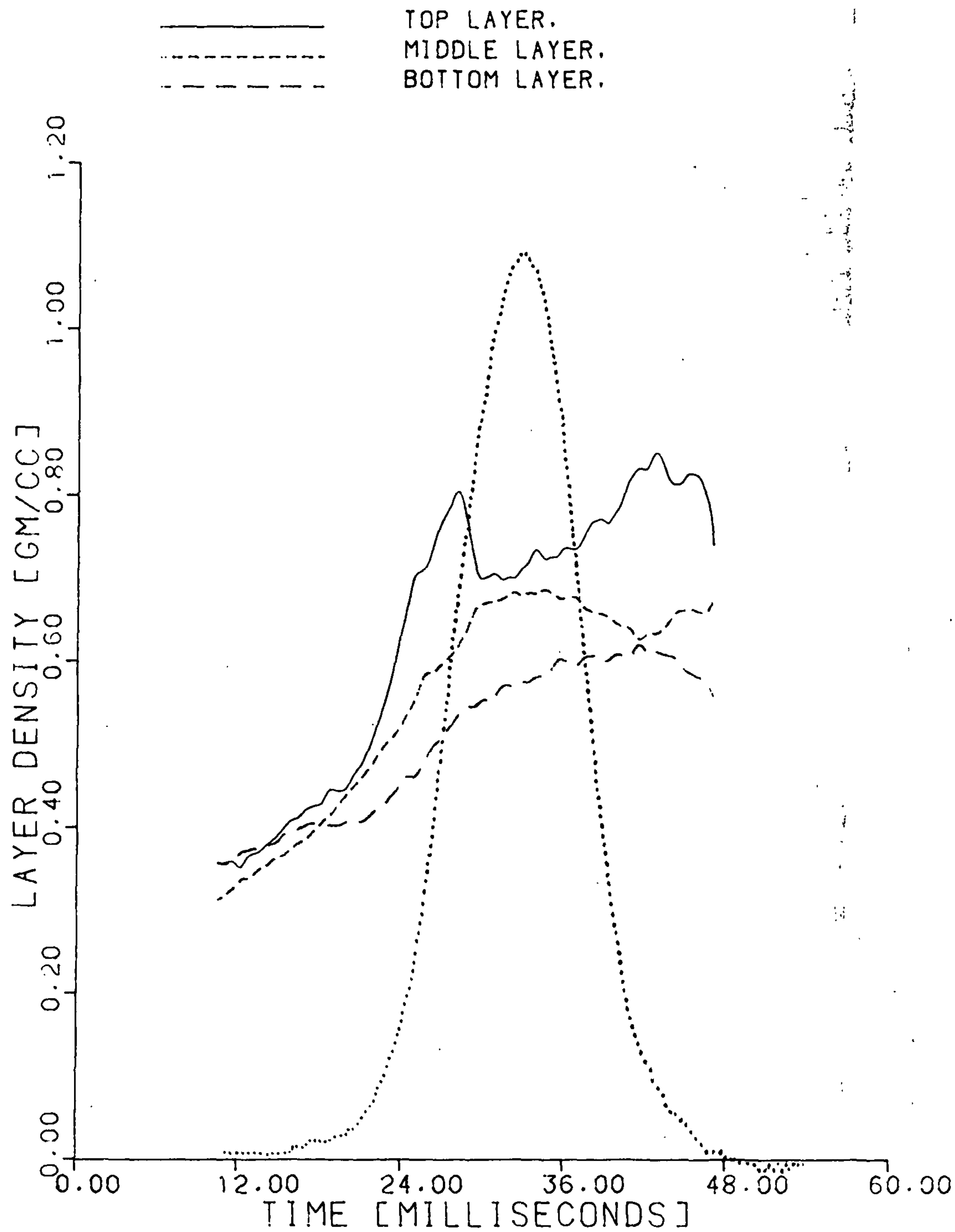

SHEET LAYER DENSITY AS A FUNCTION OF TIME FOR A 100 g/sq.m. WEB AT AN INITIAL MOISTURE RATIO OF 1.5 AND A PULP FREENESS OF 420 CSF, IMPULSE DRIED AT 600°F HOT SURFACE TEMPERATURE, 550 PSI PEAK APPLIED PRESSURE, AND A 30 MILLISECOND NIP RESIDENCE TIME. THE TOP AND BOTTOM LAYER EACH REPRESENT 25% OF THE TOTAL BASIS WEIGHT WITH THE TOP LAYER POSITIONED NEXT TO THE HEATED SURFACE. THE APPLIED PRESSURE PULSE IS INCLUDED FOR REFERENCE.

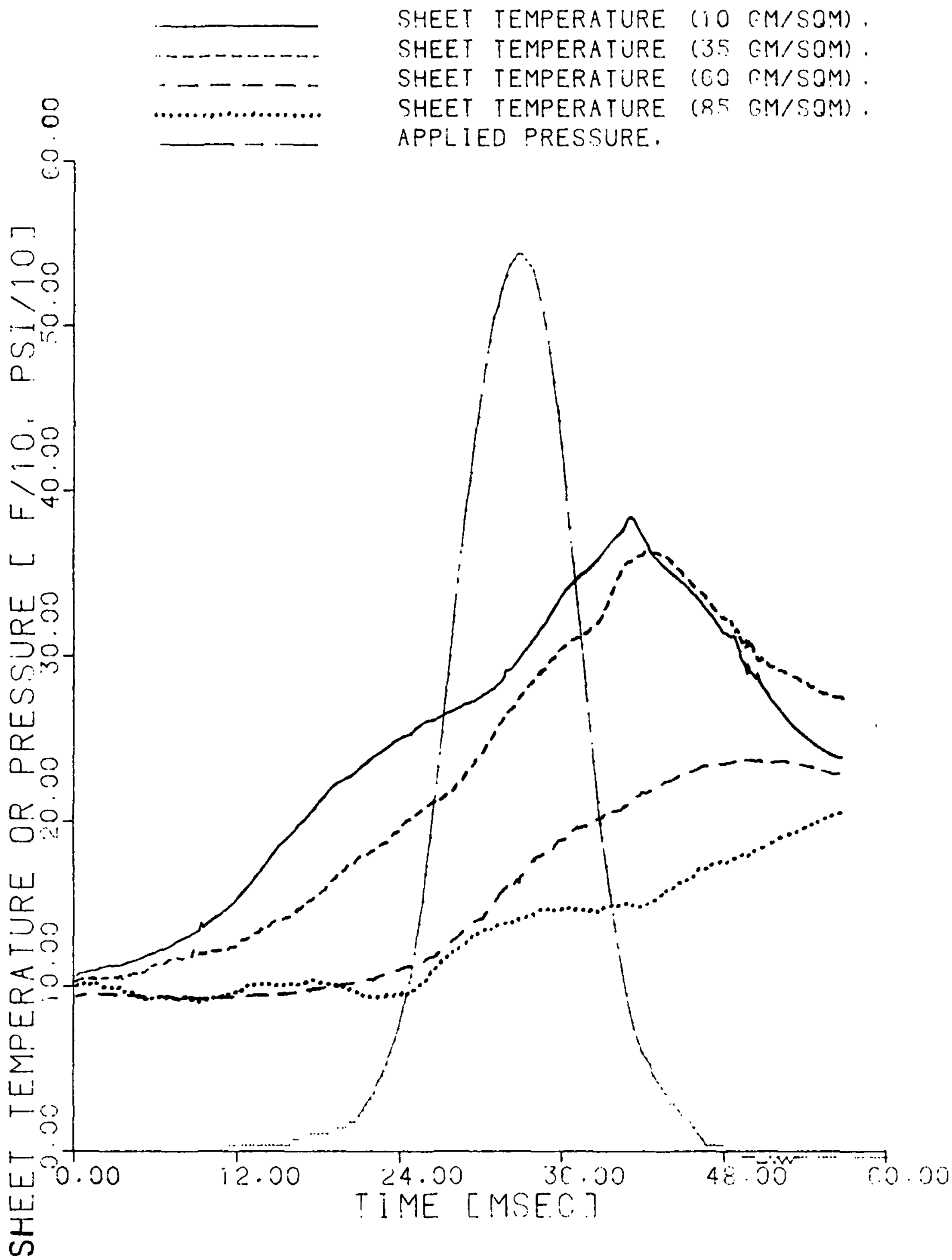

SHEET TEMPERATURE RESPONSE AS A FUNCTION OF TIME AT INCREASING DISTANCES FROM THE HOT SURFACE FOR A 100 g/sq.m. WEB AT AN INITIAL MOISTURE RATIO OF 1.5 AND A PULP FREENESS OF 420 CSF, IMPULSE DRIED AT 600°F HOT SURFACE TEMPERATURE, 550 PSI PEAK APPLIED PRESSURE, AND A 30 MILLISECOND NIP RESIDENCE TIME.

DENSIFICATION MECHANISMS
DURING IMPULSE DRYING

MOISTURE REDISTRIBUTION DUE TO EVAPORATION-CONDENSATION MECHANISM.

INTENSE DENSIFICATION OF TOP LAYER DUE TO DRYING OUT AND THERMAL SOFTENING.

ABRUPT DECREASE OR LEVELING OUT OF SHEET DENSITY NEAR THE HOT SURFACE DUE TO INTERNAL VAPOR PRESSURE GENERATION.

ENHANCED WET PRESSING MECHANISMS
IN FLOW EXITING REGION OF WEB.

COLLAPSE OF SHEET STRUCTURE DUE TO RELEASE OF VAPOR AS THE APPLIED PRESSURE DECREASES BELOW VAPOR PRESSURE.

DISRUPTION OF THE INTERNAL SHEET STRUCTURE AFTER THE PRESS NIP DUE TO CONTINUED VAPOR RELEASE.